LUMA-GIS Thesis nr 27

Accuracy Assessment in Glacier Change Analysis

Inese Linuza

2014
Department of
Physical Geography and Ecosystem Analysis
Centre for Geographical Information Systems
Lund University
Sölvegatan 12
S-223 62 Lund
Sweden

Author’s name: Inese Linuza. Title of thesis: Accuracy Assessment in Glacier Change Analysis
Supervisors: Harry Lankreijer (Lund University) and Liss Marie Andreassen (NVE, Norway)
Master degree thesis, 30 credits in Master in Geographical Information Sciences
Department of Physical Geography and Ecosystems Science, Lund University

Accuracy Assessment in Glacier Change Analysis

Inese Linuza
Master thesis, 30 credits, in Geographical Information Sciences

Harry Lankreijer
Lund University

Liss Marie Andreassen
Norwegian Water Resources and Energy Directorate

Jostefonn seen from Grovabreen.

Sundfjordbjørnen – the highest point of Jostefonn.

(Source: http://www.westcoastpeaks.com/Peaks/meneseggi.html)

Acknowledgements

I would like to express my thankfulness and appreciation to all the people who contributed to the completion of this thesis:

- Harry Lankreijer – my supervisor from Lund University
- Liss Marie Andreassen – my co-supervisor from the Norwegian Water Resources and Energy Directorate
- Paul Bailie for proofreading my English
- My children, Maija and Maris, for their love and understanding
- My mother for her love and all the help at home

Abstract

This thesis assesses the accuracy of digital elevation models (DEM) generated from contour lines and LiDAR points (Light Detection and Ranging) employing several interpolation methods at different resolutions. The study area is Jostefonn glacier that is situated in Sogn og Fjordane county, Norway. There are several ways to assess accuracy of DEMs including simple ways such as visual comparison and more sophisticated methods like relative and absolute comparison.

Digital elevation models of the Jostefonn glacier were created from contour lines for years 1966 and 1993. LiDAR data from year 2011 was used as a reference data set. Of all the interpolation methods tested Natural Neighbours (NN) and Triangular Irregular Network (TIN) algorithms rendered the best results and proved to be superior to other interpolation methods. Several resolutions were tested (the cell size of 5 m, 10 m, 20 m and 50 m) and the best outcome was achieved by as small cell size as possible. The digital elevation models were compared to a reference data set outside the glacier area both on a cell-by-cell basis and extracting information at test points. Both methods rendered the same results that are presented in this thesis.

Several techniques were employed to assess the accuracy of digital elevation models – including visualization and statistical analysis. Visualization techniques included comparison of the original contour lines with those generated from DEMs. Root mean square error, mean absolute error and other accuracy measures were statistically analysed.

The greatest elevation difference between the digital elevation model of interest and the reference data set was observed in the areas of a steep terrain. The steeper the terrain, the greater the observed error. The magnitude of the errors can be reduced by using a smaller cell size but that this is offset by a larger amount of data and increased data processing time.

Keywords: Physical Geography and Ecosystem analysis, Geographical Information Systems (GIS), accuracy assessment, glaciology, Digital Elevation Models (DEMs), interpolation.

Table of Contents

Table of Figures

Table of tables

Table of abbreviations

ANUDEM - Australian National University Digital Elevation Model

DEM - Digital Elevation Model

DSM - Digital Surface Model

DTM - Digital Terrain Model

GIS - Geographical Information Systems

GPS - Global Positioning System

IMU - Inertial Measurement Unit

IR - Infrared

IDW - Inverse Distance Weighing

LiDAR - Light Detection and Ranging

MAE - Mean Absolute Error

ME - Mean Error

NN - Natural Neighbour

NMAD - Normalized Median Absolute Deviation

NVE - Norwegian Water Resources and Energy Directorate (Norges Vassdrags og Energidirektorat)

RMSE - Root Mean Square Error

TIN - Triangular Irregular Network

1. Introduction

Glaciers are very sensitive indicators of climate changes. Changes in temperature and precipitation influence the area and volume of glaciers (Lemke *et al.* 2007). The long-term monitoring of glaciers is important for presenting information on glacier-fed water supplies, glacier-associated natural hazards and climate variability (Mennis and Fountain 2001). Glaciers provide humans with many benefits, being important water resources, hydroelectric power generators, recreational resources as well as habitats for certain species. Knowledge that is gained from monitoring glaciers is used by governments, environmental and water resource managers to make plans to better cope with the economic impacts of climate change (National Park Service, accessed 24 July, 2013).

Glacier mass balance is a critical indicator of climate change and helps to estimate the volume of water being released into the oceans, thus raising global sea waters (Pope *et al.* 2007). Therefore, glacier monitoring can yield information that is crucial for decision making. Glacier change analyses are carried out to monitor change in glacier mass balance and size. Results from glacier change analyses ought to be very precise, without biases, showing the actual situation compared to the situation in the past as well as predicting possible glacier changes in the future. Any error caused by either one or another method applied in glacier change analyses can yield inaccurate results. The possible errors ought to be investigated and made as insignificant as possible in order to get the real, up-to-date picture of today's glaciers.

Although contemporary technical possibilities provide researchers with high quality data sets as well as software to perform accurate modelling and calculations, there is still a danger of inaccuracies and biases that affect the results obtained. In order to provide governments, environmental and water resource managers and other interested entities with high quality results, uncertainty assessments should be considered.

1.1 Aims and objectives

The aim of this thesis is to investigate how sensitive the results are to different methods used in glacier change detection. The research is focusing on the quality of Digital Elevation Models (DEMs). Different approaches of DEM creation and evaluation have been tested at the Jostefonn glacier in southern Norway.

The work has been accomplished by applying different DEM creation and evaluation methods to find out which method renders the best results and whether these results can be reliable in estimating the glacier change. The accuracy of comparisons between the available data sets has been studied, with particular attention towards detecting glacier thickness changes. This involved classifying and understanding the errors, and especially biases, associated with each of the data products and methods, and to suggest corrections that may improve the accuracy and precision of the differences (Nuth and Kääb 2011).

Digital elevation models were created by different interpolation techniques and with different resolutions in order to test which technique and which resolution rendered the most reliable results. The acquired DEMs were tested against the LiDAR data that was taken as a reference data set in the glacier-free area. The elevation difference was assessed in the glacier-free area on a cell-by-cell basis between the data set to be tested and the reference data set, and by comparing the elevation at specific test points where elevation measurements are available.

The objectives of this thesis are: 1) to evaluate the suitability of various interpolation techniques to construct DEMs for glaciological studies; 2) to assess elevation differences between the DEM from LiDAR data and the DEM from topographic data in glacier-free area; 3) to discuss the methods applied and result reliability; 4) to identify the spatial distribution of elevation differences with respect to topographic characteristics (slope and aspect); 5) to ascertain the factors that affect the accuracy of the DEM; 6) to suggest methods to improve the quality of the generated DEMs; and 7) to observe the changes how the Jostefonn glacier has changed in the period between 1966 and 2011.

1.2 Structure of the work

The thesis consists of nine chapters. Chapter 1 presents the aims and objectives of the thesis. Chapter 2 presents theory and background information on methods used in glacier change analysis as well as interpolation methods that are available in creation of digital elevation models. Chapter 3 presents the study area and the available data. The methodology of creating the DEM and carrying out the analyses is discussed in Chapter 4 where different quality assessment methods are also analysed. The results are presented in Chapter 5. Chapter 6 is devoted to discussion while Chapter 7 includes a summary and conclusions. References (Chapter 8) and Appendix (Chapter 9) are available at the end of the thesis.

2. Theory and background

2.1 Methods of measuring the mass balance of a glacier

There are many methods available for measuring the mass balance of a glacier. The most common methods are the geodetic (or cartographic) method, the direct (glaciological or traditional) method, the dynamical method and the hydrological method.

The geodetic method is based on remote sensing where changes of glacier volume are studied from maps or elevation models. This mapping method can be carried out using terrestrial or aerial photogrammetry, airborne laser scanning or satellite surveys. The main principle of the geodetic method is that it determines the change of altitude in the time interval between two surveys (Pellikka and Rees 2009) and uses density estimates to convert volume change to mass change.

The direct or glaciological method is based on annual field measurements of snow/ice density and depth at certain in situ point locations using ablation stakes and snow pits in order to acquire the total glacier depth at these in situ locations. The acquired data are then extrapolated over the entire glacier surface based on in situ measurements. In order to perform extrapolation, the geodetic method is applied here. Field measurements can be quite expensive and time consuming (Andreassen 1999; Andreassen *et al*. 2012; Joerg *et al*. 2012).

The dynamic method monitors flow dynamics on a glacier surface. The mass balance of the upper part of a glacier is compared to the ice flow through its lower boundary (Pellikka and Rees 2009).

The hydrological method calculates glacier mass balance as a storage term in the water balance. Runoff and evaporation are then subtracted from precipitation, giving the glacier mass balance for the whole catchment area. This method is very seldom applied due to significant inaccuracies (Hagg *et al*. 2004; Pellikka and Rees 2009).

The geodetic method has been used in the current thesis based on the aim and objectives of the research as well as on the available data sets and software.

2.2 Sources of data acquisition for digital elevation model (DEM) generation

There are three sources that can render data for DEM generation – ground survey technique, existing topographic maps and remote sensing (Nelson *et al*. 2009). Wenzhong Shi (2010) has depicted data capture methods graphically (Fig. 1) where he differentiates between indirect and direct capture methods. The difference between these two capture methods is that in the direct capture methods the point coordinate error is the original measurement error whereas indirect capture methods include both measurement errors and further processing errors (Wenzhong Shi 2010).

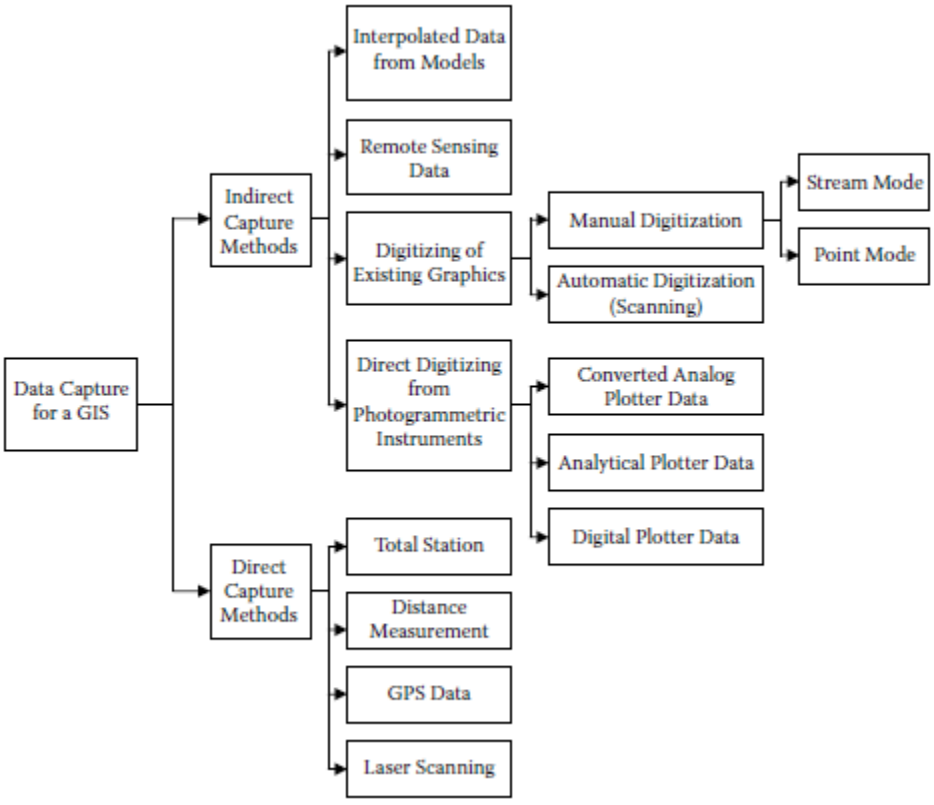

Figure 1. A classification of spatial data capture methods (Source: Wenzhong Shi 2010).

2.2.1 Ground survey techniques

Ground survey techniques are direct capture methods (Fig. 1) including the usage of total station, distance measuring equipment and global positioning system (GPS).

2.2.2 Remote sensing

Remote sensing of glaciers for glacier change analysis has developed considerably over recent years. The remote sensing platform can be airborne or situated in space. There are three sources from which DEM can be extracted – aerial photography, LiDAR and satellite imagery (Nelson *et al*. 2009).

Remote sensing refers to data acquisition using a sensor that is not in direct contact with the object such as aerial and satellite-based platforms (La Frenierre 2009; Bamber and Kwok 2003). The advantage of remote sensing lies in the fact that it renders data for all areas of the glacier surface, including areas that are otherwise difficult and dangerous to reach, and can provide an overall change in volume for a certain period of time (La Frenierre 2009; Thomas 2009). Remote sensing is also less expensive and less time-consuming compared to the glaciological method.

Remote sensing methods have some disadvantages compared to traditional glaciological methods. For example, optical satellite and aerial imagery are dependent on weather conditions. Glaciers are usually found in regions with high levels of cloud cover and precipitation, making it difficult to obtain high quality data. The high relief and complicated topography of mountains can cause distortion as well. Snow from a previous winter that has not melted as well as summer snow can make it difficult to differentiate the glacier borderline (Robson 2012).

2.2.2.1 Aerial photography and existing topographic maps

Aerial photography is the earliest technique of remote sensing, having been used in glaciology since the 1930s (Fox and Nuttall 1997). Aerial photogrammetry retrieves geometric information about objects from airborne analogue or digital image data (Pellikka and Rees 2009). It is based on single original image data, overlapping image data or transformed image data. Single image data are used in cases where individual photos are analysed. Overlapping image data (stereo-techniques) are used for three-dimensional vision and measurement. This type of data is widely applied in glaciological photogrammetry where the surface of glaciers is reconstructed with three-dimensional measurements. Transformed image data are orthoprojected images (orthorectified images, orthoimages or orthophotographs). Orthoprojection is the process whereby images from the original acquisition geometry are transformed into map geometry (Pellikka and Rees 2009).

The advantage of aerial photography is that overlapping pairs of photographs provide a three-dimensional view of the terrain. Such overlapping pairs are called stereoscopic images. Vertical stereophotos are important for visual photointerpretation and are the basis for many photogrammetric techniques (Aber *et al*. 2010). Elevation contour lines of the area can be constructed from vertical aerial photographs using a technique called stereophotogrammetry. A graphic depiction of analogue photogrammetry is seen in Figure 2.

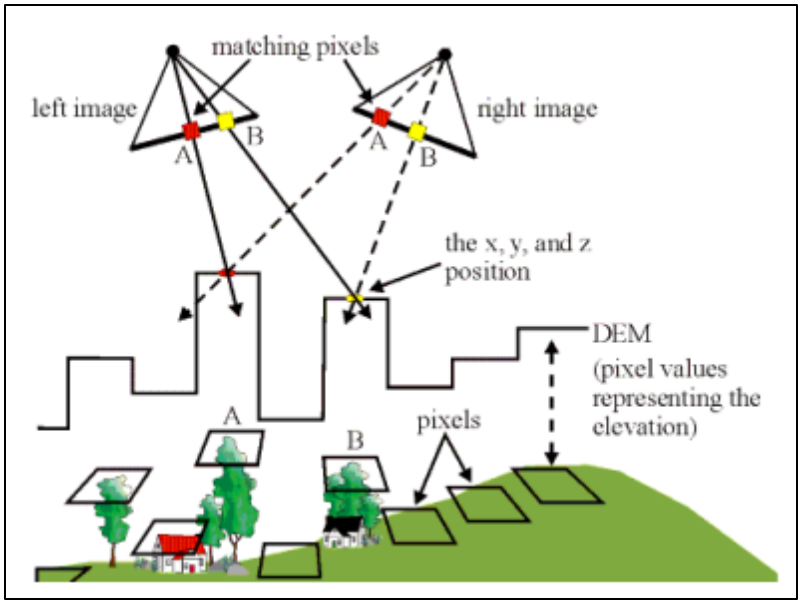

Figure 2. Analogue Photogrammetry, Extracting Elevation from Air Photos (Source: PCI Geomatics).

Aerial photographs are used in topographic mapping. The end product of aerial photographs is cartographic source material either graphic or digital. Such cartographic sources include contour lines, drainage and transportation features from topographic maps (Maune *et al.* 2007).

Contour lines can be extracted from the existing topographic maps and are thus used to generate DEM. Contour lines can either be manually digitised or extracted by using automated or semi-automated digitising methods (Nelson *et al*. 2009).

2.2.2.2 LiDAR

Light Detection and Ranging (LiDAR) is a remote sensing method that has become widely used for generating extremely accurate terrain models used in many Geographical Information Systems (GIS) applications as, for example, forestry management and planning, flood and pollution modelling as well as urban and transport planning and, of course, in glaciological studies (Bater and Coops 2009). A LiDAR system uses a laser sensor consisting of a transmitter and a receiver, a Global Positioning System (GPS) and

an Inertial Measurement Unit (IMU) (Raber and Cannistra 2005). The LiDAR sensor emits rapid pulses of Infrared (IR) light towards the earth where it is reflected by the surface it encounters. The reflected light is recorded in order to estimate the distance between the sensor and the ground surface, based on the time it takes to travel to the target and return to the sensor and at the same time compensates for the movement of the aircraft and the sensor. Each pulse can result in multiple returns where the first return will be from the tops of the trees and vegetation whereas the last return is received from the ground surface. The acquired result is thousands of points (a point cloud) where each point has three-dimensional coordinates (latitude, longitude and height) that display the position and elevation of each point. These point clouds are used to generate terrain models in the form of either digital elevation models (DEM) or digital surface models (DSM) as well as other geospatial products (Davis 2012; Bater and Coops 2009; La Frenierre 2009; Raber and Cannistra 2005; Rabber and Cannistra 2005; ESRI 2013b; Geomaps Tanzania Limited; LiDAR UK). A graphic depiction of LiDAR data acquisition is seen in Figure 3.

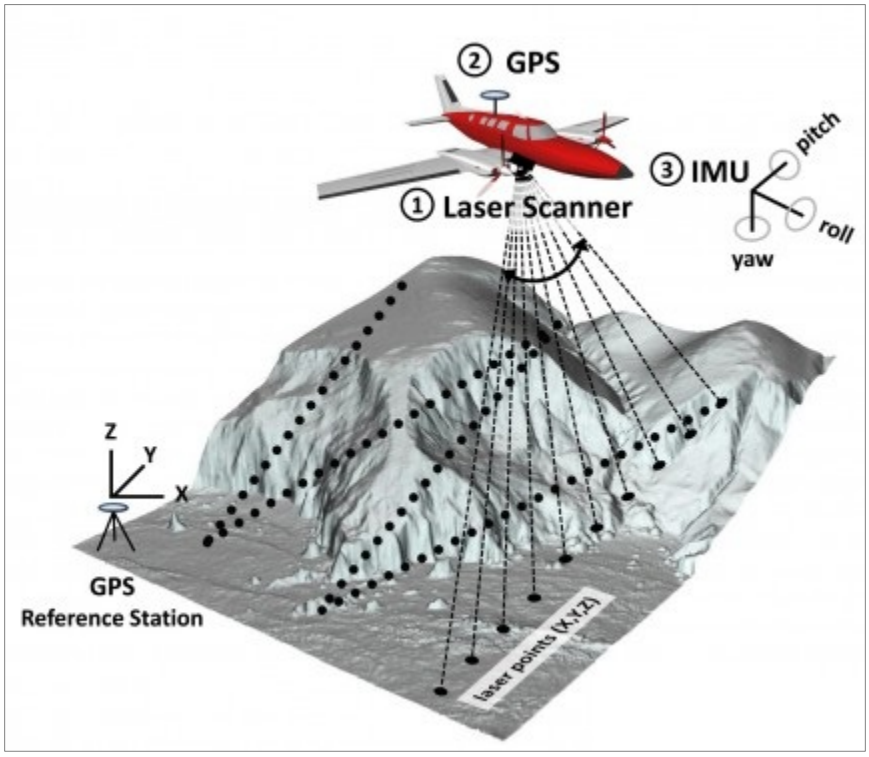

Figure 3. Principle of LiDAR data collection (Source: Höfle, 2010).

There are several advantages of LiDAR over other data capture methods that are worth mentioning, like fast capture of large amounts of elevation data, capture of distinctive detail, direct digital data collection, adequate accuracy and independence of flight conditions as well as able to be used during all seasons (Maune *et al.* 2007). Digital elevation models generated from LiDAR data render higher accuracy and resolution comparing to DEMs created from other sources. As LiDAR-derived DEMs yield better results, their use has been increasing.

There are some disadvantages of LiDAR data acquisition, though. In order to collect the data sophisticated equipment is required, making LiDAR data sets expensive. Another disadvantage is that in order to handle the large data volumes, special software and expertise is needed (Ravibabu and Jain 2008). Maune *et al.* (2007) stated that in order to check LiDAR data, imagery is needed as an additional data set and the contour lines generated from LiDAR data lack smoothness.

2.3 Interpolation methods

Interpolation is the process of predicting values at the locations where there is no recorded observation (Erdogan 2009) or estimating unknown values that fall between known values (Pringle 2010). It is essential to perform accurate interpolation of survey data in order to draw conclusions and accomplish validations (Bell 2012). There are several interpolation methods that can be classified in many ways. A classification framework that is seen in Figure 4 was developed by Lam in 1980.

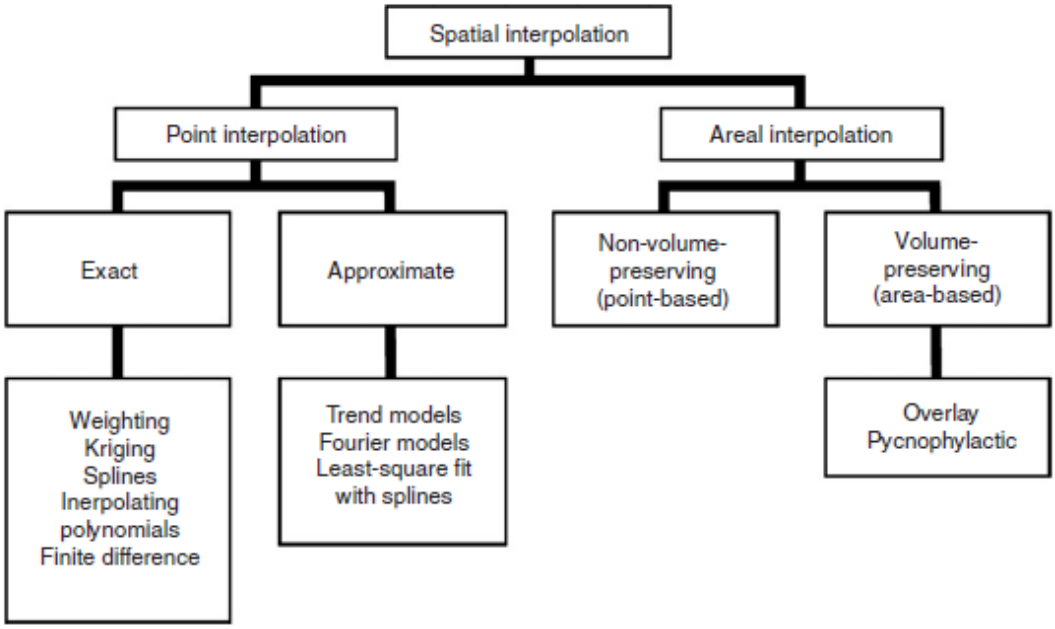

Figure 4. A classification of spatial interpolation methods (Source: Lam 1980).

Interpolation methods can be classified into local and global methods according to the spatial extent. Global methods use all the points in estimating the value of the new point that has no value, whereas local methods use only the nearby points (Erdogan 2009; Lam 2009). Another classification is into exact and approximate interpolators. These two are point interpolators which mean that the data is available at a certain point (like elevation information, temperature readings, etc.). The difference between exact and approximate interpolators is whether they preserve the original sample point values or not. Exact interpolation methods (e.g. Inverse Distance Weighing (IDW), Kriging, Splines) are used when the sample data is of relatively high accuracy, thus preserving the original value at the sample point (Lam 2009). Another way to classify interpolation methods is whether it is a statistic method or not (deterministic and geostatistical methods). For example, Kriging is a statistical interpolation method.

Point interpolation method is used in the thesis where exact interpolators like Inverse Distance Weighing (IDW) Kriging and Splines are employed.

2.3.1 Inverse Distance Weighing (IDW)

The Inverse Distance Weighing (IDW) method is one of the simplest and most commonly used interpolation methods where the value of an unknown point is calculated based on a distance-weighted average of elevation points that are within the neighbourhood. It means that the points closer to the cell have greater influence on the value of the cell than those that are further away.

The main variation of this method is the weighing function. This method has two main disadvantages. One disadvantage is that Inverse Distance Weighing is easily affected by uneven distribution of data points. It means that the same equal weight will be assigned to each of the points even if it is in a cluster of several points. Another disadvantage is that it has a smoothing effect therefore peaks and valleys will be flattened (Lam 2009).

2.3.2 Splines

The spline interpolation method uses a piecewise function where a curve is fit through all the data points. Spline interpolation is considered to work poorly with sample points that are situated close together.

There are two Splines available: the Regularized and the Tension one. The Regularized Spline creates a smooth, gradually changing surface whereas the Tension Spline creates a less smooth surface with values that are kept within the sample data range (Godone and Garnero 2013).

2.3.3 Kriging

Kriging interpolation method is named after D.G. Krige who introduced this method for mining applications in the early 1970s. There are several other variations that have been developed since then, like universal Kriging, block Kriging and co-Kriging (Lam 2009).

Kriging is a geostatistical interpolation method which is the most complex and powerful method and which is based on statistical models that include autocorrelation. Kriging is similar to IDW in that it weights the surrounding known values to obtain unknown values. Kriging analyses all the data in order to find the autocorrelation (Racoviteanu *et al*. 2007; Daix 2008; ESRI 2009c).

Kriging has several advantages over Inverse Distance Weighing method although it is a distance weighing method as well. Kriging uses semivariogram which measures the average degree of dissimilarity between unsampled values and the values that are close by. The more the sample points, the more accurate the empirically derived variogram function, thus rendering more accurate estimates. Another advantage is that Kriging provides an error estimate and confidence interval for each unknown point (Erdogan 2009; Lam 2009).

According to Lam (2009) Kriging performs best with a large number of sample points and it will still return more accurate estimates than distance weighting methods even with a smaller number of data points. Kriging is considered to be the preferred point interpolation method over other point interpolation methods (Lam 2009).

2.3.4 ANUDEM (TOPO to raster)

ANUDEM is an interpolation method that is specially designed for the creation of hydrologically correct digital elevation models from various data sources including contour lines, point elevations, streams, lakes, sinks and boundaries. ANUDEM stands for “Australian National University Digital Elevation Model” and was developed by Michael Hutchinson of the Centre for Resource and Environmental Studies at the Australian National University. This method is based on an efficient and accurate underlying interpolation procedure that simultaneously ensures a connected and downward flowing drainage structure by automatically removing artificial and

unidentified sinks, thus maintaining a realistic drainage network (Lawrence *et al.* 2008; Bater and Coops 2009).

2.3.5 TIN grid

Triangular Irregular Network (TIN) is a vector approach of handling a digital elevation model. TINs are used to interpolate surfaces using multiple triangles. Elevation points are connected to form a set of continuous and connected triangles. TIN takes the data points and triangulates them using the Delaunay triangulation method. The value of the interpolated point is calculated using linear interpolation which is done by calculating the plane equation that passes through the three vertices (Hugentobler 2004).

TIN offers a choice whether contour lines should be triangulated as hard or soft lines. Hard and soft qualifiers for lines are used to indicate whether a distinct break in slope occurs on the surface at their location. A hard line is a distinct break in slope, while a soft line will be represented on the surface as a more gradual change in slope (ESRI 2012). Figure 5 shows the difference in interpolation result when using soft or hard break lines or no break lines at all.

	No break lines	Soft break lines	Hard break lines
The Data	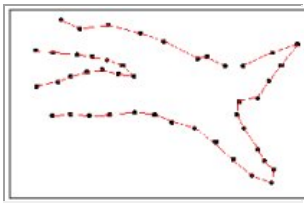	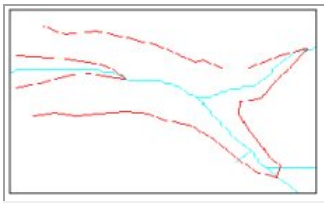	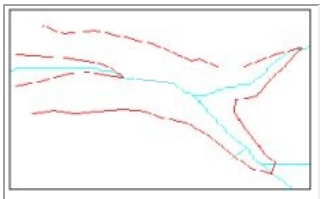
The Triangulation	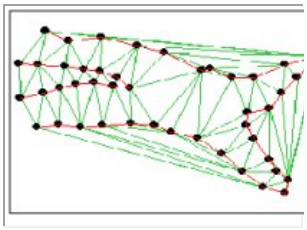	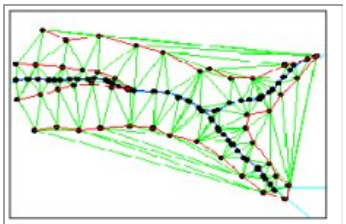	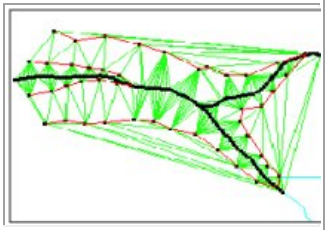
The Surface	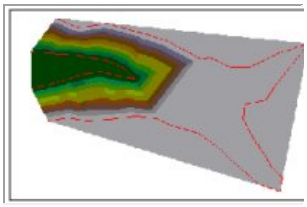	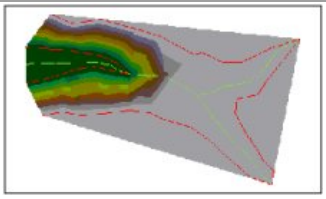	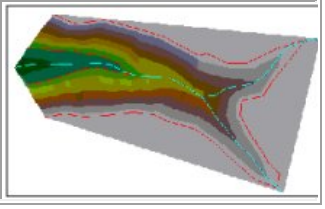

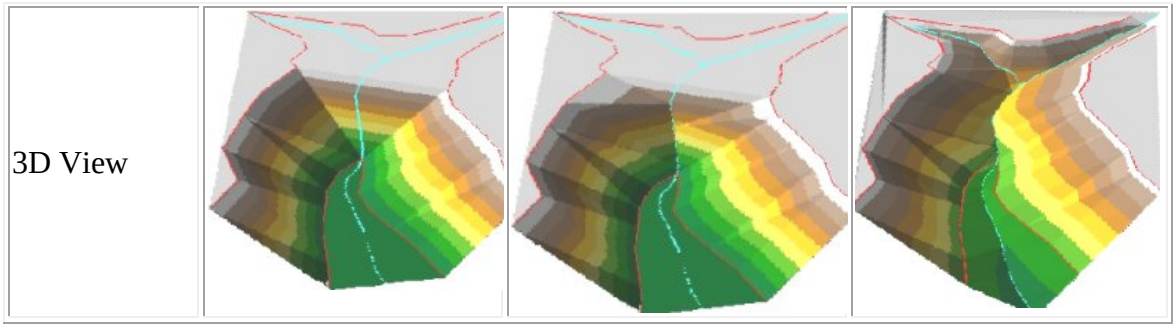

Figure 5. Difference between soft and hard break lines in TIN triangulation (Source: ET Spatial Techniques 2004b).

2.3.6 Natural neighbour interpolation

Natural Neighbour (NN) interpolation is one of the most general methods of interpolation. It is a local interpolation method that uses only a subset of samples that surround the point of interest. The interpolated heights will definitely be within the range of the samples used. It will not produce any peaks or pits (ESRI 2009b).

Natural neighbour interpolation uses a Triangular Irregular Network (TIN) to identify nearby points and Voronoi (Thiessen) polygons to determine the influence or weighting of each point (Bater and Coops 2009).

2.4 Digital elevation models and their application in glacier change analyses

Digital Elevation Model (DEM) is the general term for digital topographic and bathymetric data, in all its various forms. It is called "model" not only because computers can use such data to model and automatically analyse the earth's topography in 3-dimensions (Maune *et al.* 2007) but also because it is only a representation of the surface.

Digital Elevation Models have been used in many applications since the late 1950s. It is a valuable tool for applications that are concerned with the Earth's surface such as

glaciology, hydrology, geology, cartography, geomorphology, engineering applications, landscape architecture and other applications (Erdogan 2009).

DEM is a useful tool in glaciology to monitor the spatial and temporal change of glacier surfaces, thus assessing glacier response to climate change. The advantage of a DEM lies in the fact that large areas can be modelled and analysed with only minimal field-based input. However, glacier surface change that has been derived from remote sensing does not provide the user with detailed information that direct methods would provide (Pope *et al*. 2007).

DEM subtractions are a frequent application in glaciology in order to estimate glacier volume changes. DEM applications are also used to model glacier mass movements and ice thickness distribution of glaciers as well as to predict glacier evolution in the future (Frey 2011).

2.4.1 Definitions

There are three types of terrain models: Digital Elevation Models (DEM), Digital Terrain Models (DTM) and Digital Surface Models (DSM). These models are digital three dimensional representations of the surface of the terrain. Digital Surface Models depict the terrain including all the objects that that are elevated above the ground (e.g. buildings and other man-made objects, trees, plants, vegetation, etc.) whereas Digital Terrain Models and Digital Elevation Models depict bare earth without any objects. In some countries DTMs are synonymous with DEMs. Although DTMs are similar to DEMs, DTMs frequently incorporate the elevation of significant topographic features on the land as well as mass points and breaklines, thus depicting the true shape of the bare earth terrain better and the distinctive terrain features are more clearly defined and precisely located. DTMs are technically superior to DEMs for many applications (Maune *et al.* 2007).

A DTM may be also used as a digital model of any single valued surface, like information on geology, air temperature or pressure, population density, the amount of precipitation, the level of pollution, soil type, etc. (Droj 2000).

2.4.2 Benefits and drawbacks of DEMs

DEMs are easy to compute and can be easily used in a GIS environment. A number of other terrain-related data sets can be derived from digital elevation models, like slope, aspect, curvature, flow direction and wetness index (Carlisle 2002). DEMs have a uniform spatial structure where almost all properties are defined by a single characteristic – a cell size (Hengl and Evans 2009). Another advantage of DEM data sets is that it is possible to perform statistical and spatial analyses as well as creating pseudo images (like shaded relief images) that can help visualize the data (Maune *et al.* 2007).

On the other hand, the use of DEMs can have disadvantages as well. There might be a high level of data redundancy in areas of a similar terrain, thus a smooth topography can get over-sampled (Carlisle 2002; Hengl and Evans 2009). Another issue is that digital elevation models are subject to errors of data source and processing. The data source should be of high quality in order to obtain high quality DEMs. The same refers to data processing as the quality of a DEM is dependent on the choice of interpolation method as well as cell size.

2.4.3 Creation of DEMs from contour lines / elevation points

Contour lines are isolines that connect points of equal elevation (Maune *et al.* 2007). Thus elevation in topographic maps is represented by contour lines and spot heights. There are four factors that can affect the accuracy of point interpolation estimates when the grid approach is applied. Firstly, the result is influenced by the cell size. However, there is no general rule on how small or large the grid cell size should be. Secondly, the result is affected by the number of data points. There is an assumption that a larger amount of

points render a more accurate result. However, that is not always true, as some points can exhibit more information (e.g., peaks, pits) than others. Thirdly, the spatial distribution of data points has an effect on the outcome. Sample points that are more evenly spread out can contribute more information than sample points that are clustered. Finally, the interpolation method itself can seriously affect the accuracy of the estimates (Lam 2009).

Spatial under-sampling and a generalization of topography are the biggest problems in DEMs that are generated from contour lines according to Reuter *et al*. (2009). Contour lines show different density in different parts of the study area and such data is very sensitive to interpolation algorithms that can lead to errors in the resulting DEM. The most common errors are terraces that are formed in between two contour lines (Reuter *et al*. 2009).

According to Maune *et al.* (2007) contour lines are not considered to be a good input data set to an interpolator due to the fact that there are a large amount of sample points along the contour line and hardly any sample points between the contour lines. Therefore the DEMs generated from contour lines are often biased to the values of the contour lines. That can lead to a terraced surface or an abrupt change in elevation can be noticed (Maune *et al.* 2007).

The interpolated DEM is only an estimate and should not be considered to be reality, where every terrain surface is unique. Reasonable approximations of terrain surface can be achieved by using interpolation techniques however no interpolation method will render superior results in all cases (Carlisle 2002).

2.5 Assessment of DEM quality

DEMs have become an important tool in many applications - including in glaciology, therefore it is important to assess their accuracy. Otherwise, using DEMs can lead to inaccurate results (Aguiler et al. 2006).

It is important to keep in mind that the DEM is usually the end product of several modelling and processing steps each of them adding error to the overall error of the result (Fisher and Tate 2006). Borisov et al. (2009) and Fisher and Tate (2006) have shown these steps in a graphical way depicted in Figures 6 and 7.

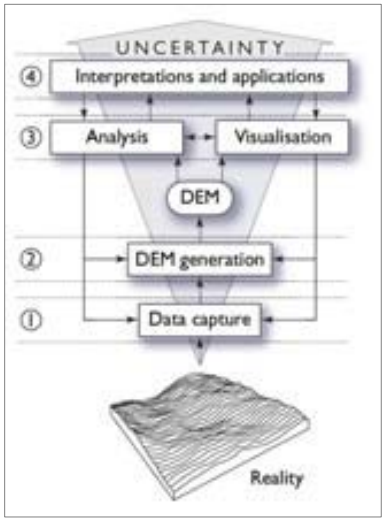

Figure 6. Phases in which uncertainty is introduced (Source: Borisov et al. 2009).

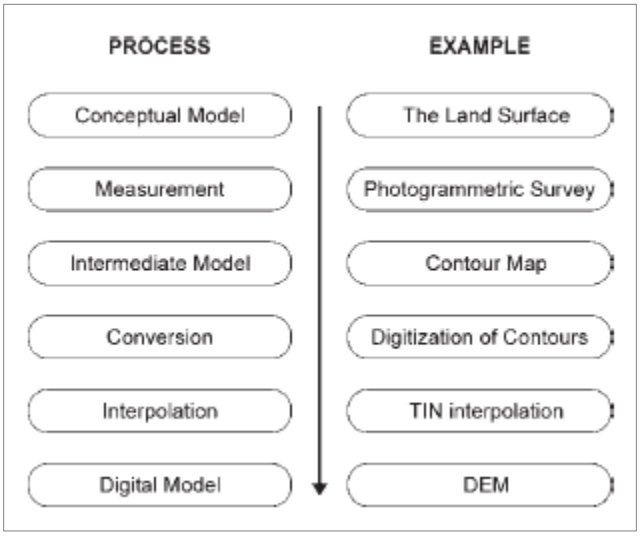

Figure 7. A flow chart showing the steps of DEM acquirement (Source: Fisher and Tate 2006).

DEM quality assessment can be absolute or relative. Absolute methods are carried out by comparing the elevation difference between a reference DEM and the DEM that needs to be validated. The whole data set is used on a pixel-by-pixel basis. Relative assessment methods are based on sample points, either obtained from field surveys or extracted from a more accurate reference data set. Two results are rendered when using an absolute assessment – the statistical measures as well as an error map showing the error variation in the entire area (Kyarizu 2005). Relative accuracy is a measure of just random errors whereas absolute accuracy accounts for the combined effects of systematic and random errors. Relative vertical accuracy is especially important for DEM derivatives like slope and aspect (Maune *et al.* 2007).

There are three approaches in assessing DEM quality: visual assessment, geomorphometric characterization and empirical approach (Wood 1996; Carlisle 2002; Kyarizu 2005).

2.5.1 Visual Assessment

Visual assessment is done by inspecting the visual appearance of a DEM and DEM derivatives. Visualization helps identify the pattern, spatial distribution and possible causes of DEM errors especially in cases where no ground truth or higher accuracy validation data are available (Kyarizu 2005). In order to understand spatial data in general as well as to assess the data quality visually, there are several visualization techniques available. Although visualization is a subjective and qualitative approach to quality assessment which is heavily dependent on how the user decides to visualize a DEM, it is an effective way of understanding spatial data (Wood 1996; Carlisle 2002). Fisher and Tate (2006) state that visualization is one of the most diagnostic methods for investigating errors. The advantage of visual analysis is that the user can apply various rendering techniques like 3D view, orthographic display as well as the use of exaggeration factors to better view the terrain (Kyaruzi 2005).

2.5.1.1 Orthographic display

Another approach of visual assessment is orthographic display. By an orthographic display, sometimes referred to as pseudo 3D projection, additional topographic information can be revealed. The DEM surface can be viewed obliquely and in perspective (Wood 1996). Wood (1996) suggested a “fishnet” approach. By using the 3D projection another data set can be draped over the surface and coloured, thus displaying more information (Wood 1996). For example, orthophotographs can be draped over the surface to make a visual sense of images (Wood 1996; Carlisle 2002). Figure 8 shows orthographic displays of the Jostefonn glacier: a) fishnet display and b) fishnet display with orthophotos.

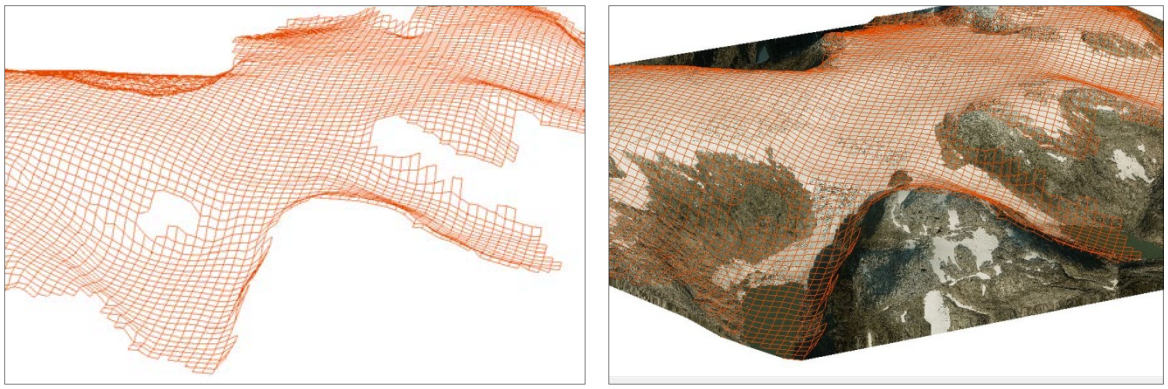

(a) (b)

Figure 8. Ortographic displays, (a) fishnet display, (b) fishnet display with ortophotos. Source: Own elaboration

2.5.2 DEM derivatives

Geomorphometry is an approach to characterize the landform. There are several parameters that can be derived from a DEM including slope, aspect, hillshade and curvature (Wang *et al.* 2010).

Slope represents the rate of change of elevation for each cell of a DEM, either as a per cent rise or in degrees. By deriving the slope it is possible to determine how steep or flat the terrain is. The lower the slope value, the flatter the terrain and the higher the slope value, the steeper the terrain (Maune *et al.* 2007).

An aspect map shows the direction to which side a slope is orientated. Aspect is calculated in degrees where 0 degrees represents north direction, 90 degrees – east, 180 degrees – south and 270 degrees – west. The value of each location in an aspect data set indicates the direction to which the surface slope faces (Maune *et al.* 2007).

Hillshading is often used to better visualize topography by simulating illumination of the surface. A hypothetical light source is used to calculate the illumination and shadow values for each raster cell. The default azimuth (horizontal angle of the light source) and

altitude (vertical angle of the light source) values of the artificial light source are 315 and 45 degrees respectively (Findlay 2005; ESRI 2011d). A hillshade map helps distinguish between valleys, peaks and ridges. A hillshade map is usually used as a background layer to enhance the topographic relief of the landscape and is a very common cartographic technique.

Three different curvature raster data sets can be created – an output curvature raster, an optional profile curve raster, and an optional plan curve raster. The Curvature extension from Jenness Enterprises DEM Surface Tools offers options to calculate even seven types of landscape curvature including the already mentioned curvature raster data sets as well as others like Tangential Curvature and Total Curvature (Jenness 2013). Profile curvature is parallel to the direction of the maximum slope. Plan curvature is perpendicular to the direction of the maximum slope. Both plan and profile curvature together allows a more accurate understanding of the flow across a surface (ESRI 2010).

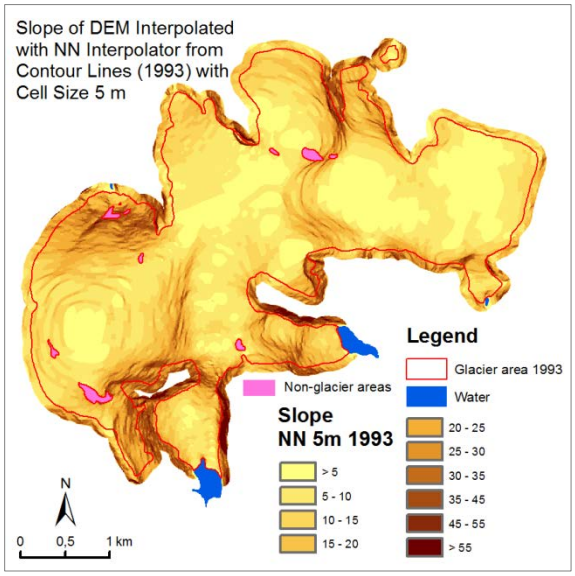

(a)

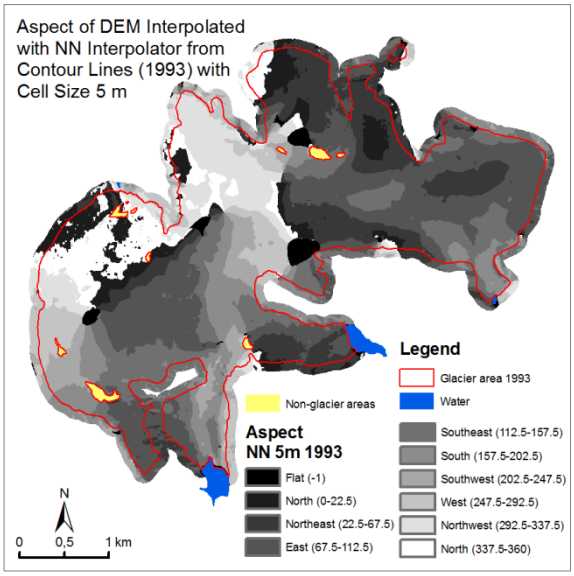

(b)

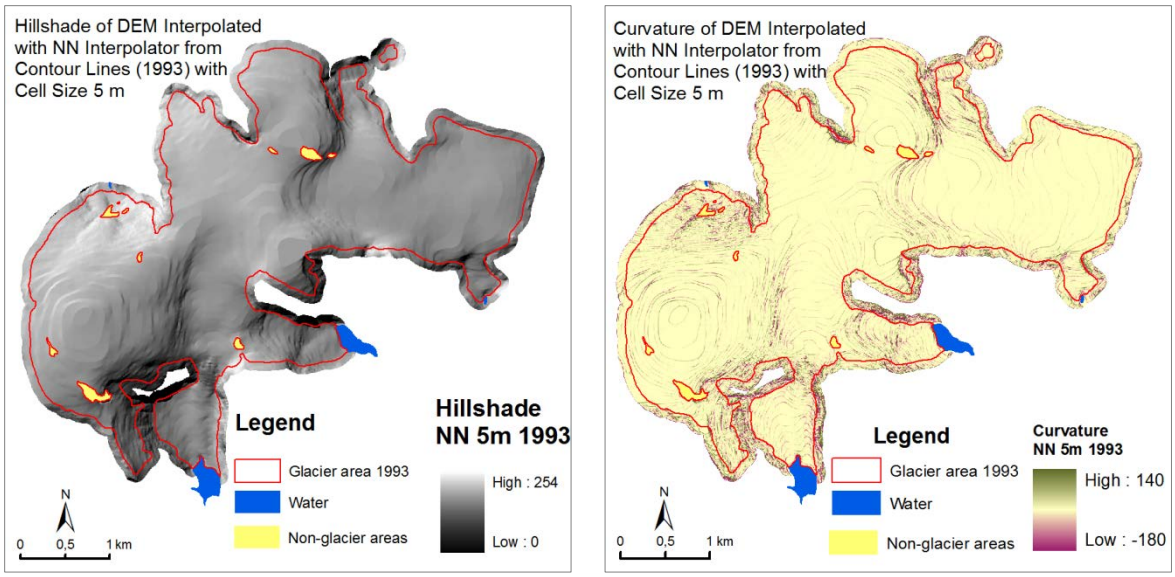

(c) (d)

Figure 9. DEM derivatives: (a) slope, (b) aspect, (c) hillshade, (d) curvature.
Source: Own elaboration
Coordinate System: WGS 1984 UTM Zone 32N

Figure 9 shows slope, aspect, hillshade and curvatuve maps derived from the DEM that was created using natural neighbour interpolator with a resolution of 5m.

According to Fisher and Tate (2006) the most diagnostic visualization methods rely on either summary graphs or mapping DEM derivatives like slope and shaded relief. Such visualization methods are effective for detecting systematic errors like terracing in DEMs generated from contour lines. Terracing can be detected by inspecting histograms where spikes of high frequency are observed (Fig.10a). The same terracing error can be detected in slope maps (Fig.10b) where steep slopes will be noticed due to relatively sudden changes from one contour value to another (Fisher and Tate 2006; Maune *et al.* 2007).

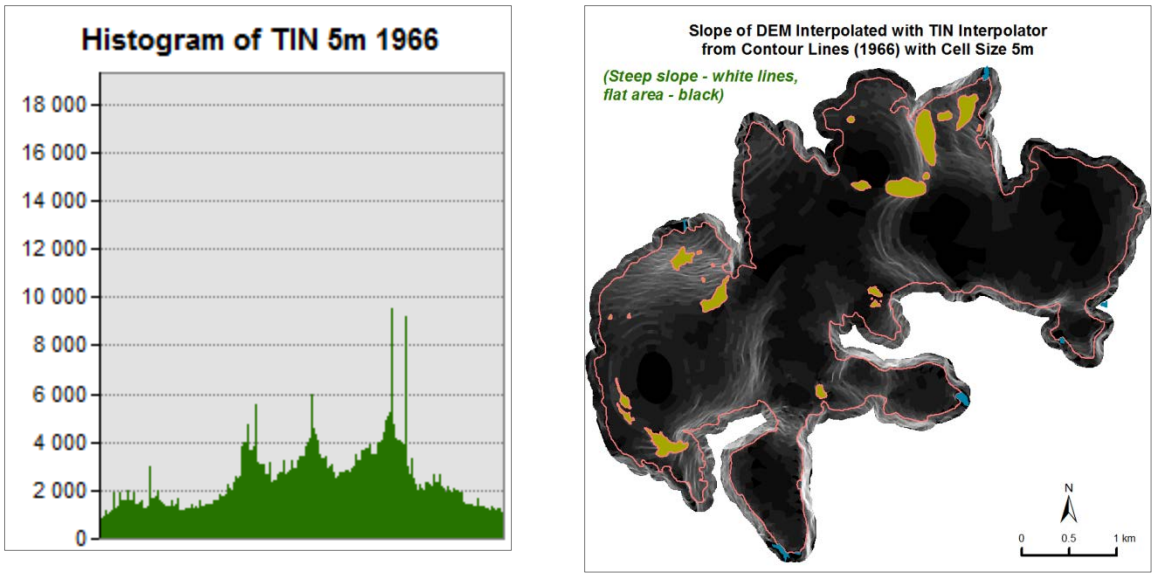

a) b)

Figure 10. Histogram showing cyclic peaks indicating overrepresentation at the contour lines (a) and a slope map showing steep slopes at contour positions (very steep slopes – white lines) (b). DEM interpolated with TIN interpolator from contour lines (1966) with cell size 5m.
Source: Own elaboration
Coordinate System: WGS 1984 UTM Zone 32N

2.5.3 Empirical approach

The accuracy of any DEM can be obtained by comparing it with measurements made to a known higher order of accuracy. There are statistical methods that help determine the accuracy of a DEM in comparison to a reference DEM. Quality control statistics like the Root Mean Square Error (RMSE) is often used in the validation of vertical accuracy (Sharma *et al*. 2009; Balan and Mather 2010; Hirt *et al*. 2010).

The empirical approach depends on validation data sets, either reference DEM or ground truth points, in order to calculate statistical quality measures. According to D'Agata and Zanutta (2007), a measure of DEM quality is the Root Mean Square Error (RMSE) between the true elevation and the DEM value. The RMSE is affected by several

parameters, such as the accuracy of the source data, the characteristics of the terrain surface or the, method for DEM surface generation (D'Agata and Zanutta 2007).

2.5.3.1 Accuracy measures

According to Congalton and Green (1999) there are two types of map accuracy assessment: positional and thematic. Positional accuracy deals with the accuracy of the location of map features and measures how far a spatial feature on a map is from its true or reference location on the ground whereas thematic accuracy deals with the attributes of the features of a map and measures whether the mapped feature attributes are different from the true feature attribute (Congalton and Green 1999).

One of the most commonly used methods to evaluate accuracy in a DEM is to determine the Root Mean Square Error (RMSE). RMSE is the standard deviation of the difference between the elevations and the corresponding pixel elevation on the DEM (Carlisle 2005; Aguilar *et al*. 2006; Bates 2007; Ziadat 2007). The RMSE is defined in Equation 1. The RMSE is a statistical method that is based on the assumption of a Gaussian distribution with zero mean error, and therefore there is no systematic bias in the DEM (Barringer and Lilburne 1997; Sharma *et al.* 2009).

$$RMSE = \sqrt{\frac{\sum(h_i - h_t)^2}{n}} \quad (1)$$

where h_i is the interpolated DEM elevation of a test point, h_t is the true value of the test point and n is number of test points.

"The mean root square of the square of the differences is used instead of the mean of the simple arithmetic differences to compensate for the fact that the errors can have positive and negative values. An alternative estimator that would also deal with negative values would be to take the absolute value of the arithmetic mean of the errors." (Congalton and Green 1999).

The RMSE is a global spatial measure and therefore local spatial characteristics are not assessed. The RMSE gives the user information on the accuracy of the interpolation approach (Bell 2012).

The mean error (ME) is used for determining the degree of bias in the estimates and it is calculated with the following equation:

$$ME = \frac{\sum(h_i - h_t)}{n} \quad (2)$$

The mean absolute error (MAE) is the average absolute difference between the values in reference data set and the values in the obtained DEM.

$$MAE = \frac{\sum|h_i - h_t|}{n} \quad (3)$$

Höhle and Potuckova (2011) have presented a table of the accuracy measures (Table 1) for the assessment of the vertical accuracy for both a normal distribution of vertical errors and a distribution that is not normal.

Table 1. Accuracy measures for DEM presenting a normal distribution of vertical errors (Source: Höhle and Potuckova 2011).

Difference from reference data	Δh
Number of tested points	n
Root Mean Square Error	$RMSE = \sqrt{\frac{\sum (\Delta h)^2}{n}}$
Maximum difference	$\lvert \Delta h_{max} \rvert$
Definition of a blunder (threshold)	S > 3* RMSE
Number of blunders	N
Number of points without blunders	$n' = n - N$
Mean	$\mu = \frac{\sum \Delta h}{n'}$
Standard deviation	$\sigma = \sqrt{\frac{\sum (\Delta h - \mu)^2}{(n'-1)}}$

Table 2. Robust accuracy measures for vertical errors of DEM (Source: Höhle and Potuckova 2011).

accuracy measure	error type	notational expression
Median (50% quantile)	Δh	$\hat{Q}_{\Delta h}(0.50) = m_{\Delta h}$
Normalized Median Absolute Deviation	Δh	$NMAD = 1.4826 \cdot median_j(\lvert \Delta h_j - m_{\Delta h} \rvert)$
68.3% quantile	|Δh|	$\hat{Q}_{\lvert \Delta h \rvert}(0.683)$
95% quantile	|Δh|	$\hat{Q}_{\lvert \Delta h \rvert}(0.95)$

The Median (m) (Table 2) is the middle value if all errors are put in an order starting with the lowest value to the highest value. The Normalized Median Absolute Deviation (NMAD) estimates the scale of the error distribution and corresponds to the standard

deviation if there are no outliers. The 95% quantile (Q) means that 95% of the absolute errors have a magnitude within the interval from 0 to 0.95. 68.3% quantile indicates the value where all differences smaller than this value amount to 68.3% of all errors (Höhle and Potuckova 2011).

Höhle and Potuckova (2011) suggest the procedure for the determination of the DEM accuracy measures depicted in Figure 11.

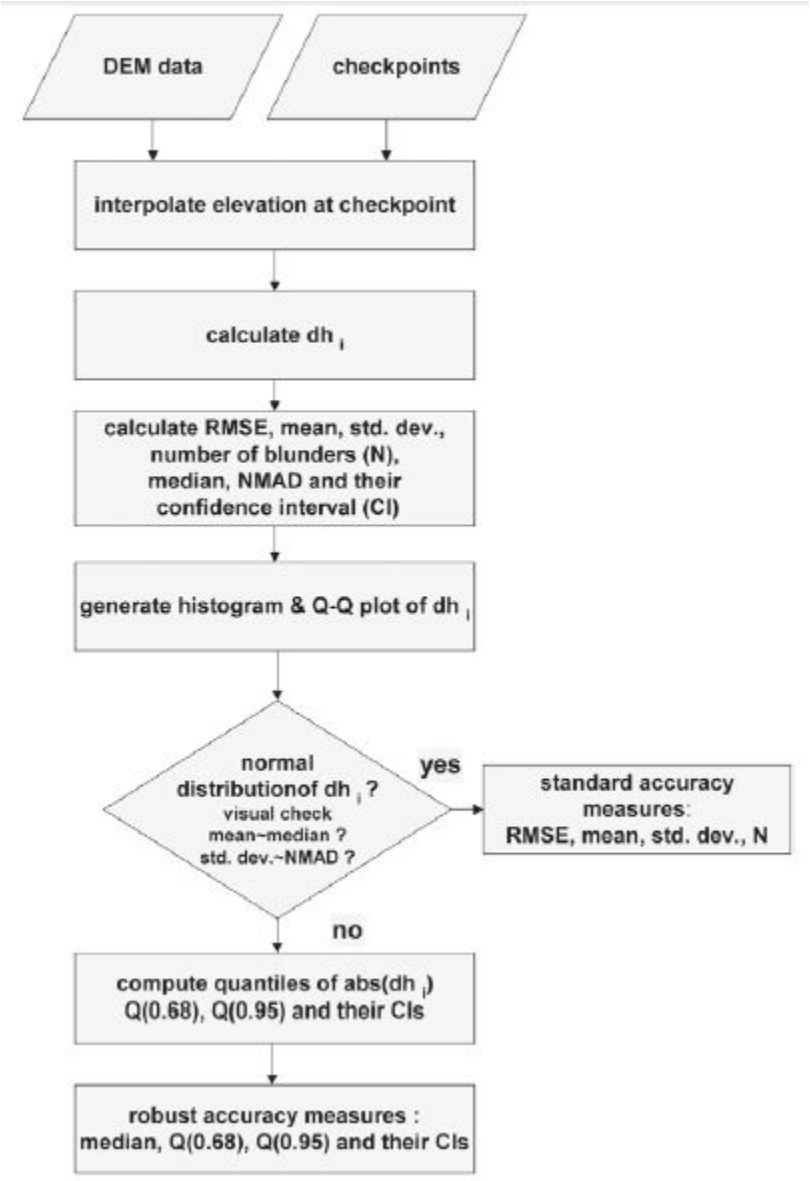

Figure 11. Suggested procedure for the determination of DEM accuracy measures (Source: Höhle and Potuckova 2011).

2.5.4 Errors in DEMs

According to Maune *et al.* (2007) accuracy of a single measured elevation point is defined as the closeness of its estimated elevation to a standard or accepted correct value. No DEM is completely accurate, with each one having its limitations based on production methods as well as taking into consideration the data set each DEM has been derived from. Wechsler (2003) pointed out several sources of possible error in DEMs mentioning data age, errors of spatial sampling, data measurement errors as well as data entry mistakes. Interpolation errors are also mentioned in this list (Wechsler 2003). The accuracy of digital elevation models is one of the factors that influence the overall quality of a data set. Accuracy is defined as the difference between a value in the data set and the corresponding true value (Ravidabu and Jain 2008).

There are several types of errors mentioned in Maune *et al.* (2007) – random errors, systematic errors and blunders. The errors that are measured in accuracy calculations are referred to as random errors that are produced by irregular causes. Systematic errors follow some fixed pattern and are usually the result of data capture procedures and systems. Systematic errors are predictable while random errors are not. A blunder is an error of major proportion that is usually identified and removed in the editing or processing stage. A potential blunder may be identified as any error that is more than three times the standard deviation of the error (Maune *et al*. 2007).

Errors in a DEM can be observed in elevation or vertical (Z) coordinates as well as planimetric or horizontal (XY) coordinates, but the focus is usually on the vertical coordinates as planimetric error will also produce elevation error (Fisher and Tate 2006). Vertical accuracy is the main criterion in assessing the quality of digital elevation data (Maune *et.al.* 2007). Elevation (vertical coordinate Z) is also the main coordinate of interest in glaciological applications because changes in surface elevation over time can be an indicator of mass balance changes (Etzelmüller 2000).

According to Maune *et al.* (2007), 90% of elevation points should have a maximum error of one-half of the contour interval and the remaining 10% of elevation points should have an error less than one contour interval.

2.6 Comparison of DEM quality

The quality of a DEM can be compared using different techniques. Visual assessment of the quality of a DEM is performed by visual means giving the first perception of the data. There are also absolute and relative assessments where the data of interest are compared to a data set of a higher accuracy, either performing the comparison on a cell-by-cell basis or by employing a test data points. Statistical accuracy measures with their corresponding graphs are used to characterize the difference between the DEM that has been tested with the reference data set.

2.7 Causes of reduced quality

The quality of a DEM is a result of several individual factors according to Erdogan (2009). He has grouped these factors into three classes: the accuracy of the source data, the interpolation process and the characteristics of the surface (Erdogan 2009).

2.7.1 Quality of data sources

The accuracy of data sources is dependent on the techniques used in order to gather the data. Map digitization, active airborne sensors, airborne laser scanning techniques, photogrammetric methods as well as field surveying are the techniques worth mentioning (Erdogan, 2009).

Table 3 shows a comparison of various DEM acquisition methods and the accuracy of the data they render as well as the speed, cost and application domain. Table 4 gives comparison of the accuracy of DEM data obtained by different techniques.

Table 3. A comparison of various DEM acquisition methods (Source: Li *et al.* 2005).

Acquisition Method	Accuracy of Data	Speed	Cost	Application Domain
Traditional surveying	High (cm–m)	Very slow	Very high	Small areas
GPS survey	Relatively high (cm–m)	Slow	Relatively high	Small areas
Photogrammetry	Medium to high (cm–m)	Fast	Relatively low	Medium to large areas
Space photogrammetry	Low to medium (m)	Very fast	Low	Large areas
InSAR	Low (m)	Very fast	Low	Large areas
Radargrammetry	Very low (10 m)	Very fast	Low	Large areas
LIDAR	High (cm)	Fast	High	Medium to large areas
Map digitization	Relatively low (m)	Slow	High	Any area size
Map scanning	Relatively low (m)	Fast	Low	Any area size

Table 4. Comparison of the accuracy of DEM data obtained by different techniques (Source: Li *et al.* 2005).

Methods of Data Acquisition	Accuracy of Data
Ground measurement (including GPS)	1–10 cm
Digitized contour data	About 1/3 of contouring interval
Laser altimetry	0.5–2 m
Radargrammetry	10–100 m
Aerial photogrammetry	0.1–1 m
SAR interfereometry	5–20 m

2.7.1.1 Ground survey sources

Ground survey of elevation data is performed by the actual measurement of elevation in the field (Ravibabu and Jain 2008). Although ground survey techniques render high quality data, they are time-consuming and expensive. There can be limited accessibility in mountainous terrain which is the case in this glacier study. GPS equipment is considered to be more practical in such areas of limited access being cheaper and more portable than other traditional surveying equipment. However, GPS equipment has its own limitations, such as inaccessibility, the trade off between portability and accuracy and between speed and accuracy as well as poor satellite visibility (Ravibabu and Jain 2008).

2.7.1.2 Photogrammetric sources

Photogrammetry provides the most frequently used data sources and techniques for generating DEMs. Although photogrammetric sources have several advantages, especially in areas that are difficult to access, they also have a number of problems. One of the drawbacks is constant cloud or lengthy snow covers, which limits the acquisition of good and clear aerial photographs. Areas of high relief mountain topology can affect the quality of aerial photographs having areas that are shaded or obscured from view. These problems can lead to data with lower accuracy (Ravibabu and Jain 2008).

Scale and resolution of the aerial photography as well as the flying height influence the accuracy of the data captured by photogrammetric techniques (Ravibabu and Jain 2008).

2.7.1.3 Cartographic sources

The available equipment, map distortion as well as operator or machine error influence the accuracy of cartographic sources. The operator or machine error is of great significance as these errors are difficult to quantify and these undetected errors should be taken into consideration when assessing the quality of a DEM generated from cartographic sources (Ravibabu and Jain 2008).

2.7.2 Quality of interpolation

Another factor that affects the accuracy of a DEM is the interpolation method that is used to generate DEMs. There are many interpolation algorithms but there is no single interpolation method that is considered to be the best and most suitable (Erdogan, 2009). Each study case is unique and the researcher should test and find out which interpolation method suits best for the particular research project. “The crucial point is that since different methods of interpolation produce different estimates for height values at the same point, these methods will also produce different quantities of error in the DEM.” (Fisher and Tate 2006). There are a number of studies (see Discussion 6.2) that have

tested several interpolation methods, each of them concluding that one method has proved to be superior over others. If the majority of the studies have proved that one exact interpolation method has rendered the best results, that method will most probably show good results in other studies too.

2.7.2.1 Contour line and point interpolation

The accuracy of the contour lines is dependent on the quality and scale of the aerial photographs from which they are derived, as well as on the characteristics of the photogrammetric device and on the skill of the operator (Carrara *et al.* 2010). Nearly all interpolation methods tested in the current project have elevation points as the input data set (except TIN and ANUDEM). The result of interpolation is affected by the contour line interval. If the contour interval is large, the elevation points used in the interpolation process will be clustered along the contour lines, having no points in between the contour lines, thus decreasing the quality of the output DEM.

2.7.2.2 Different interpolation methods

There is a variety of interpolation methods that can be used in order to generate a digital elevation model. Jin Li and Heap (2011) who present a review on comparative studies of spatial interpolation methods, have stated that there are many factors that affect the performance of the methods but there are no consistent findings about their effects. They have looked at 53 comparative studies where the performance of 72 methods / sub-methods have been analysed. They also have mentioned that spatial interpolation methods are developed for specific data types or a specific variable and are used in at least ten fields that employ geostatistics (Li and Heap 2011).

3. Study area and data

3.1 Study area

Jostefonn glacier is situated in Sogn og Fjordane county, Norway and covers an area of 10.5 km^2 (Andreassen *et al.* 2012) (Figs 12 and 13). Jostefonn is a plateau glacier located approximately 10 km west of Fjærland and about 10 km southwest of Jostedalsbreen glacier which is the largest glacier in continental Europe (Andreassen 1998). Jostefonn glacier is considered to be the thirtieth largest glacier in Norway (Andreassen *et al.* 2012). Mass balance investigations were carried out at Jostefonn in 1996-2000 by the Norwegian Water Resources and Energy Directorate. Detailed map surveys were accomplished in 1966, 1993 and 2011 (Andreassen *et al.* 2012). Volume change analysis between 1966 and 1993 was performed by L.M.Andreassen (1998).

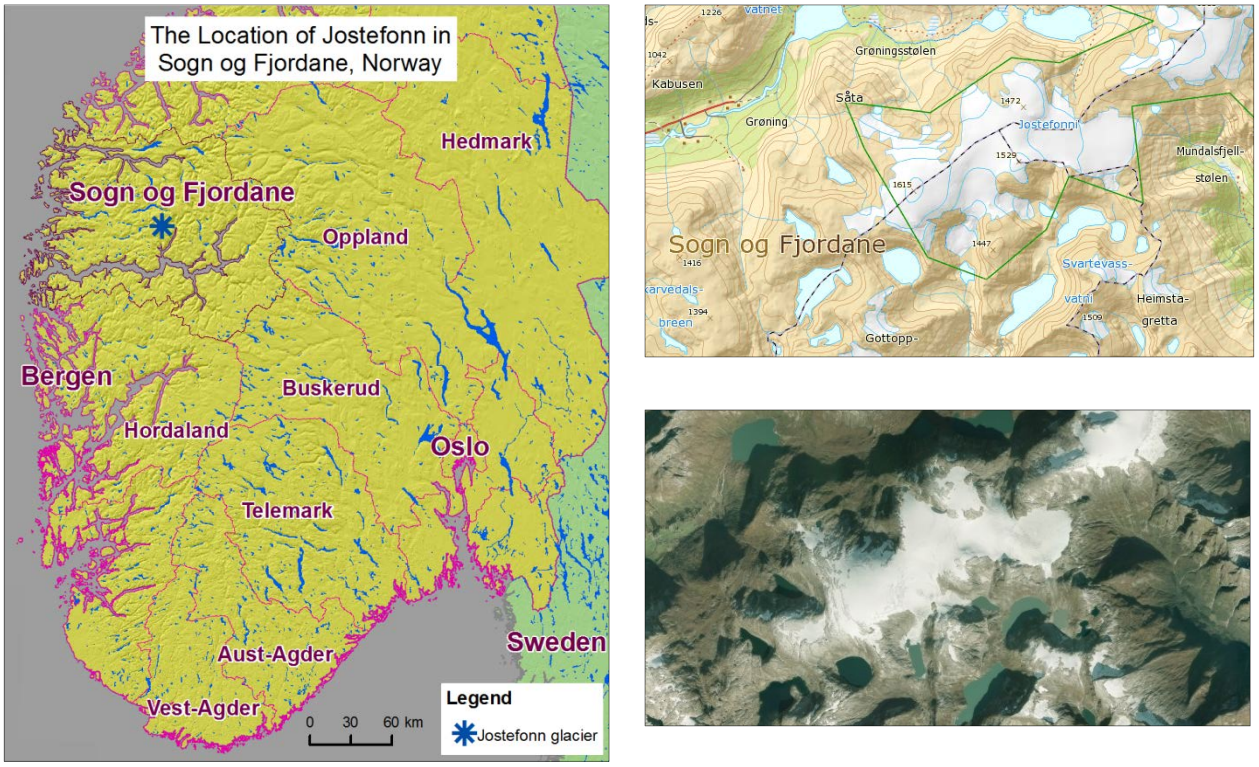

Figure 12. Maps showing the study area – the location of Jostefonn glacier.
Source: Own elaboration, data acquired 24 July, 2013 from DIVA-GIS (http://www.diva-gis.org), DEM Explorer (http://ws.csiss.gmu.edu/DEMExplorer/), Norge i bilder (http://norgeibilder.no/), Norgeskart (http://www.norgeskart.no).

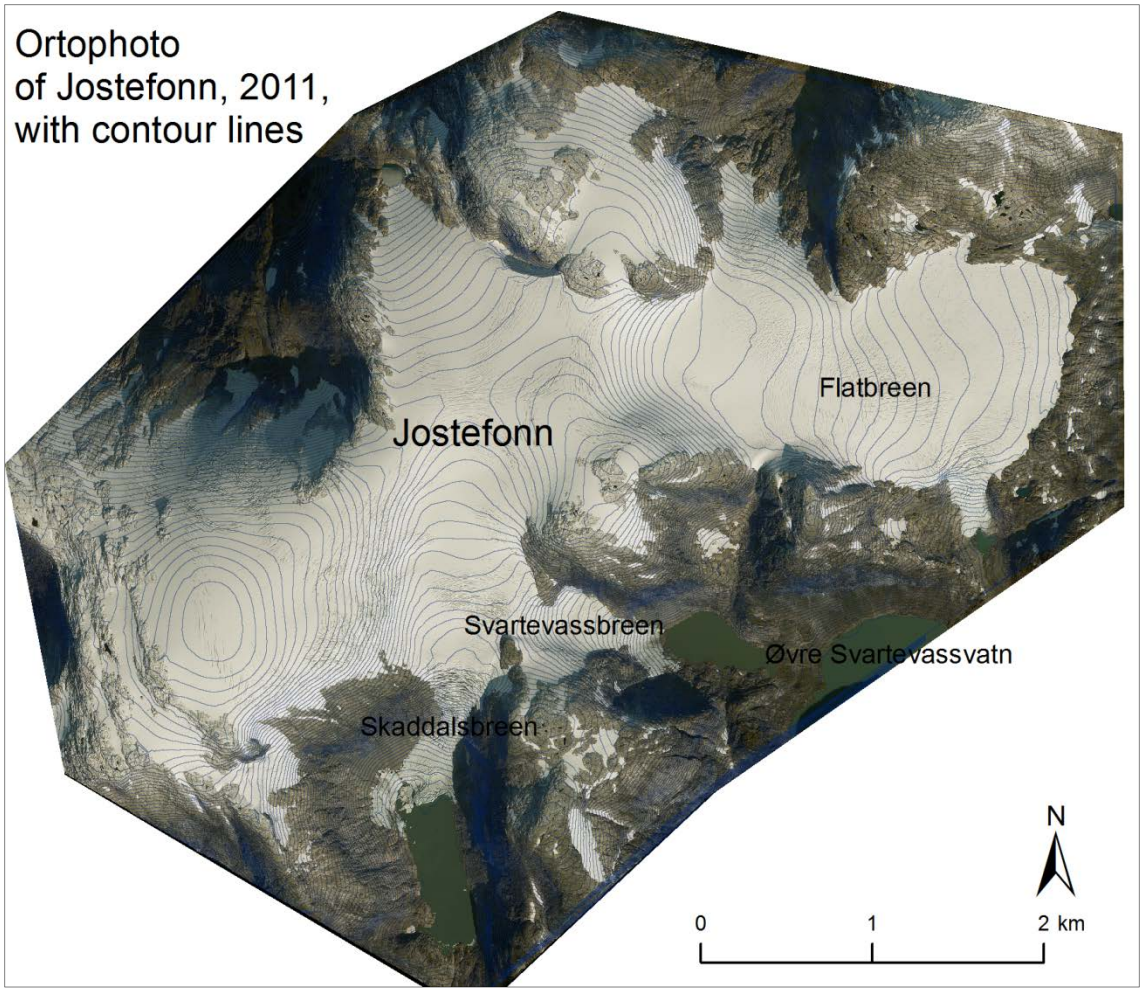

Figure 13. Maps showing the study area – the location of Jostefonn glacier.
Source: Own elaboration, data used - Ortophoto (NVE).

3.2 Data

Contour lines derived from aerial photographs and LiDAR data were used in order to generate DEMs for the area of interest. The available data for this study are shown in Table 5 and Figure 14.

Table 5. An overview of the available data for the study. Data provided by NVE.

Map				Photos				
Year	**Method**	**Scale**	**Contour interval (m)**	**Contract no.**	**Date**	**Flight hight**	**Scale**	**Remarks**
1966	Analogue photogrammetry (vertical aerial photos)	1:10 000	10	Widerøe Flyveselskap A/S 1833	21.07.1966	7800	1:38 000	Good contrast
1993	Analogue photogrammetry (vertical aerial photos)	1:10 000	10	Fjellanger Widerøe A/S 11534	27.08.1993	7200	1:40 000	Partly covered by snow, poor contrast
2011	LiDAR and othophoto			COWI A/S	17.09.2011	3080 - 3600		

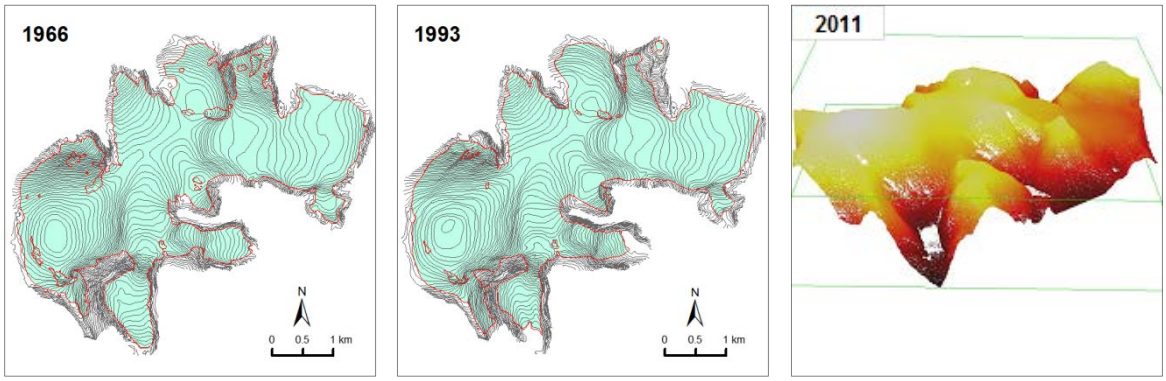

Figure 14. Source of DTMs of Jostefonn : contour maps made from aerial photos in 1966 and 1993 and LiDAR data from 2011 (MultiPoints).
Source: Own elaboration
Coordinate System: WGS 1984 UTM Zone 32N

Free access weather and climate data from historical to real time observations are available from web portal eKlima provided by the Norwegian Meteorological Institute and they were used to observe the changes in the Jostefonn glacier in the period between 1966 and 2011.

3.2.1 LiDAR data

LiDAR data used in the thesis was provided by the Norwegian Water Resources and Energy Directorate (Norges Vassdrags og Energidirektorat – NVE). Laser scanning of Jostefonn glacier was performed on 17th September, 2011 by COWI AS who also processed the raw laser data.

3.2.2 Orthophotos

24 tiles of orthophoto images taken on 17th September, 2011 by COWI in conjunction with the LiDAR data are available for the current project as shown in Figure 15.

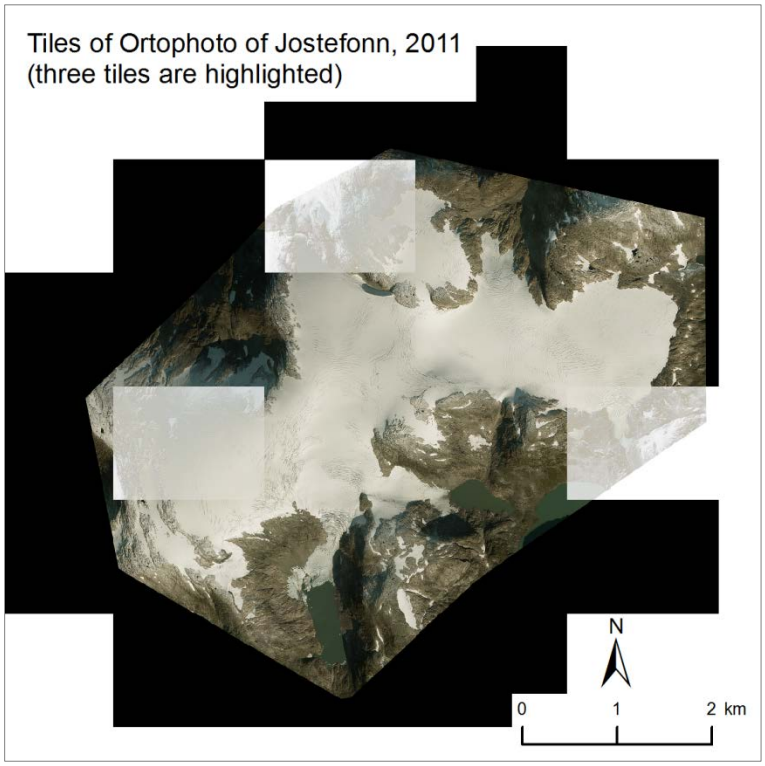

Figure 15. The available ortophoto tiles for Fostefonn glacier. (Three tiles are displayed lighter to show the size of a tile.)
Source: Own elaboration
Coordinate System: WGS 1984 UTM Zone 32N

3.2.3 Maps 1966 and 1993

The two sets of vertical aerial photographs from 1966 and 1993 were used in this study are. The digital photogrammetry work for the aerial photographs taken in 1966 and 1993 was performed by Fjellanger Widerøe A/S. Analogue photogrammetry was used to construct the 1966 map and analogue stereo plotters were used to generate the 1993 map, where elevations were registered with a digital encoder (Andreassen *et al*. 2002). Contour lines at 10 m intervals were constructed for the glacier area, and at 100 m intervals outside the glacier area. The accuracy of the map depends on the scale of the aerial photographs as well as snow and ice surface conditions at the time when the aerial photographs were taken, as snow and clouds can make it difficult to draw accurate contour lines (Andreassen 1998). There are also other factors that can influence the accuracy of the map, e.g. the flying height of the aircraft, the type of stereo-plotter and the skill of the operator (Østrem 1986). Aerial photographs from 1966 had good contrast whereas photographs from 1993 had poorer contrast (Andreassen 1998).

4. Methodology

4.1 Data preparation

All available data were projected to the WGS 1984 UTM Zone 32N coordinate system. A buffer zone of 100m was created round the glacier outline for the years 1966 and 1993, in order to have information of a DEM not only in the glacier area but also outside it. Elevation points were then generated from contour lines, as elevation points are required as the input data for most of the interpolation methods.

4.2 Software

All data processing and calculations were performed in a Geographical Information Systems (GIS) with ARC/Info software (ESRI 2009a). Geostatistical Analyst was used for geostatistical analyses. ArcMap 10.2 (ESRI 2013a) was used to work with the LiDAR data and perform statistical analysis for the original LAS data set and the thinned LAS data set.

Microsoft Excel was used to perform the statistical analyses as well as to do other calculations needed for this thesis.

4.3 DEM generation

In the current study, DEMs were generated both from elevation points (contour lines) and LiDAR points using several interpolation methods.

By using an interpolation procedure a DEM is computed as a continuous surface from discrete measurements (Godone and Garnero 2013). The interpolated DEM accuracy is influenced by the choice of the interpolation method as each of the interpolators behave in different ways depending on the cell size as well as data density (Godone and Garnero 2013).

4.3.1 Interpolation from contour lines / elevation points

In the present study, DEMs were created from the digital contour maps acquired from vertical aerial photographs taken in 1966 and 1993. The contour lines were converted to points at vertices. The resulting point shapefile contained 38799 points for the year 1966 and 38265 points for the year 1993. Two subsets of points were created to train (31039 points (1966) and 30612 points (1993), 80% of the total) and test (7760 points (1966) and 7653 points (1993), 20% of the total) the interpolation methods used. The ratio of 80/20 was used here as it is a very commonly used ratio sometimes referred to as the Pareto principle. The Pareto principle states that, for many events, 80% of the effects come from 20% of the causes (Melini 2013; Boslaugh and Watters 2008). M.Peravlo (2003), S.Maroju (2007) and D.Melini (2013) suggested using this ratio in order to test how well the interpolation method has performed. The training data set was used to generate DEMs while the testing data set was used as an independent data set to estimate vertical interpolation errors.

The training data set consists of randomly selected data that constitutes 80% of the original data. In a similar manner to the original data, they are concentrated along the contour lines, thus forming an uneven distribution. The training data sets for the years 1966 and 1993 were interpolated by six different interpolation algorithms: Inverse Distance Weighing, Kriging, Natural Neighbours, Triangulated Irregular Network, Tension Spline and ANUDEM. The surfaces were interpolated in four different resolutions: 5m, 10m, 20m and 50m. The interpolations were carried out using the parameters presented in Table 6.

Table 6. The interpolation parameters for IDW, Kriging and Spline.

Interpolation parameters	IDW	Kriging	Spline
Power	2		
Search radius	variable	variable	
Max number of points	12	12	12
Method		Ordinary	
Semivariogram model		Spherical	
Weight			0.1
Triangulate			

No parameters were set for Natural Neighbours, for TIN creation – both the elevation points and contour lines were used setting Triangulate as to hard lines. Interpolating using ANUDEM both elevation points and contour lines were used. A better result was achieved by using both elevation points and contour lines where possible (in TIN creation and ANUDEM).

In order to find out whether the sampling size of the grid influences the result, different cell sizes were tested. The purpose of evaluating DEMs at different resolutions is to detect possible differences and find out which resolution depicts the evaluation data most accurately (Hasan *et al.* 2011). In the current study the cell size of 5 m, 10 m, 20 m and 50 m was tested in a similar manner to the cell sizes studied by Andreassen (1999).

4.3.2 DEM generation from LiDAR points

Digital elevation models were created from thinned LiDAR data points (ANY_RETURNS) applying the same interpolation methods that were used in DEM creation from contour lines (IDW, Kriging, Spline, NN, ANUDEM and TIN). With the available software and equipment it was not possible to acquire the results with the Kriging interpolator. Resolutions of 5 m, 10 m, 20m and 50 m were tested.

The generated MultiPoints from LiDAR data were used to create a terrain data set. A terrain data set is a multiresolution, TIN-based surface built from measurements stored as features in a geodatabase (ArcGIS Desktop Help). A feature data set was created in the

already existing geodatabase, as a terrain data set can only be created in a feature data set. It is important to set the Z coordinate system as well as the XY coordinate system. Defaults were used for the next steps. The MultiPoints were dragged into the newly created empty feature data set, before terrain data set was created in the feature data set. The terrain data set was added in ArcMAP and explored. When zooming in it was noticed that the terrain was redrawn in more detail. The unique feature of the terrain data set is that it can easily deal with large volumes of data. Comparing to TIN, TIN would have taken much more time to build, redraw and generate.

In the next step the terrain was converted to a raster data set. The output data type was set to Float, and Natural Neighbours were used as the interpolation method. The natural neighbour interpolation method was used due to the fact that is considered to work better than the linear interpolation method. It is not as fast as linear interpolation but generally produces better results both in terms of aesthetics and accuracy (ESRI 2011b). The cell size was set to 1 m.

4.3.2.1 The use of all LiDAR data

The use of all the LiDAR data slowed the analysis process considerably. That is why the original data was thinned as described below.

4.3.2.2 Thinning of LiDAR data

The number of LiDAR data points was reduced as a larger point density was observed in overlapping areas due to the route of the aircraft. That was done by using the LAStools lasthin option to thin LiDAR points by placing a uniform grid over the points and keeping within each grid cell only the point with the lowest (or the highest or the random) Z coordinate (LAStools).

4.5 Assessment of DEM quality

Several approaches were applied to assess the quality of the interpolated DEMs including visualization, absolute and relative quality assessment, by means of geomorphometry (slope and aspect), and statistical analysis.

4.5.1 Visual assessment of DEM quality

Visual assessment of DEM quality was applied as the initial step in the DEM quality assessment as this approach gives a general overview of the quality of the terrain data sets.

The original contour lines from maps from the years 1966 and 1993 were compared to the contour lines generated from the interpolated DEMs. By comparing the contour lines it was possible to visually see how precisely they overlapped each other or how great the differences were. This visual approach already gave some hints which interpolation method or methods rendered the best results.

Another approach of visual assessment used in the thesis was to compare the original contour lines of maps from the years 1966 and 1993 with the contour lines generated from the reference data set (LiDAR data 1m) in the area that is glacier free.

4.5.2 Geomorphometry

Slope and aspect maps were derived from the DEMs that were created using natural neighbour and TIN interpolators with resolutions of 5m and 10m for years 1966 and 1993. These slope and aspect maps were used to assess the accuracy of DEMs.

4.5.3 Estimating DEM accuracy

4.5.3.1 Accuracy measures / Statistical analysis

The accuracy of interpolation methods was evaluated by using accuracy measures such as mean error (ME), mean absolute error (MAE), root mean square error (RMSE), standard deviation of error.

4.5.3.2 Validation and cross-validation

In order to assess only the quality of the used interpolation methods but not the quality of the original elevation data a common strategy was applied that has been mentioned in several sources (Carrara *et al*. 1997; Desmet 1997; Barringer *et al*. 2002; Carlisle 2002). Some data was withheld from the DEM generation process and assumed as ground truth. 20% from the total available points was used as the test data set whereas 80% - was used for DEM generation. The value at each withheld location (test sample points) was compared to the interpolated surface value and a statistical measure like root mean square error was calculated (Maune 2007). Such an approach only represents partial quality assessment and can only provide limited knowledge of DEM quality sometimes even decreasing the accuracy of the DEM, as less points are used in the interpolation process (Carrara *et al*. 1997; Barringer *et al*. 2002; Carlisle 2002). On the other hand interpolation methods are the only factor that causes DEMs to differ from each other as the same input data has been used. Thus, in order to test the quality of the DEMs generated by different interpolation methods, this approach seems to be feasible (Carrara *et al*. 1997). This approach is also referred to as performing validation on a geostatistical layer from a subset where original data set is divided into two parts. One part is used for creating an output surface whereas the other part is applied for testing or validating the obtained output surface (ESRI 2008).

Cross-validation is a technique used as an exploratory procedure to find the most suitable model among a number of other models. The cross-validation method uses all the raw data

available for comparison (Erdogan 2009). In the cross-validation process each point is removed in turn and, a value for that location is predicted based on the rest of the data and then the measured and predicted values are compared.

4.5.3.3 Comparing to sources of more accurate data

Another approach of assessing the accuracy of a DEM is to test it against a high-resolution reference DEM which is known to be of a higher order of accuracy. In this study, the LiDAR DEM was chosen as the reference data set to obtain the vertical accuracy of the DEMs generated from contour lines. The corresponding RMSE cannot be referred to as being the absolute vertical accuracy but the elevation error relative to the reference DEM (Junfeng Wei *et al*. 2012). According to Gens (1999) the reference DEM is considered to be correct and error free and at least one order better than the DEM that is evaluated.

5. Presentation of results

5.1 Interpolation from contour lines

Four DEM surfaces using cells sizes of 5m, 10m, 20m and 50m were created for each interpolator (IDW, Kriging, NN, TIN, Spline and ANUDEM) for both the years (1966 and 1993). 24 DEM surfaces were created both for the years 1966 and 1993. 48 DEM surfaces interpolated from contour lines were used in the research.

The histograms of all the DEMs are found in Appendix 9.1 and two histograms from each of the years are depicted in Figure 16 – one with distinctive peaks (yielded by IDW interpolation) and another with considerably fewer peaks (yielded by TIN interpolation). Histograms of IDW, Kriging and Spline interpolation methods show the greatest peaks whereas NN, TIN and ANUDEM have considerably fewer peaks. There is a difference between the years 1966 and 1993 as well. The DEMs generated from contour lines in 1966 display more peaks than the DEMs generated from contour lines in 1993.

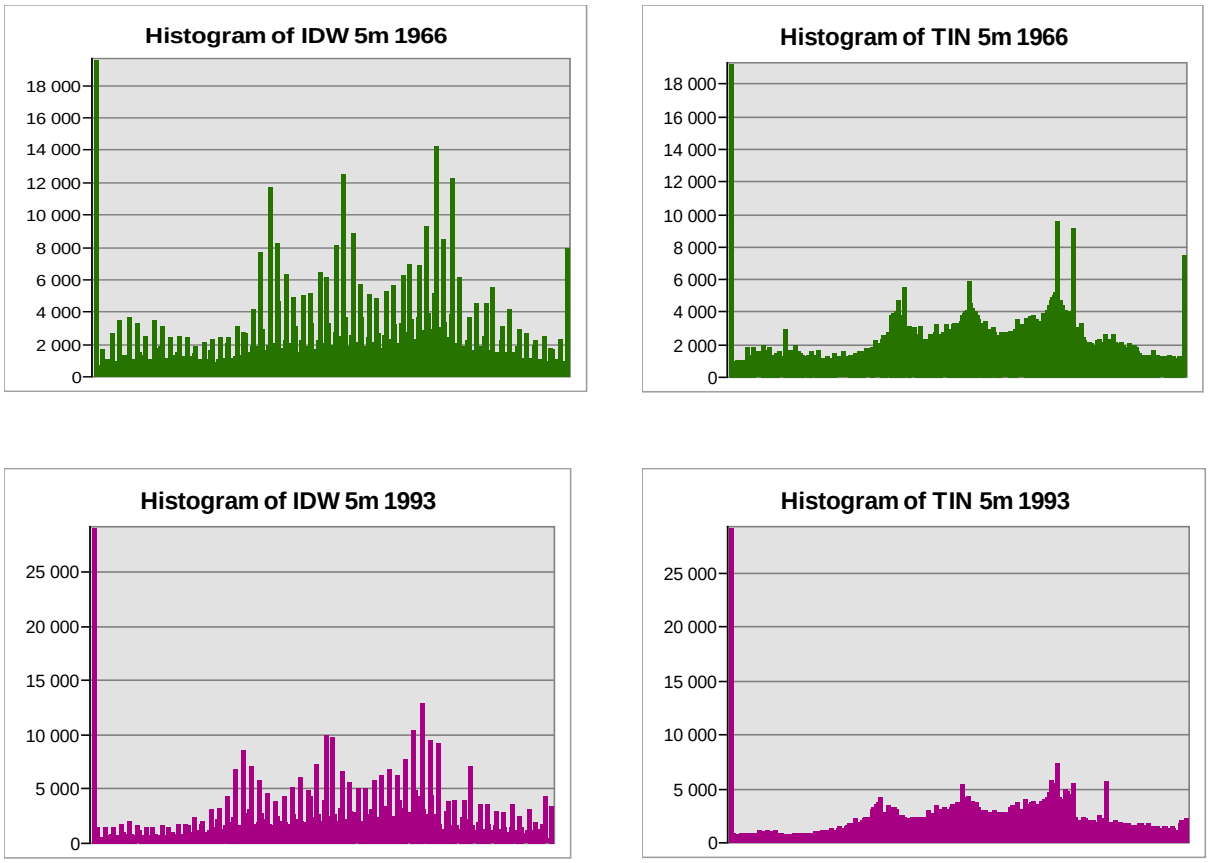

Figure 16. Histograms showing cyclic disposition of peaks due to overrepresentation of elevations equal to the digitized contours. DEMs created by IDW and TIN interpolators for years 1966 and 1993 with cell size 5m. X axis shows the data frequency / distribution.

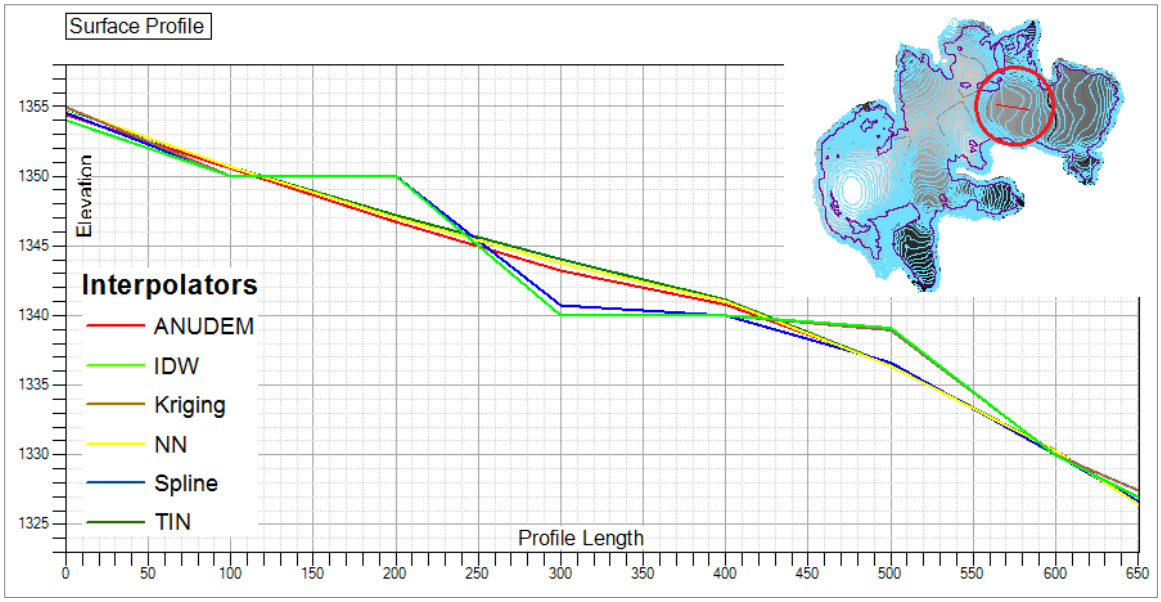

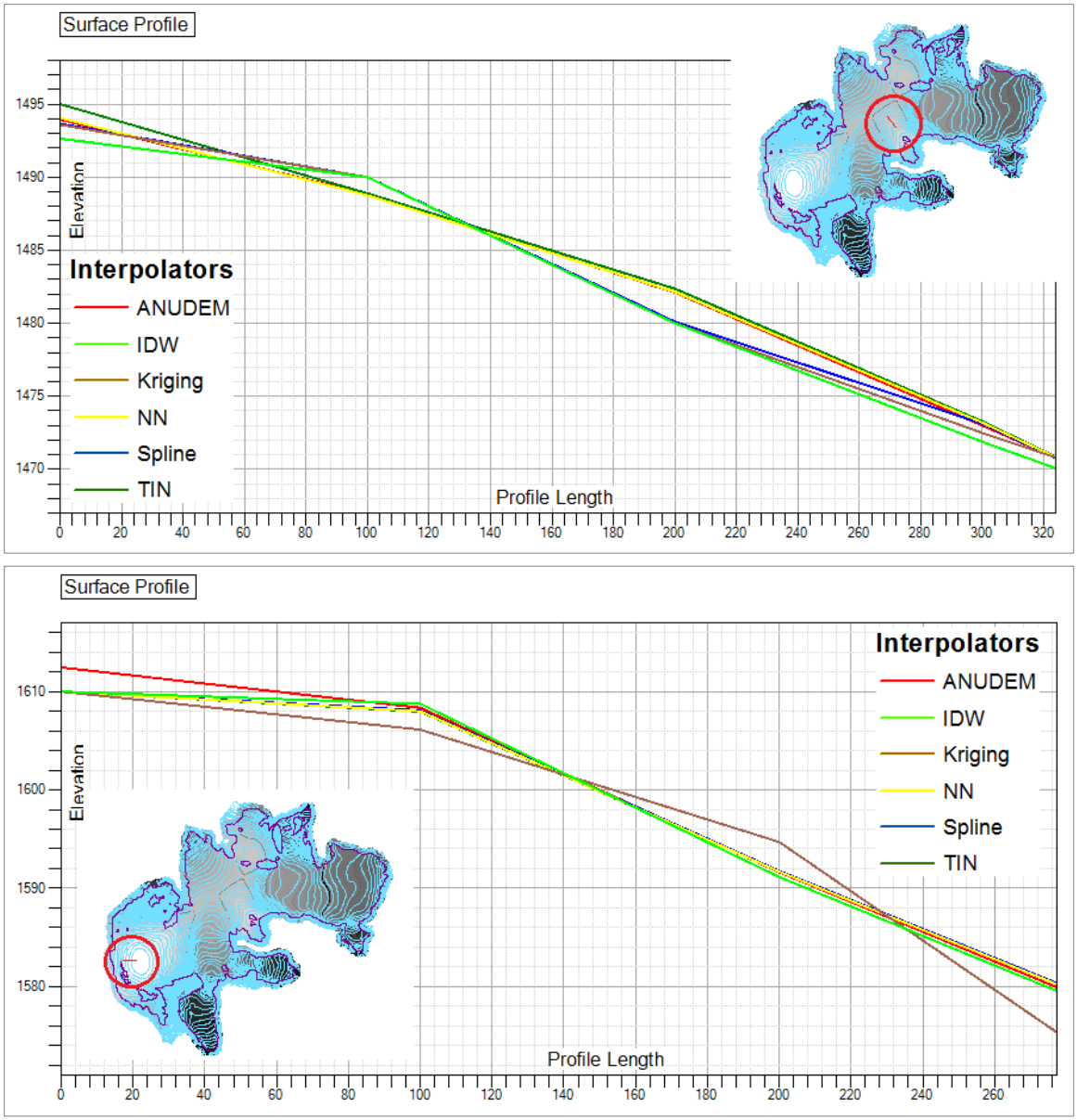

Figure 17. Surface profile through interpolated DEMs (cell size 5m, 1966), taken perpendicular to contour lines. X axis depicts profile length and Y axis depicts elevation.
Source: Own elaboration
Coordinate System: WGS 1984 UTM Zone 32N

Figure 17 shows the surface profiles of interpolated DEMs with a cell size of 5m (1966). The surface profiles show that IDW and Kriging interpolation methods form terracing as it was discovered before (See Appendix 9.1 Histograms of interpolated surfaces). The terracing is observed due to the fact that the same elevation values are clustered around the contour lines. A step wise transition from one elevation line to another is observed.

The spline method also shows some deviations. The best results were obtained by using NN, TIN and ANUDEM interpolators. The ANUDEM interpolator was the only interpolator to retain the highest value of Sundfjordbjørnen – the highest point of Jostefonn which is over 1610 m.

5.2 DEM from LiDAR data

A DEM with a 1 m resolution was created as a reference data set. In the analysis where DEMs were compared on a cell-by-cell basis and DEMs with different resolution were needed, the Aggregate function was used with the help of which reduced resolution versions of the 1 m DEM were generated.

5.2.1 Tninning of LiDAR data

Figure 18 shows the amount of original LiDAR data points compared to thinned data points.

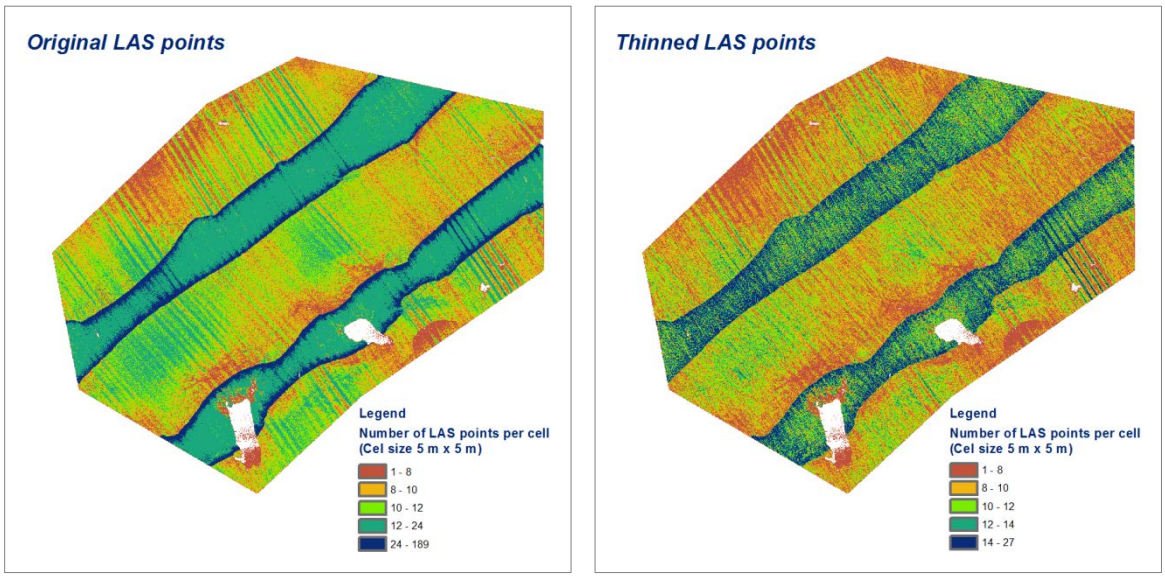

Figure 18. The amount of original and thinned LAS points per cell with resolution of 5m.
Source: Own elaboration
Coordinate System: WGS 1984 UTM Zone 32N

The amount of original LAS points reached even 189 points per cell with resolution of 5 m in the overlapping areas. The amount of points was reduced to maximum of 27 points per cell.

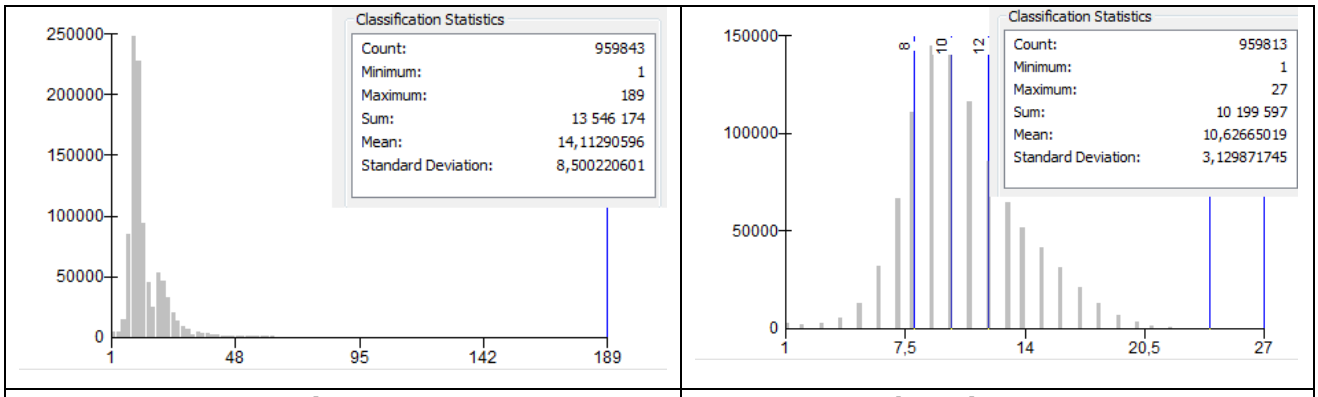

Original LAS points	Thinned LAS points

Figure 19. Histograms and statistics of original and thinned LAS points per cell with resolution of 5 m.

The histogram (Fig. 19) of original LAS data is skewed to the left with standard deviation of 8.5 points and the mean amount of points per cell (5 m x 5 m = 25 m^2) is 14 points. The histogram of thinned LAS points is close to normal distribution with standard deviation of 3 points and the mean amount of points per cell is almost 11 points.

5.3 Visual assessment of the results

Figure 20 shows the visual comparison of interpolation methods where contour lines generated from the created DEMs are compared to the original contour lines. The original contour lines which are yellow are shown along with the contour lines derived from the interpolated DEMs which are depicted purple. For the ANUDEM interpolator both lines nearly coincided. The original contour lines and the contour lines generated from the raster interpolated with the NN interpolator were also nearly overlapping each other. That could be said about other interpolators (IDW, Kriging and Spline) as rather big differences were observed there.

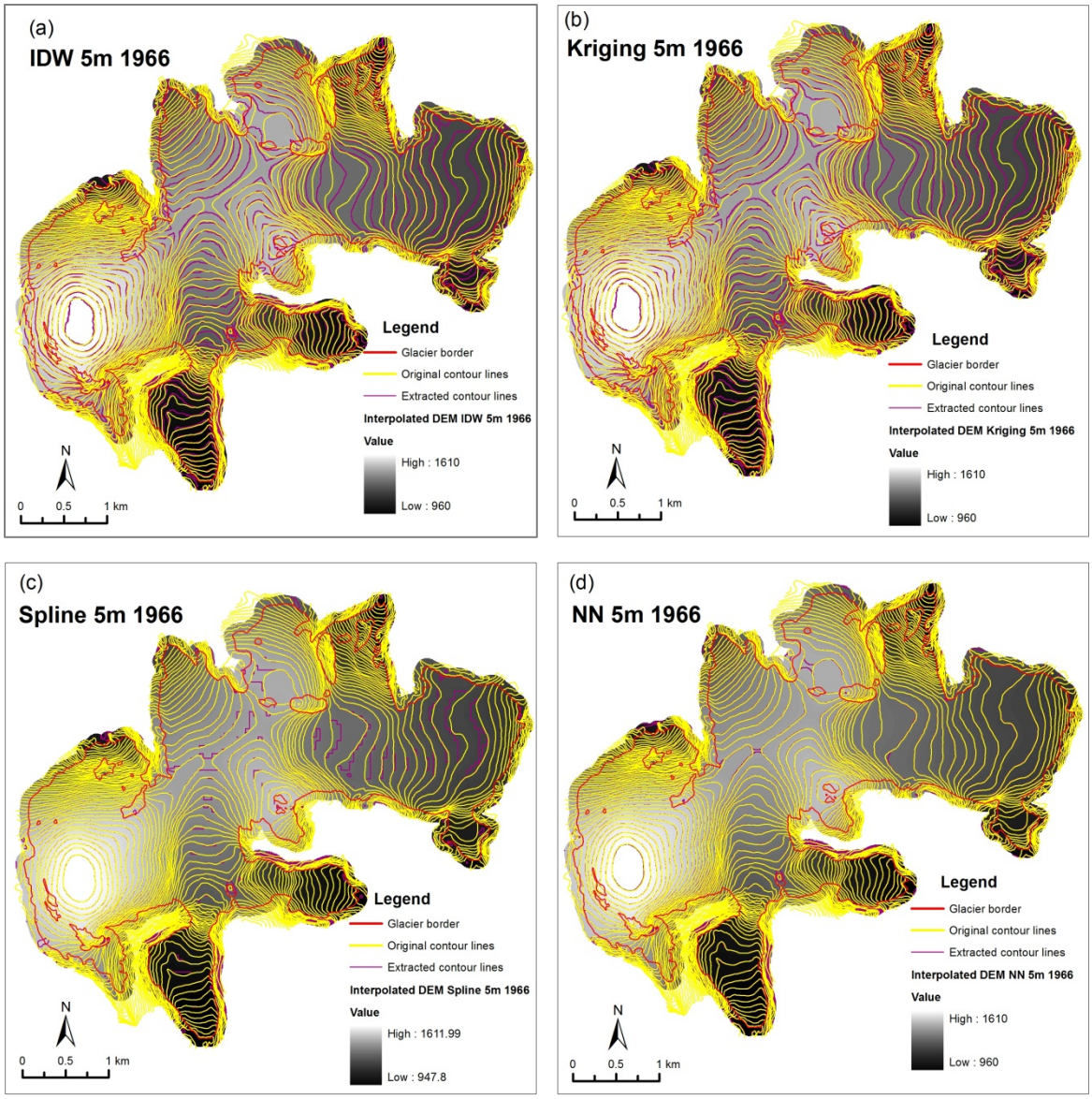
(a)
IDW 5m 1966
Legend
Glacier border
Original contour lines
Extracted contour lines
Interpolated DEM IDW 5m 1966
Value
High : 1610
Low : 960
N
0 0.5 1 km
(b)
Kriging 5m 1966
Legend
Glacier border
Original contour lines
Extracted contour lines
Interpolated DEM Kriging 5m 1966
Value
High : 1610
Low : 960
N
0 0.5 1 km
(c)
Spline 5m 1966
Legend
Glacier border
Original contour lines
Extracted contour lines
Interpolated DEM Spline 5m 1966
Value
High : 1611.99
Low : 947.8
N
0 0.5 1 km
(d)
NN 5m 1966
Legend
Glacier border
Original contour lines
Extracted contour lines
Interpolated DEM NN 5m 1966
Value
High : 1610
Low : 960
N
0 0.5 1 km

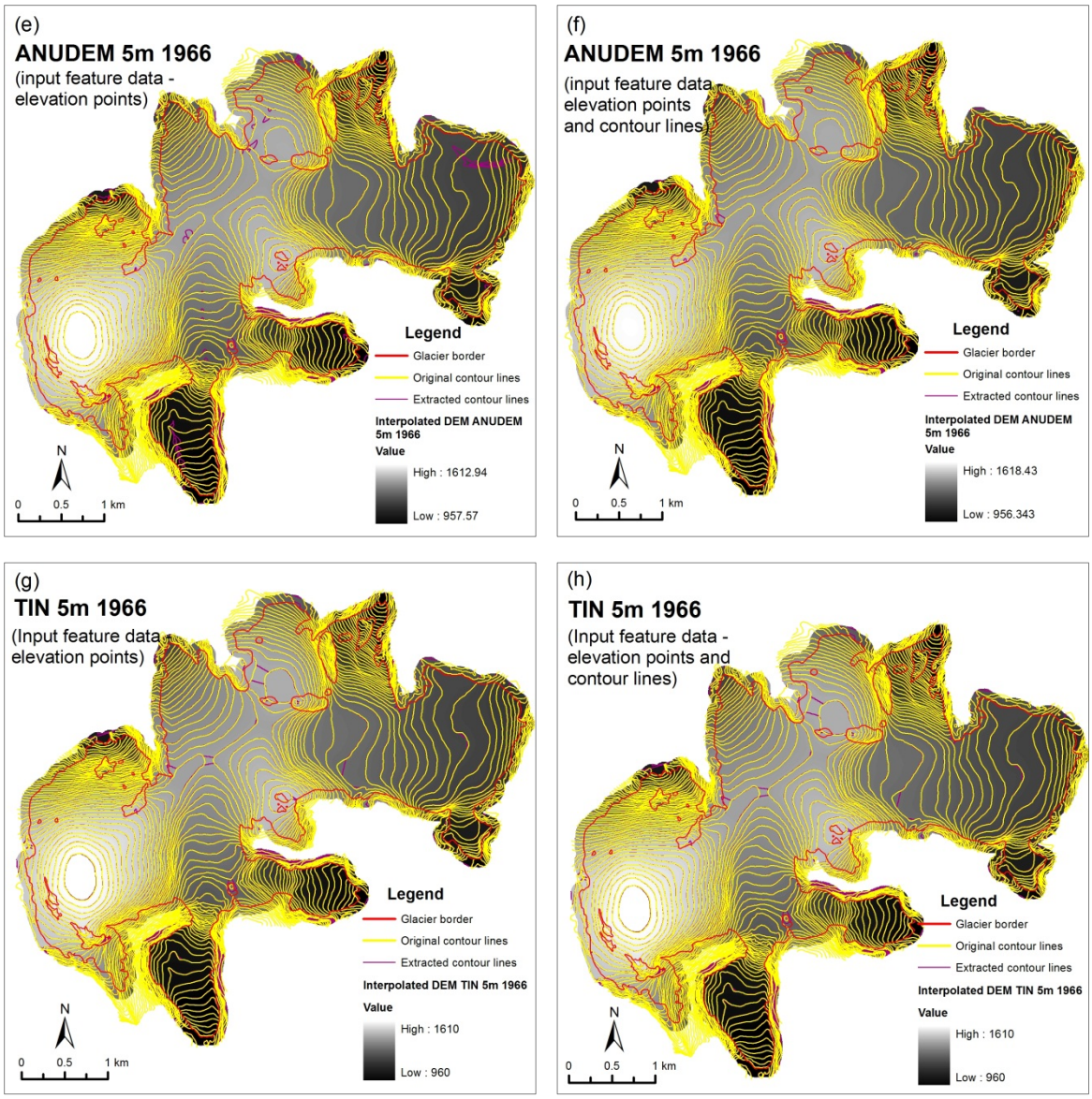

Figure 20. A comparison between the modelled and the reference contour lines for (a) IDW, (b) Kriging, (c) Spline, (d) Natural Neighbours, (e) ANUDEM interpolated using only elevation points as the input data, (f) ANUDEM interpolated using both elevation points and contour lines, (g) TIN interpolated using only elevation points and (h) TIN interpolated using both elevation points and contour lines for the year of 1966. The extracted contour lines are shown in purple and the original contour lines are depicted in yellow. The cell size for all the maps is 5 m.
Source: Own elaboration
Coordinate System: WGS 1984 UTM Zone 32N

The visual comparison of the interpolation methods with cell sizes 10m (1966), 5m (1993) and 10m (1993) are found in Appendix 9.2. There are also found two bigger figures of the two interpolators (b and f from Fig.20).

By increasing the cell size, the generated contour lines become ragged. They can be smoothed. The smooth line tool smooths sharp angles in lines to improve aesthetic and cartographic quality (ESRI 2011a) (Fig.21).

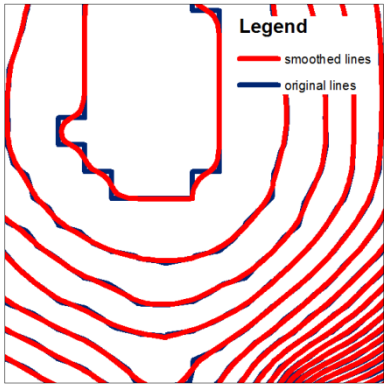

Figure 21. Smoothed lines versus original lines.
Source: Own elaboration.

Another approach in order to test how accurate the contour maps were was to generate contours from the reference grid and compare them with the original contours from the years 1966 and 1993 in the ice-free terrain. When the two maps are placed upon each other and the contour lines for all areas outside the glacier coincide well, one may anticipate that the two maps are reliable (Haakensen 1986).

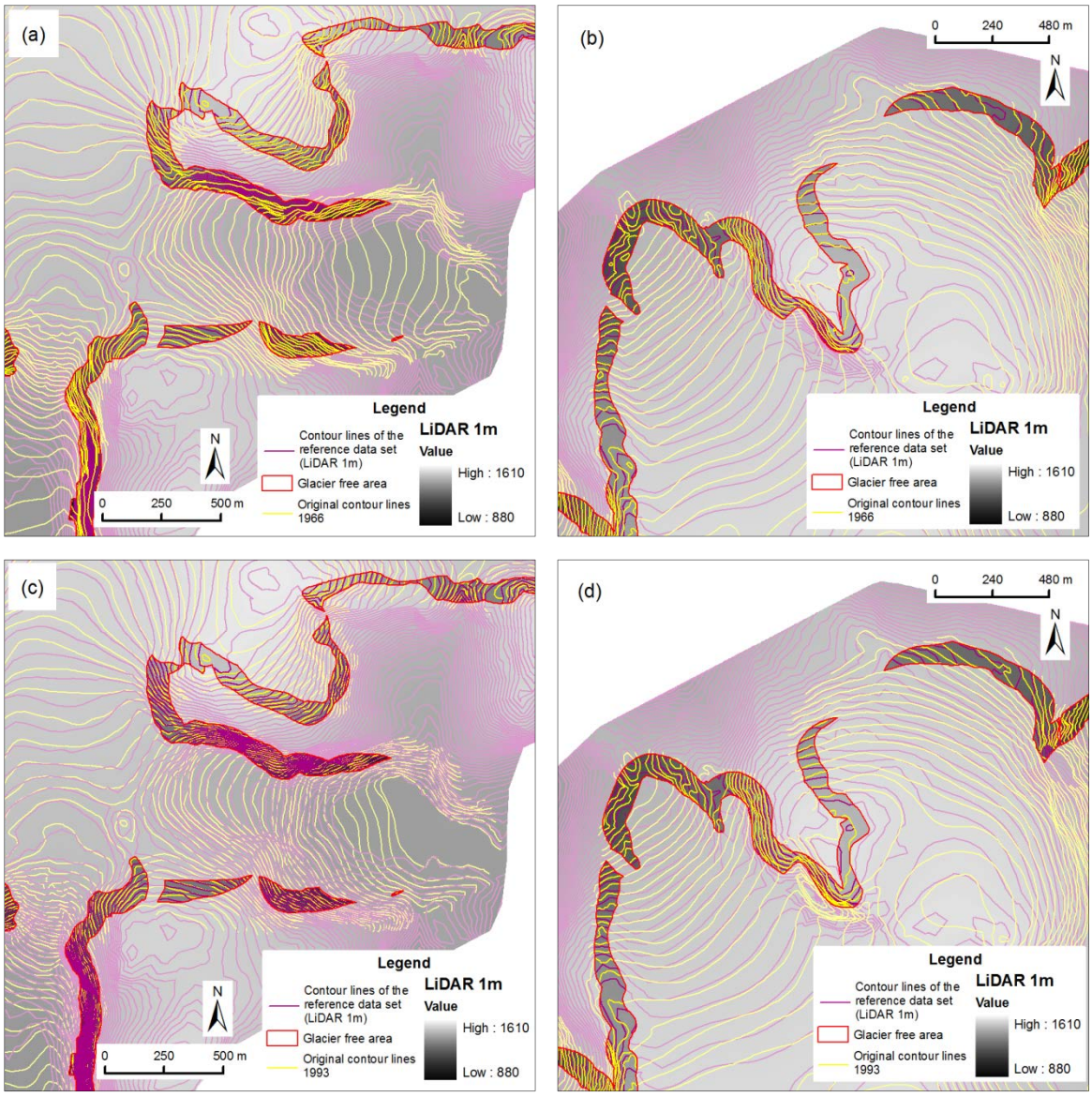

Figure 22. A comparison between the original contour lines and the contour lines derived from the reference data set (LiDAR 1m). (a) and (b) depict the contour lines from the year of 1966, (c) and (d) – the contour lines from the year of 1993. Two areas for both the years have been zoomed in to show a closer look of the contour lines. The original contour lines are depicted in yellow whereas the contour lines derived from the reference data set are shown in purple.

Source: Own elaboration

Coordinate System: WGS 1984 UTM Zone 32N

The maps displayed in Figure 22 show no great distortions between the original contour lines and the contour lines from the reference grid in glacier free areas which means that the DEMs tested are reliable.

5.4 Comparison of accuracy measures

Figures 23, 24 and 25 show the results of a comparison of two accuracy measures (RMSE and MAE) for all three years studied (1966, 1993 and 2011). The statistical analysis was performed for all the acquired DEMs generated with the chosen interpolators and chosen resolution by applying training and testing data sets (4.3.1). Other accuracy measures are found in Appendix 9.3.

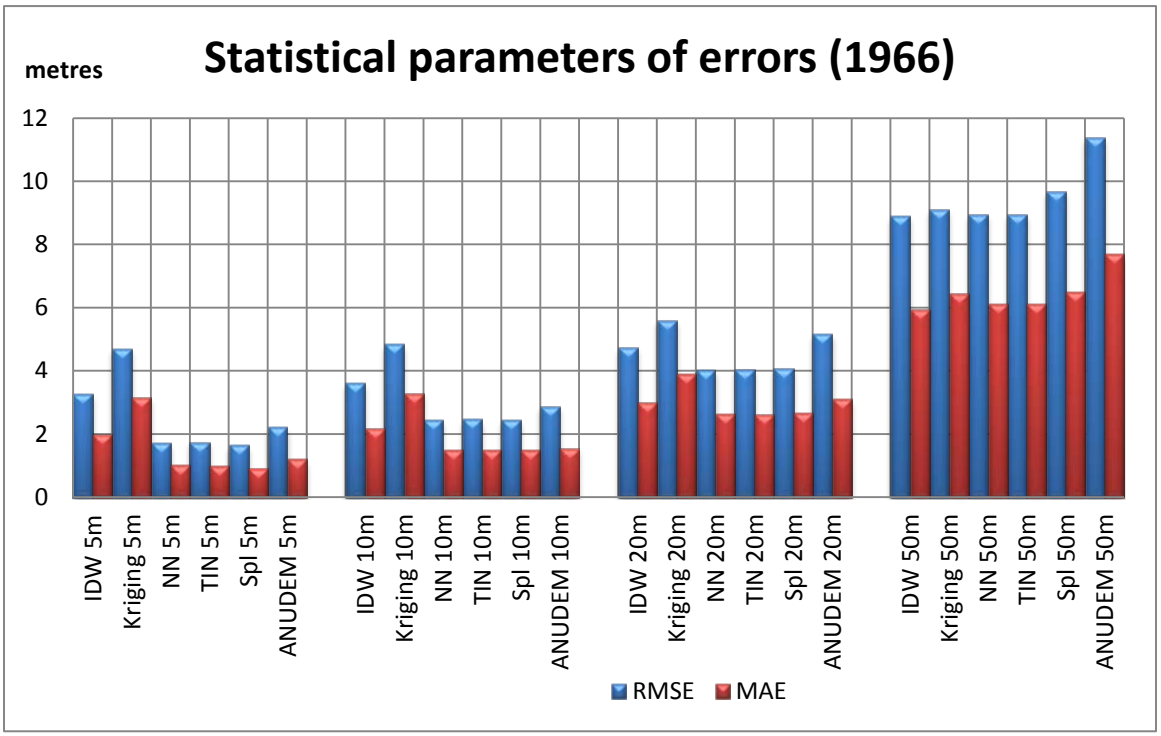

Figure 23. Comparison of accuracy measures (RMSE and MAE) for the year of 1966. The statistical measures of RMSE and MAE are depicted for all the interpolated DEMs with four resolutions tested (5 m, 10 m, 20 m and 50 m).

Figure 23 shows the statistical measures (RMSE and MAE) of all the interpolated surfaces at different resolutions for the year 1966. The IDW and Kriging interpolators

show higher values in the descriptive statistical measures at all resolutions compared to other interpolators. Natural neighbours, TIN and Spline showed the best performance. However, that can be said only about resolutions of 5m and 10m as the RMSE and MAE values for resolutions of 20 m and 50 m are as high as for other interpolators.

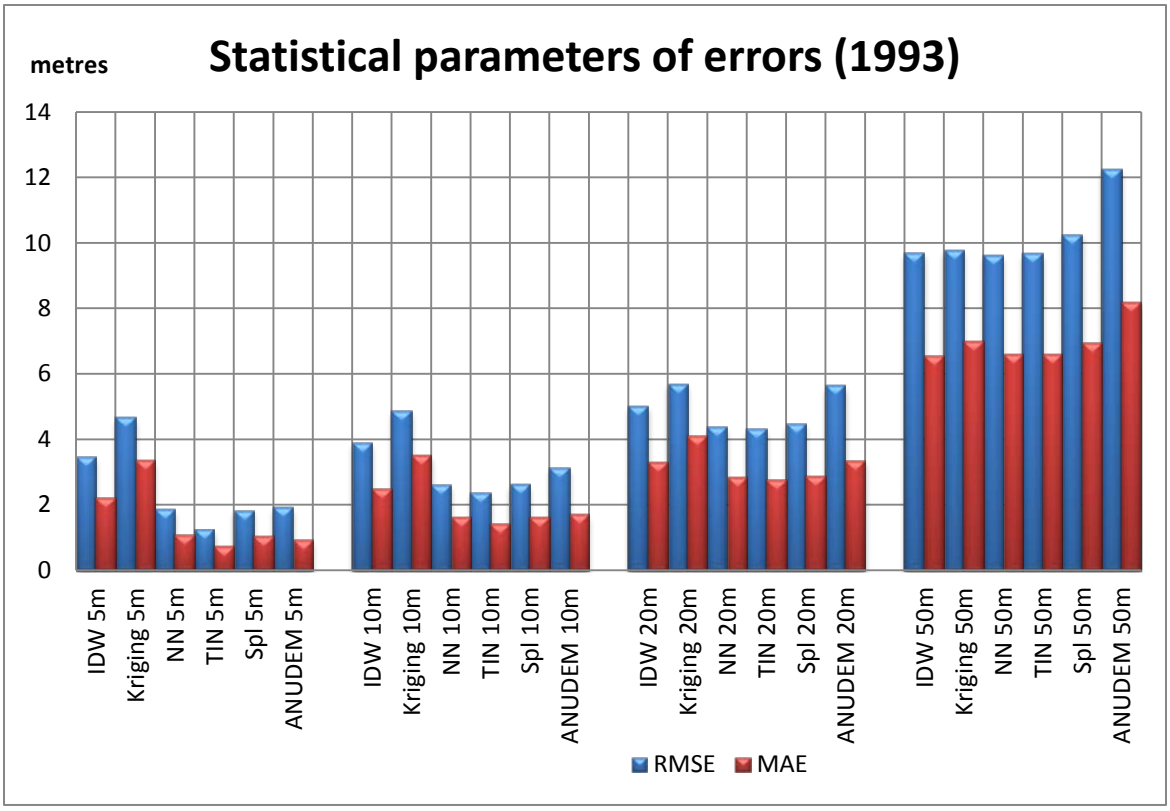

Figure 24. Comparison of accuracy measures (RMSE and MAE) for the year of 1993. The statistical measures of RMSE and MAE are depicted for all the interpolated DEMs with four resolutions tested (5 m, 10 m, 20 m and 50 m).

Figure 24 shows the statistical measures (RMSE and MAE) of all the interpolated surfaces at different resolutions for the year 1993. As for 1966, the highest values in each of the descriptive statistical measures are shown by IDW and Kriging interpolators. Natural neighbours and TIN showed the best performance. However, that can be said about resolutions of 5m and 10m as in the case of the year 1966.

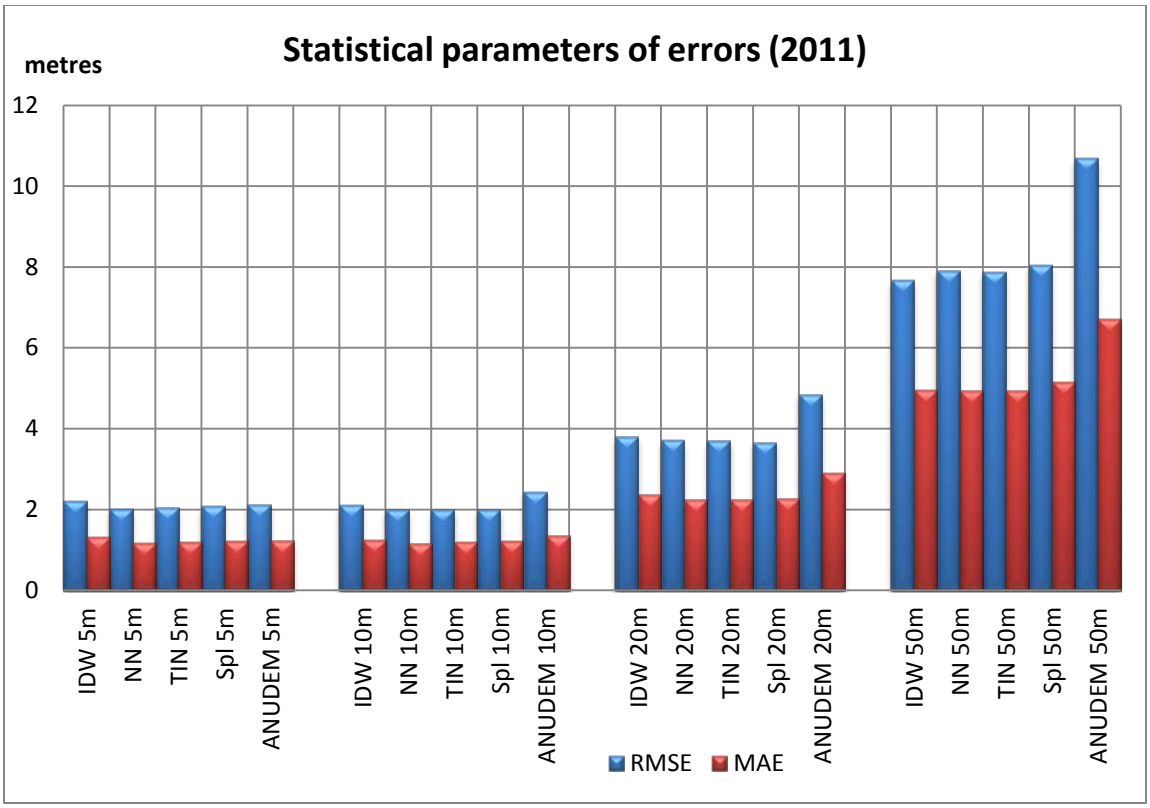

Figure 25. Comparison of accuracy measures (RMSE and MAE) for the year of 2011. The statistical measures of RMSE and MAE are depicted for all the interpolated DEMs with four resolutions tested (5 m, 10 m, 20 m and 50 m).

Figure 25 shows the statistical measures (RMSE and MAE) of all the interpolated surfaces at different resolutions for the year 2011. Due to the large amount of data, it was not possible to generate DEM surfaces with the Kriging interpolator. The RMSE and MAE values are quite similar at 5m and 10m resolution. By increasing the cell size, the RMSE and MAE values increase.

The corresponding research testing interpolation methods confirmed that the interpolation methods used (IDW, Kriging, Spline Tension, ANUDEM and TIN) were quite similar in respect to their RMSE and MAE for the years 1966 and 1993 and especially for the year of 2011. The natural neighbour and TIN interpolators tended to render the lowest overall range of errors (cell size 5m and 10m) and that is why the surfaces interpolated using these two interpolation methods were used in the comparison with LiDAR data in non-glacier areas.

In order to find out whether the distribution of errors is normal or not, histograms or quantile-quantile (Q-Q) plots were generated. Histograms of the error distribution for all the interpolated surfaces are found in Appendix 9.3.

A Q-Q plot is a graph that is used to detect a deviation from the normal distribution. The plot compares the standardized errors to a normal distribution. If the errors are normally distributed, the Q-Q plot should yield a straight line. It is important that the errors are normally distributed when probability and quantile maps are made.

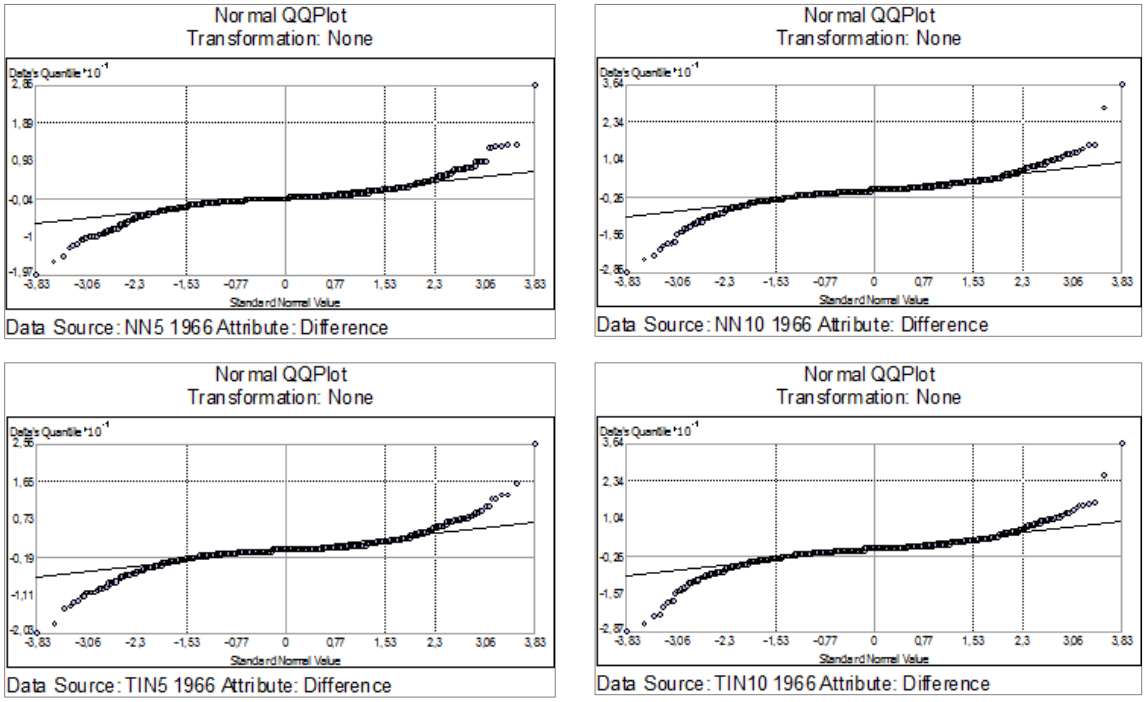

Figure 26. Normal Q-Q plots for the distribution of elevation differences (NN 5m, NN 10m, TIN 5m, TIN 10m, year 1966).

The Q-Q plots in Figure 26 show that there are deviations from the normal distribution. There are high elevation differences. Höhle and Potuckova (2011) state that if either the histogram of the errors or the Q-Q plot do not reveal normal distribution, then robust accuracy measures should be applied.

The statistical parameters of error for all of the interpolated surfaces at the chosen resolutions are found in Appendix 9.4. The minimum and maximum errors were the ones of particular interest as they seemed to be quite large compared to the mean error and mean absolute error. The errors that were outside the range from -5m to 5m were selected. The selected error values from the test data set for all of the interpolation methods tend to be in the areas where there is steep terrain. The same tendency is observed for all the years of interest. The number of test points where the elevation difference was outside the defined range (from -5m to 5m), increased with the increased cell size. This was observed for all of the interpolation methods. The smallest number of test points that were outside the defined range were observed in the surfaces interpolated with natural neighbours, TIN and Spline interpolators. However, ANUDEM showed quite similar results. IDW and Kriging rendered the greatest number of test points that showed large elevation differences, even at finer resolutions. The results are shown in Figure 27. The results yielded by other interpolators and other resolutions are found in Appendix 9.4.

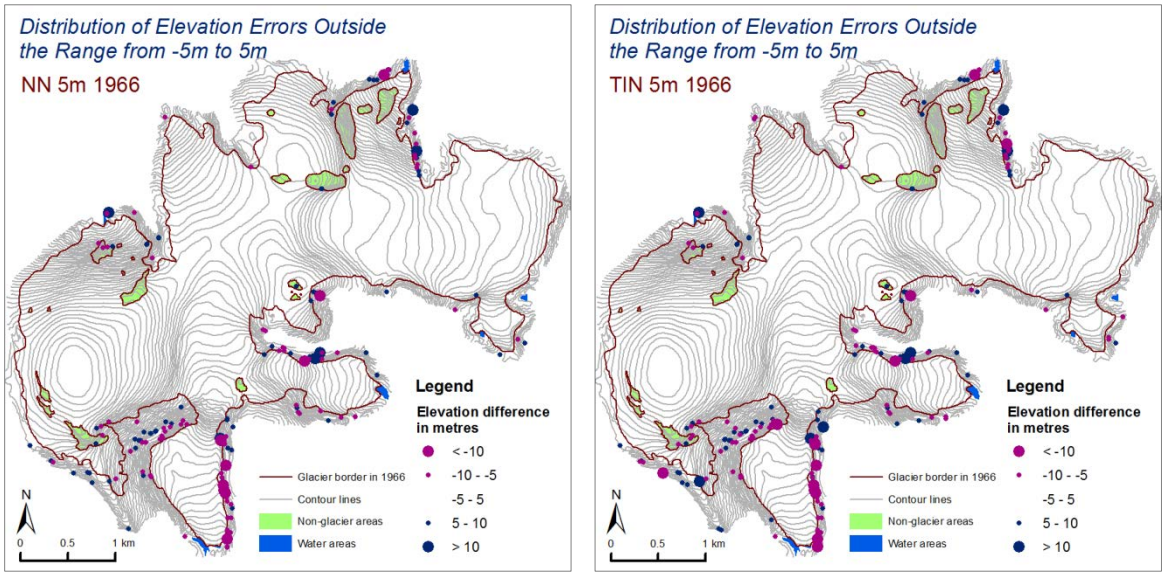

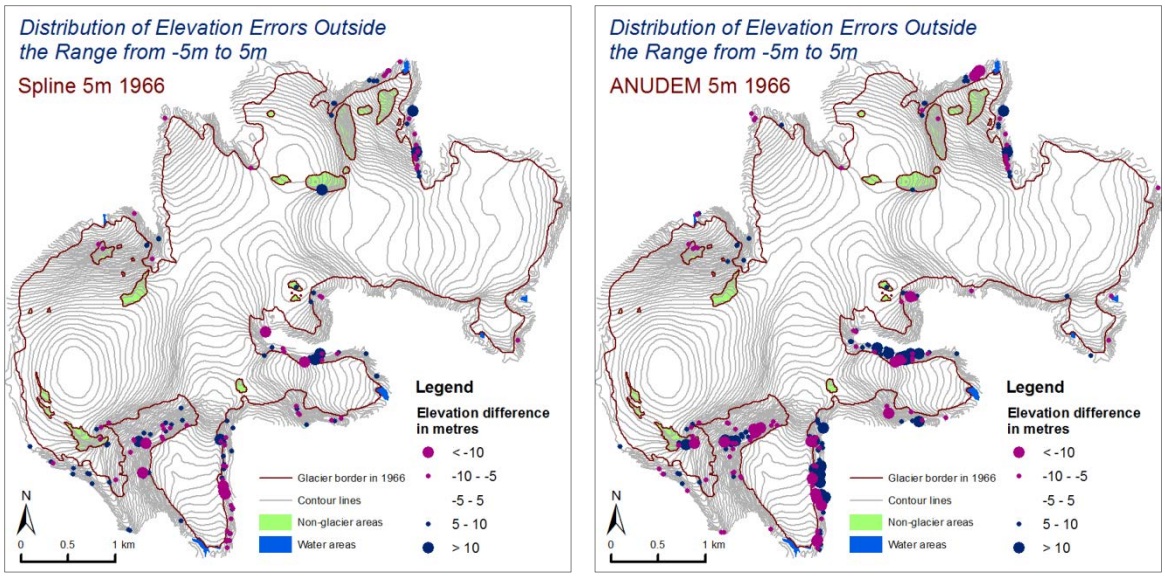

Figure 27. Distribution of elevation errors that are outside the specified range from -5m to 5m. The interpolation methods that have chosen the best results are chosen (NN, TIN Spline and ANUDEM). The following test is done for the year 1966. The elevation differences that are lower than the interpolated raster value are shown in purple and the elevation differences that are higher than the interpolated raster are depicted in blue. Nearly all erroneous values are outside the glacier area.
Source: Own elaboration
Coordinate System: WGS 1984 UTM Zone 32N

Figure 28 shows an overall picture of all the test points and the elevation differences from the interpolated raster. The natural neighbour interpolator was chosen as it showed good results. It can be seen that all the test points where the elevation difference is within the range of -1m and 1m are mostly found in the glacier area and the test points that have larger elevation differences are outside the glacier area and in the areas where there is steep terrain.

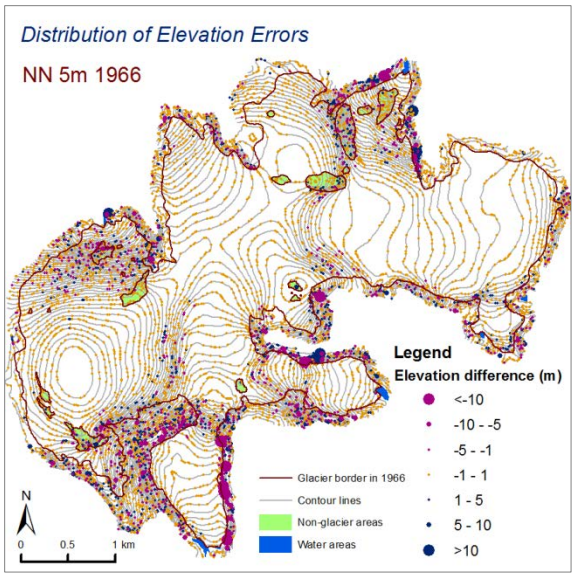

Figure 28. Distribution of elevation differences between the test points and the interpolated raster (NN 5m 1966). The elevation difference that is within the range from -1m to 1m is depicted in yellow.
Source: Own elaboration
Coordinate System: WGS 1984 UTM Zone 32N

As the most erroneous elevation differences were found to be in the area outside the glacier that could lead to inaccuracies while comparing the interpolated rasters with the reference data set in non-glacier areas. The DEM derivatives (aspect, slope etc.) would render inaccuracies in the areas outside the glacier as well as in areas of steep terrain due to the interpolation errors in those areas.

The contour line density is very high in steep terrain areas, resulting in two or more elevation values in one output raster cell. That is why a considerably larger amount of test points displayed an elevation difference in coarser resolutions. The finer the resolution, the fewer the number of test points that exhibited remarkable elevation difference. If the cell size is equal to the contour line interval in the steep areas, the output raster will be more accurate.

For example, testing the natural neighbour interpolation method (contour lines 1966) with a validation technique, 2.24% (cell size – 5m) of all the test points rendered high elevation difference (lower than -5m or higher than 5m). For the surface with a cell size of 10m there were 4.51% of all the test points which had either lower elevation than -5m or higher than 5m compared to the value in the interpolated raster, with values of 15.03% and 43.76% for the cell sizes of 20m and 50m respectively. The cell size of 1m was

tested although it was not chosen in the previous testing processes. Only 1.52% of all the test points displayed greater elevation difference compared to the raster surface value.

5.5 Cross-validation

In order to find out which model provides the best predictions, cross-validation can be employed. By using cross-validation, one or more data samples were withheld and then the prediction was done at the same data location. In such a way a predicted value was compared to the observed value, thus getting information about a certain interpolation method. Cross-validation used all the data to estimate the autocorrelation model (Johnston 2004). Cross-validation was performed for the available interpolation methods offered by Geostatistical Analyst Tools from ESRI Software. The cross-validation results are shown in Figure 29 and Table 7.

Inverse Distance Weighted (Prediction)	Inverse Distance Weighted (Error)
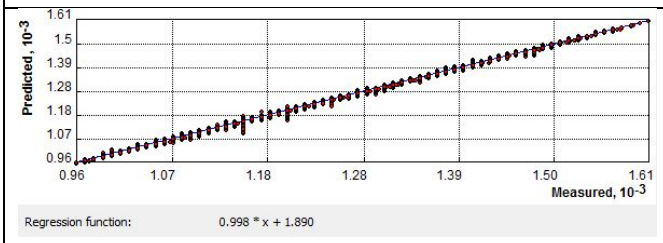	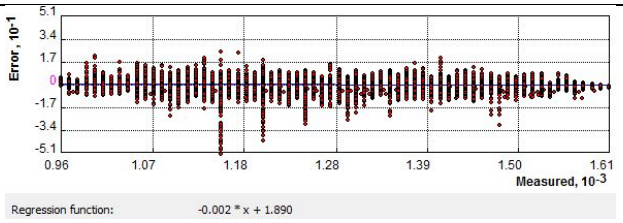
Local Polynomial Interpolation (Prediction)	Local Polynomial Interpolation (Error)
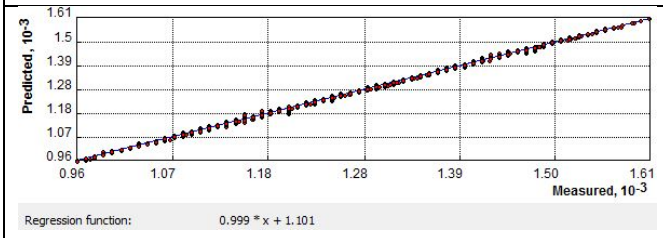	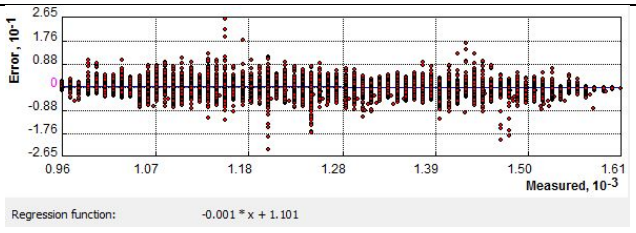
Radial Basis Functions (Prediction)	Radial Basis Functions (Error)
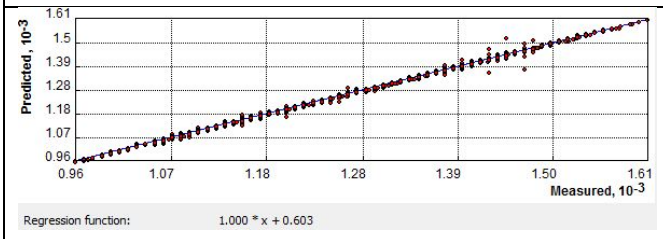	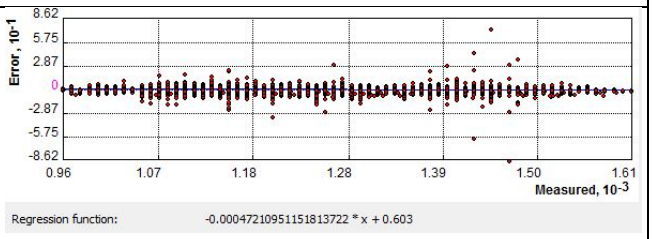
Ordinary Kriging (Predicted)	Ordinary Kriging (Error)

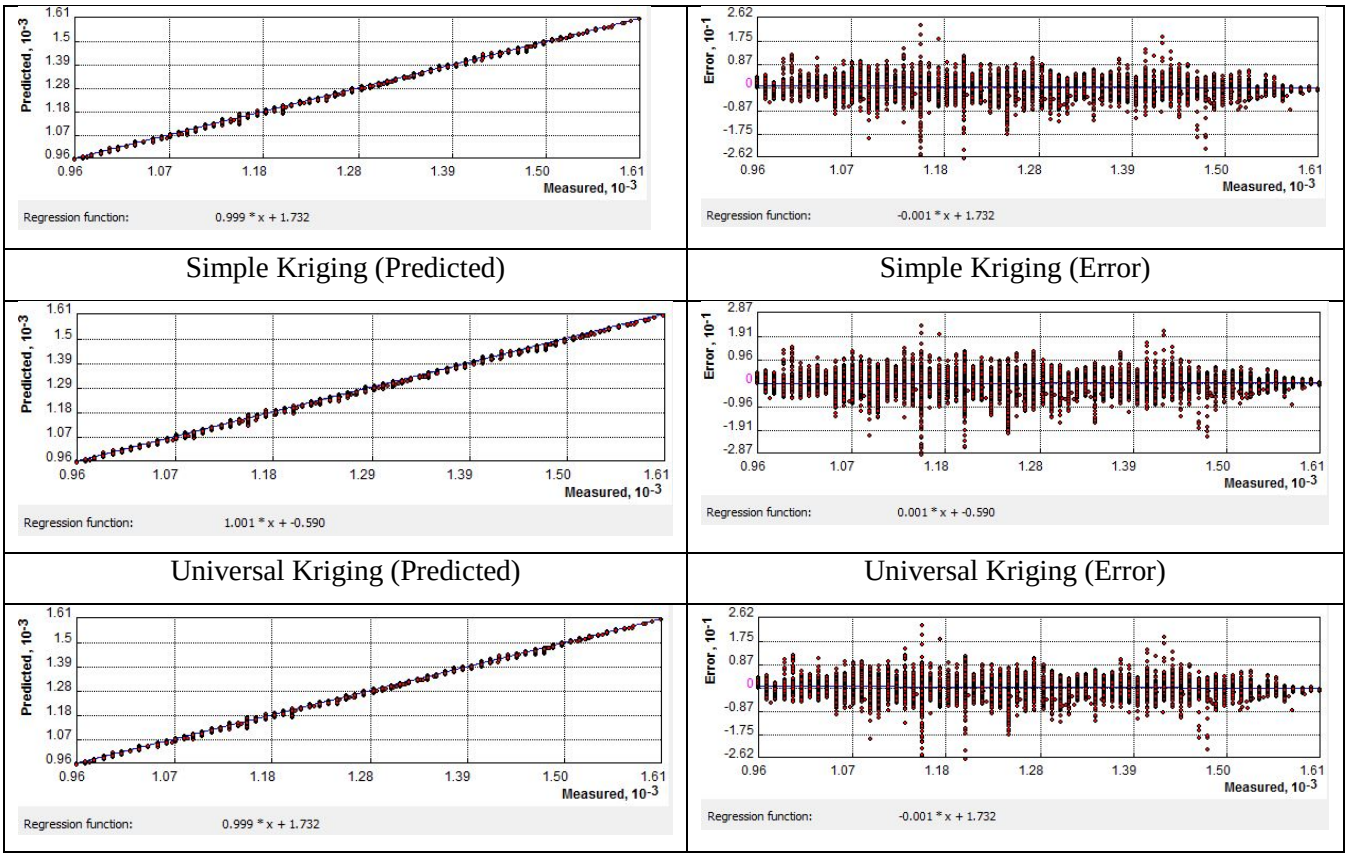

Figure 29. Results of cross-validation for year 1966 for the interpolation methods available in Geostatistical Analyst.

Table 7.Statistical measures acquired as the result of cross-validation.

Interpolation Method	1966	
	Mean	RMSE
Inverse Distance Weighting	-0.1394	3.013
Local Polynomial Interpolation	0.01412	1.534
Radial Basis Functions	-0.03173	1.686
Ordinary Kriging	-0.00191	1.839
Simple Kriging	0.08234	2.332
Universal Kriging	-0.00191	1.839

5.6 Accuracy of the DEM for terrain on different slopes and aspects

It was found that there were larger errors in elevation in areas where the terrain is steep compared to the areas where it is flat. Lower resolution (larger cell size) generated lower

values of slope. The reason for this tendency is quite logical as the elevation points are located at a specified maximum distance from the cell centre, leading to a greater deviation in steeper terrain (Hasan *et al.* 2011). Hasan *et.al.* (2011) suggested associating the accuracy of a DEM with the slope of the terrain, especially in high accuracy modelling on a detailed scale.

The graphs in Appendix 9.5 show the effect of slope on the elevation difference in the glacier free areas. The mean absolute elevation difference was calculated at the test points on each respective slope. The graphs clearly show that the mean absolute elevation difference tended to increase with slope. On slopes that are less than 40 degrees the mean absolute elevation difference was within 2 m for the DEMs with a 5 m resolution (NN and TIN interpolators). For the DEMs with a 10 m resolution the mean absolute elevation difference was bigger – exceeding 2 m. The rapid increase in the mean absolute elevation difference was observed on slopes that are greater than 60 degrees – even up to 18 m. From the graphs it can be seen that the TIN interpolator rendered smaller mean absolute elevation differences on each respective slope compared to NN interpolator. In addition, it was observed that the smaller the pixel size, the smaller mean absolute elevation difference.

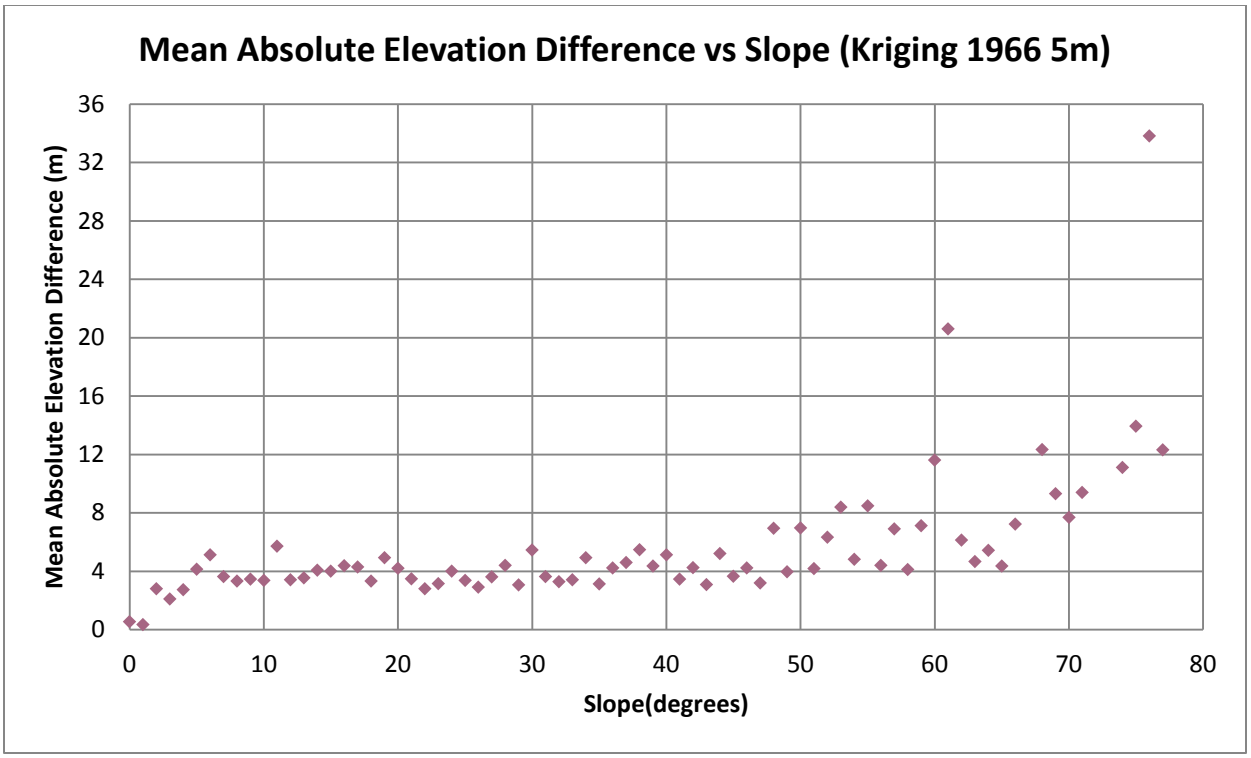

Figure 30. Mean absolute elevation differences plotted against slope (DEM Kriging 1966 5m).

Figure 30 shows a graph of mean absolute elevation difference with respect to slope for the DEM with a 5 m resolution created with the Kriging interpolation method. NN and TIN interpolators showed better results compared to other interpolators in the visual assessment (Chapter 5.3) and by applying the statistical measures (Chapter 5.4). Once again the DEM created by the Kriging interpolation method is less accurate that the DEMs created by NN or TIN interpolation methods. The mean absolute elevation difference on each respective slope is higher in the DEM created using the Kriging method than the previously mentioned methods – NN and TIN. While the mean absolute elevation differences are within 2 m on slopes less than 40 degrees for NN and TIN (5 m resolution), they exceed 4 m for the DEM created by the Kriging interpolation method.

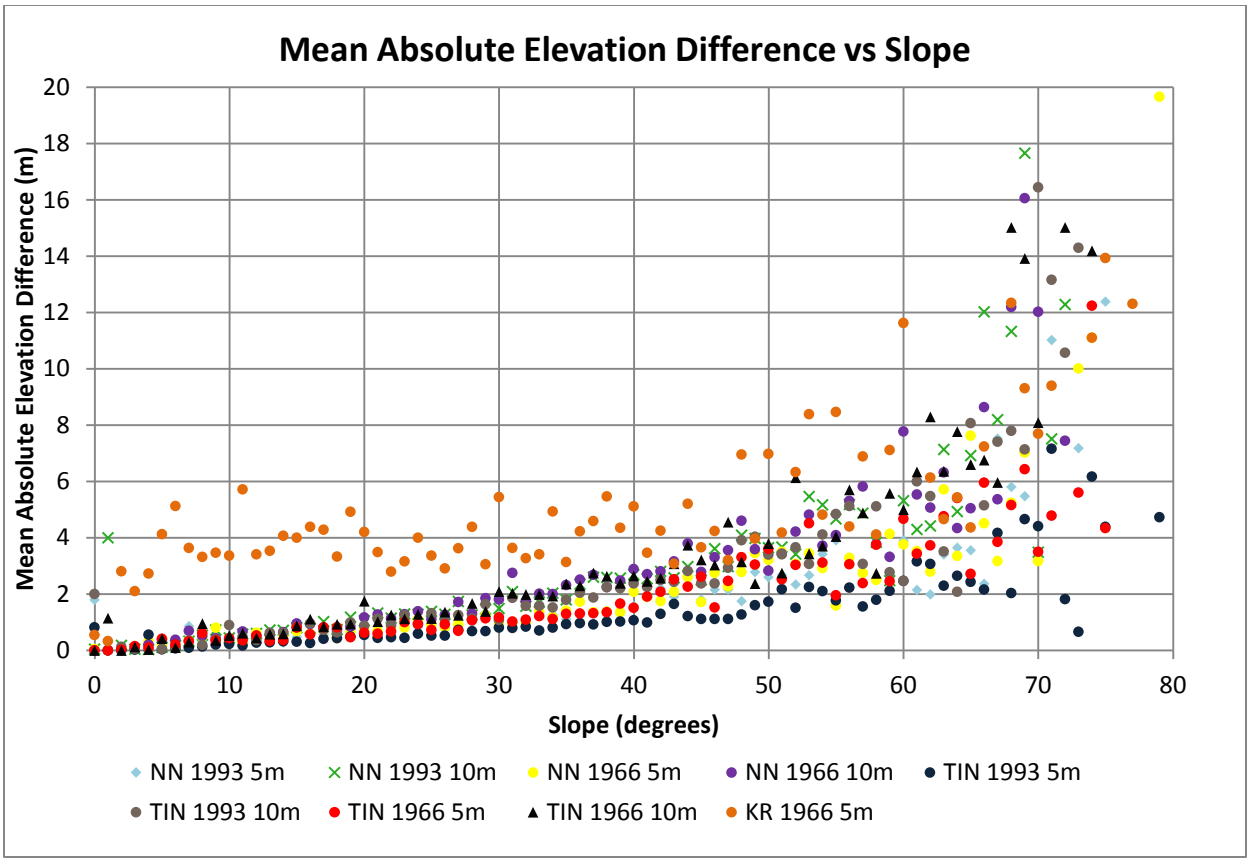

Figure 31. Mean absolute elevation differences plotted against slope.

Figure 31 shows an overall picture where the mean absolute elevation differences from the chosen DEMs (NN 1966 and 1993 5m, TIN 1966 and 1993 10m, and Kriging 1966 5m) are plotted against slope, giving a clearer picture of the trend that larger differences occur on steeper slopes. A more rapid increase is noticed on slopes that are steeper than 50 degrees.

Table 8. The coefficient of determination.

Raster data sets	R^2
NN 1993 5m	0.6098
NN 1993 10m	0.6072
NN 1966 5m	0.5443
NN 1966 10m	0.6886
TIN 1993 5m	0.6509
TIN 1993 10m	0.6119
TIN 1966 5m	0.7090
TIN 1966 10m	0.6828
KR 1966 5m	0.3607

Table 8 shows the coefficient of determination (R^2) for the chosen DEMs where the mean absolute elevation difference is plotted against slope. The R^2 value indicates the relationship between the variables. All the raster data sets except for Kriging show quite a strong relationship between the variables. This confirms the above mentioned trend that the mean absolute elevation difference increases with slope.

In order to find out whether there is a correlation between the mean absolute elevation differences and aspect, the following study was carried out in a similar manner as studied by Racoviteanu et al. (2007). Aspect maps were created for each DEM of interest (NN 1966 and 1993, with resolutions of 5 and 10 m, TIN 1966 and 1993, with resolutions of 5 and 10 m). The aspect value was extracted at the test points in the glacier-free area. The mean absolute elevation difference was calculated for each slope aspect of interest. The acquired results are seen in Figure 32. The graphs show that elevation differences do not depend on slope aspect. The mean absolute elevation differences do not exceed 3.5 m. Smaller differences are observed on slopes facing to the E compared to the slopes facing to SW. Larger mean elevation differences were observed in DEMs with a resolution of 10 m compared to DEMs with a resolution of 5 m.

Mean Absolute Elevation Difference vs Aspect
(NN 1966 5 m)

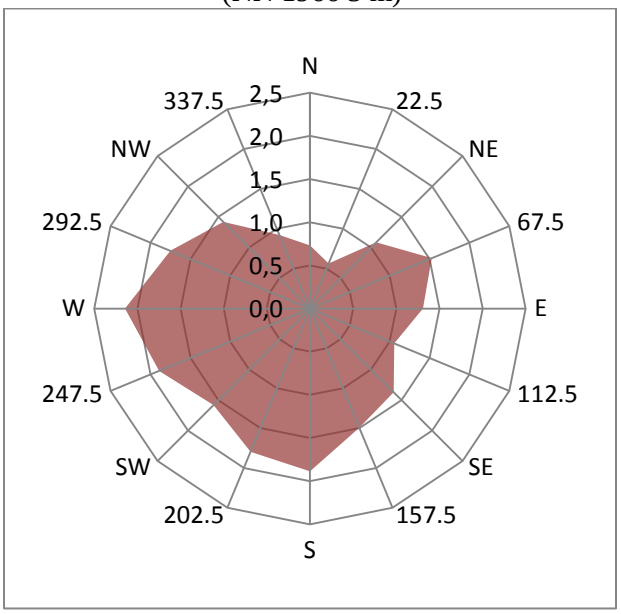

Mean Absolute Elevation Difference vs Aspect
(NN 1966 10 m)

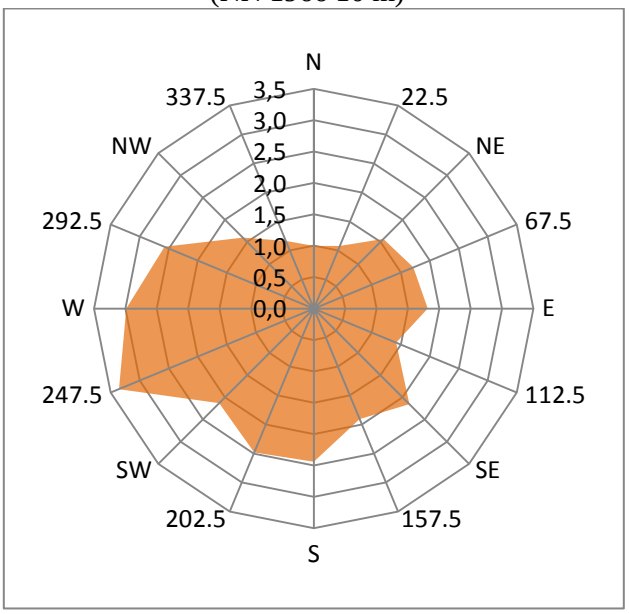

Mean Absolute Elevation Difference vs Aspect
(TIN 1966 5 m)

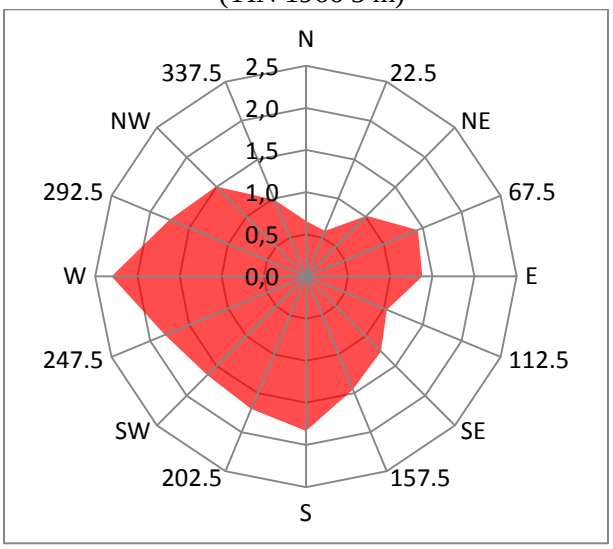

Mean Absolute Elevation Difference vs Aspect
(TIN 1966 10 m)

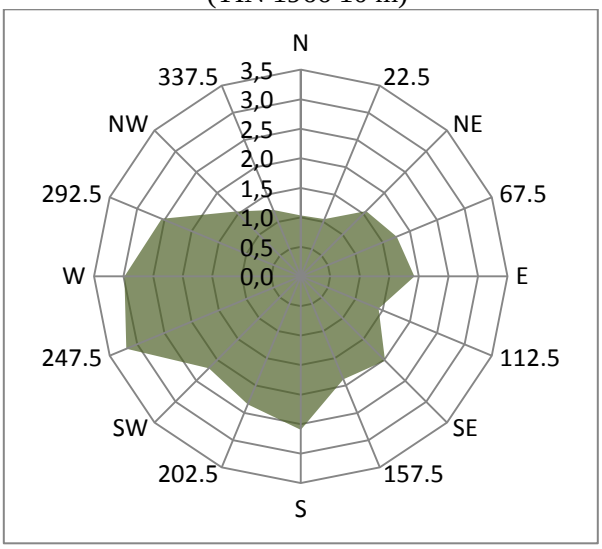

Mean Absolute Elevation Difference vs Aspect
(NN 1993 5 m)

Mean Absolute Elevation Difference vs Aspect
(NN 1993 10 m)

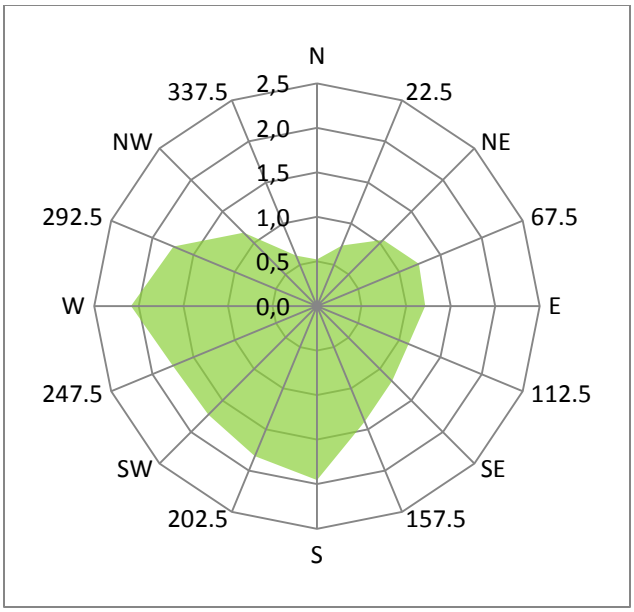

Mean Absolute Elevation Difference vs Aspect (TIN 1993 5 m)

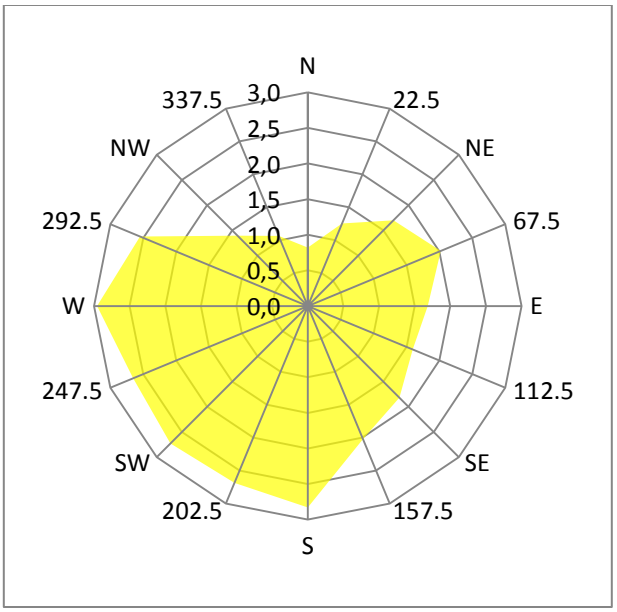

Mean Absolute Elevation Difference vs Aspect (TIN 1993 10 m)

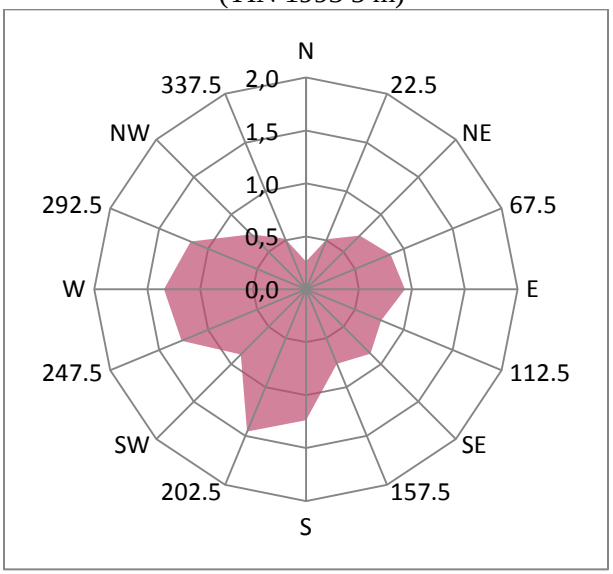

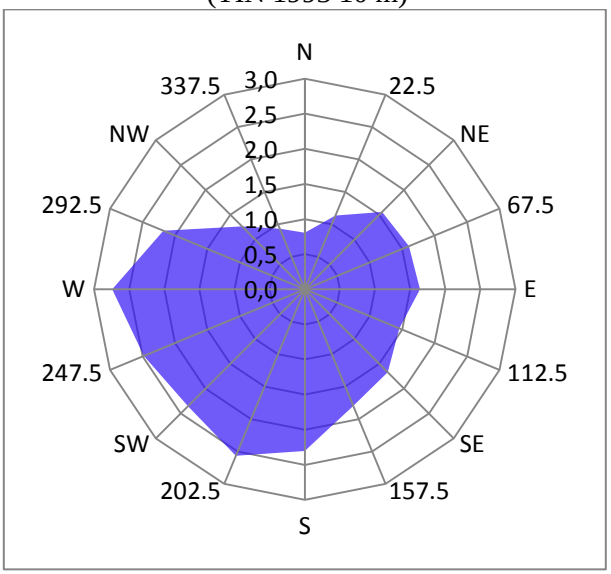

Figure 32. Radar graphs of mean absolute elevation differences as a function of aspect.

5.7 DEM comparison with LiDAR data in non-glacier areas

The quality of the contour maps was tested by comparing them with the reference data which was a LiDAR DEM in the current study. This testing was performed in a glacier-free area that was considered to be stable and where no elevation change was expected.

The DEM grid generated from LiDAR data with a 1 m resolution outside the glacier was considered to be a reference model for the accuracy assessment of the other digital terrain models. The corresponding LiDAR model with a 1 m resolution was assumed 100% accurate, representing the real terrain elevation. It was also used for generating LiDAR DEMs with 5m and 10 m resolutions. The AGGREGATE algorithm was used for this generalization process. Each pixel in the 5 m DEM was calculated as a mean value of all 25 pixels in the 1 m resolution model following the research by Burdziej and Kunz (2007).

Two approaches were tested comparing the contour maps to the reference grid – by subtracting the contour map from the reference grid and by testing the elevation change in sample points taken from the LiDAR data. The DEM surfaces interpolated with the natural neighbour and TIN algorithms were tested as they showed the best results (resolution 5m and 10m). Figures 33 - 40 show the results of the performed DEM (5 m resolution) analyses in the glacier-free area. The DEM (10 m resolution) analyses is found in Appendix 9.6.

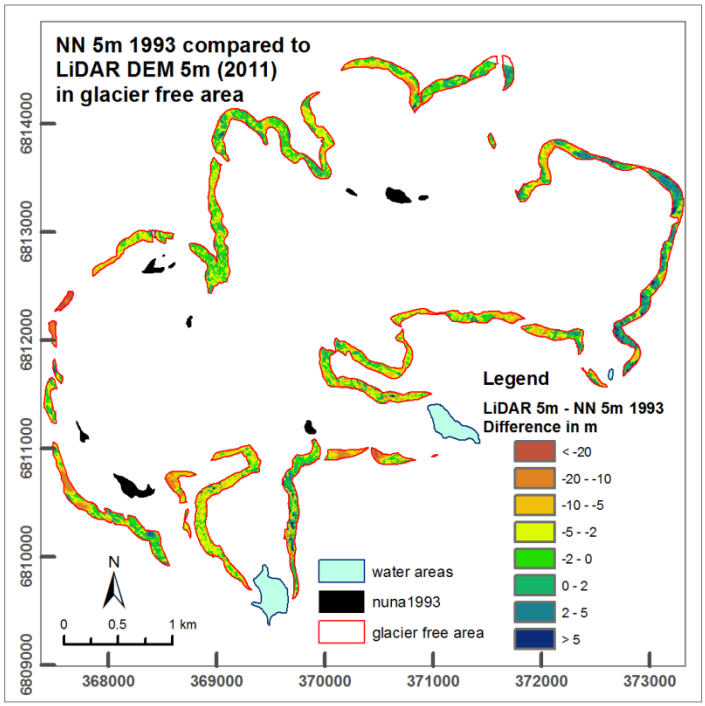

Figure 33. Difference in elevation comparing LiDAR (2011) DEM (resolution 5m) and DEM interpolated from contour lines from 1993 using natural neighbour method (resolution 5m). Surface elevation differences were calculated by subtracting DEMs on a cell-by-cell basis.
Source: Own elaboration
Coordinate System: WGS 1984 UTM Zone 32N

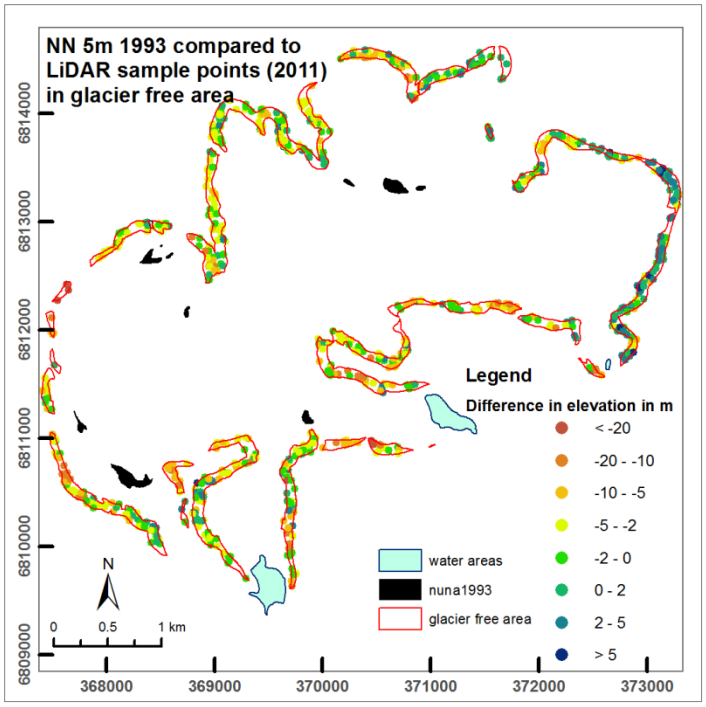

Figure 34. Difference in elevation comparing LiDAR sample points and DEM interpolated from contour lines from 1993 using natural neighbour method (resolution 5m). Surface elevation differences were calculated by extracting the cell values of the interpolated raster based on a set of sample points of LiDAR data (2011).
Source: Own elaboration
Coordinate System: WGS 1984 UTM Zone 32N

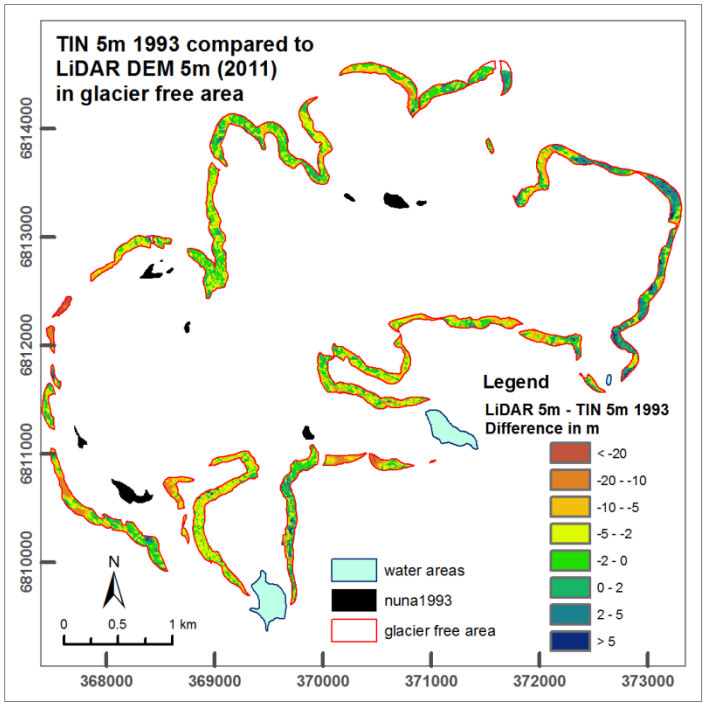

Figure 35. Difference in elevation comparing LiDAR (2011) DEM (resolution 5m) and DEM interpolated from contour lines from 1993 using TIN method (resolution 5m). Surface elevation differences were calculated by subtracting DEMs on a cell-by-cell basis.
Source: Own elaboration
Coordinate System: WGS 1984 UTM Zone 32N

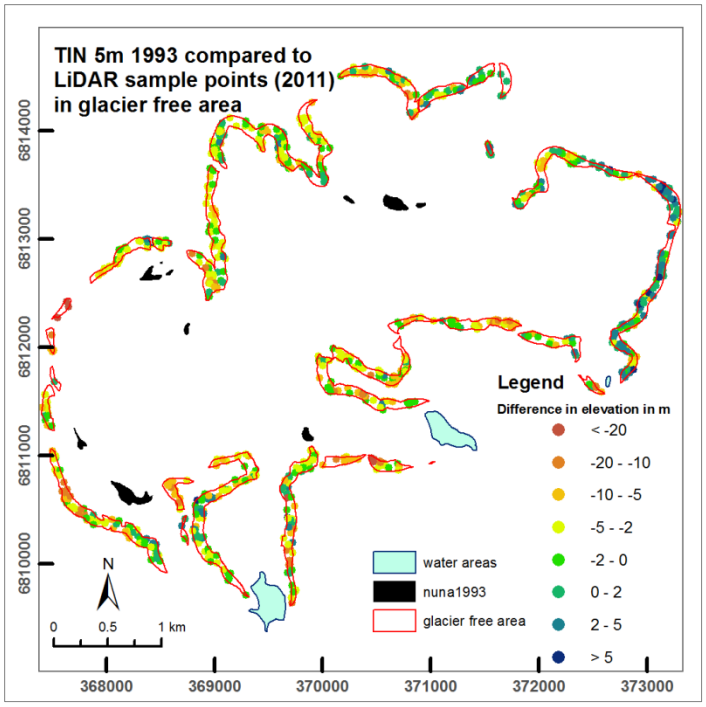

Figure 36. Difference in elevation comparing LiDAR sample points and DEM interpolated from contour lines from 1993 using TIN method (resolution 5m). Surface elevation differences were calculated by extracting the cell values of the interpolated raster based on a set of sample points of LiDAR data (2011).
Source: Own elaboration
Coordinate System: WGS 1984 UTM Zone 32N

Both approaches yielded very similar results. The greatest elevation differences were observed at the east side of the glacier where the elevation differences has increased and on the west side of the glacier (west side of Sundfjordbjørnen) where the elevation has decreased.

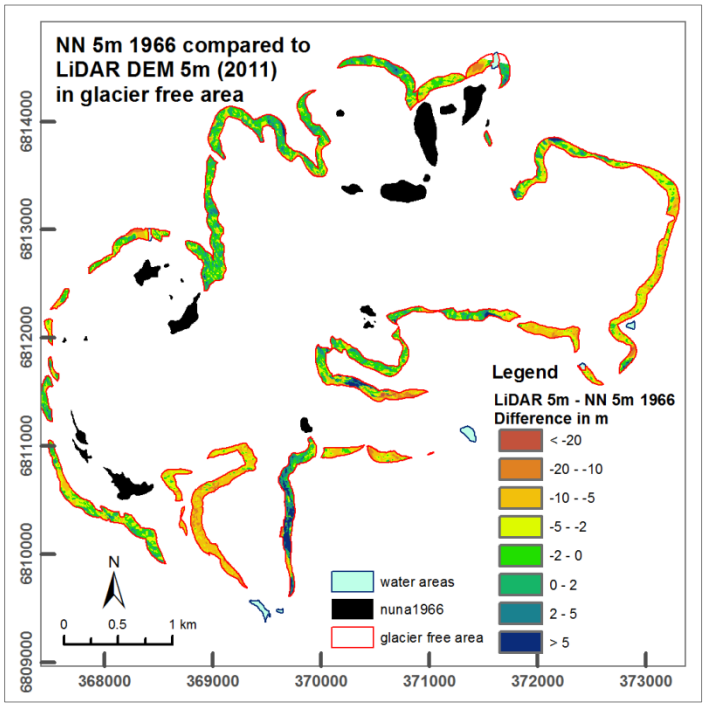

Figure 37. Difference in elevation comparing LiDAR (2011) DEM (resolution 5m) and DEM interpolated from contour lines from 1966 using natural neighbour method (resolution 5m). Surface elevation differences in a glacier free area were calculated by subtracting DEMs on a cell-by-cell basis.
Source: Own elaboration
Coordinate System: WGS 1984 UTM Zone 32N

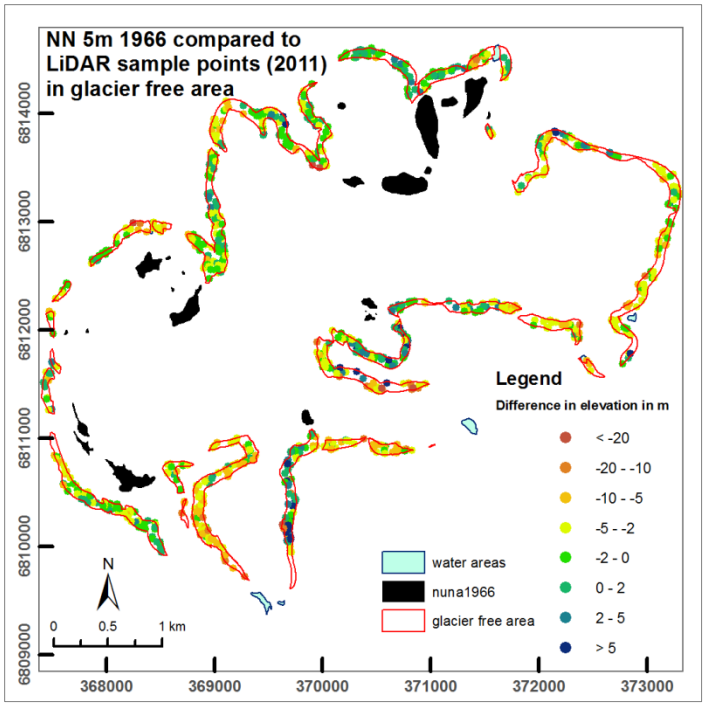

Figure 38. Difference in elevation comparing LiDAR sample points and DEM interpolated from contour lines from 1966 using natural neighbour method (resolution 5m). Surface elevation differences were calculated by extracting the cell values of the interpolated raster based on a set of sample points of LiDAR data (2011).
Source: Own elaboration
Coordinate System: WGS 1984 UTM Zone 32N

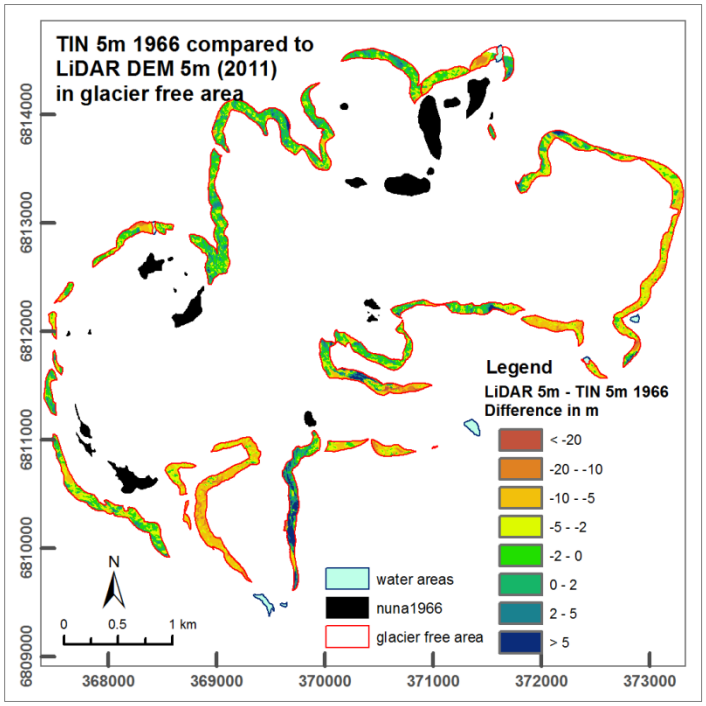

Figure 39. Difference in elevation comparing LiDAR (2011) DEM (resolution 5m) and DEM interpolated from contour lines from 1966 using TIN (resolution 5m). Surface elevation differences in a glacier free area were calculated by subtracting DEMs on a cell-by-cell basis.
Source: Own elaboration
Coordinate System: WGS 1984 UTM Zone 32N

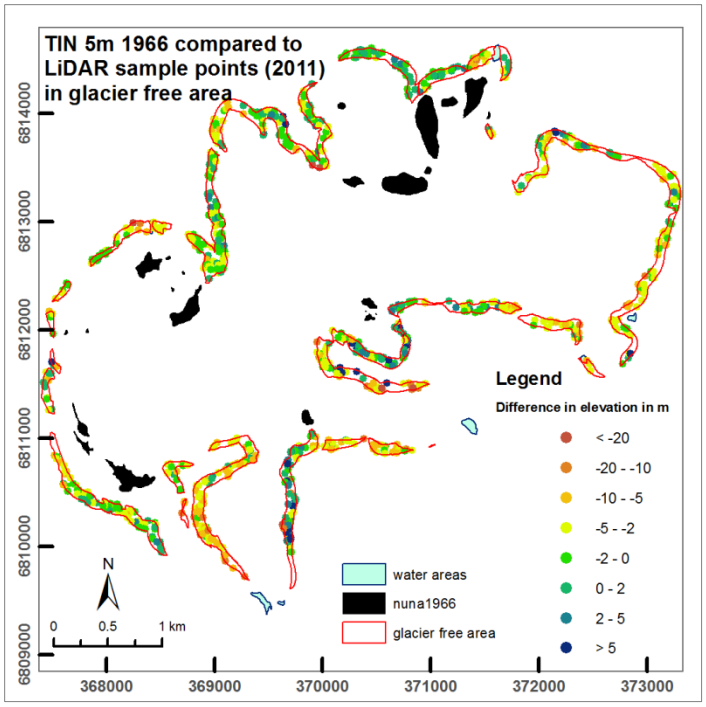

Figure 40. Difference in elevation comparing LiDAR sample points and DEM interpolated from contour lines from 1966 using natural neighbour method (resolution 5m). Surface elevation differences were calculated by extracting the cell values of the interpolated raster based on a set of sample points of LiDAR data (2011).
Source: Own elaboration
Coordinate System: WGS 1984 UTM Zone 32N

The results for the year 1966 showed an increase in elevation differences on the east side of Skaddalsbreen (the very south tongue of Jostefonn). A greater decrease in elevation differences than in other places was observed on the west side of Skaddalsbreen and on the east side of Jostefonn glacier.

Table 9. RMSE for the tested interpolated glacier free surfaces against the reference grid (LiDAR) (1) using sample points from the reference grid and extracting elevation values from the interpolated raster and (2) performing calculations on a cell-by-cell basis between the raster surfaces.

Glacier free area	RMSE		Glacier free area	RMSE	
LiDAR versus NN 5m 1993	5.542	Sample point method	LiDAR versus NN 5m 1966	5.042	Sample point method
LiDAR versus NN 10m 1993	5.711		LiDAR versus NN 10m 1966	5.436	
LiDAR versus TIN 5m 1993	5.498		LiDAR versus TIN 5m 1966	5.053	
LiDAR versus TIN 10m 1993	5.694		LiDAR versus TIN 10m 1966	5.436	
LiDAR versus NN 5m 1993	5.245	Calculations on cell-by-cell basis between the rasters	LiDAR versus NN 5m 1966	5.256	Calculations on cell-by-cell basis between the rasters
LiDAR versus NN 10m 1993	5.665		LiDAR versus NN 10m 1966	5.145	
LiDAR versus TIN 5m 1993	5.217		LiDAR versus TIN 5m 1966	5.489	
LiDAR versus TIN 10m 1993	5.635		LiDAR versus TIN 10m 1966	5.131	

The following results (Table 9) show that the contour lines for the year 1966 are slightly more accurate than the contour lines for the year 1993. It was already mentioned before (Chapter 3.2) that due to the fact that the glacier area was partly covered by snow the aerial photographs taken in 1993 had poor contrast that have lead to errors in generating contour lines as well as in estimating the glacier border line.

Comparing the two methods used, the calculations between the DEMs on a cell-by-cell basis and by extracting values from the raster by sample points of the reference grid rendered very similar RMSE values. The RMSE here was not affected by the interpolating method and there was only a slight difference between the resolutions tested (5m and 10m). Again, as the smaller the cell size (Chapter 5.1.2), the better the results that can be achieved.

5.8 DEM comparison with LiDAR data in glacier areas

Figures 41 to 44 depict the elevation changes in the glacier area. These figures show the changes that have occurred in the period from 1993 to 2011. Figures 45 to 48 show how the glacier has changed in the period from 1966 to 2011. The results with a resolution of 10m are found in Appendix 9.6.

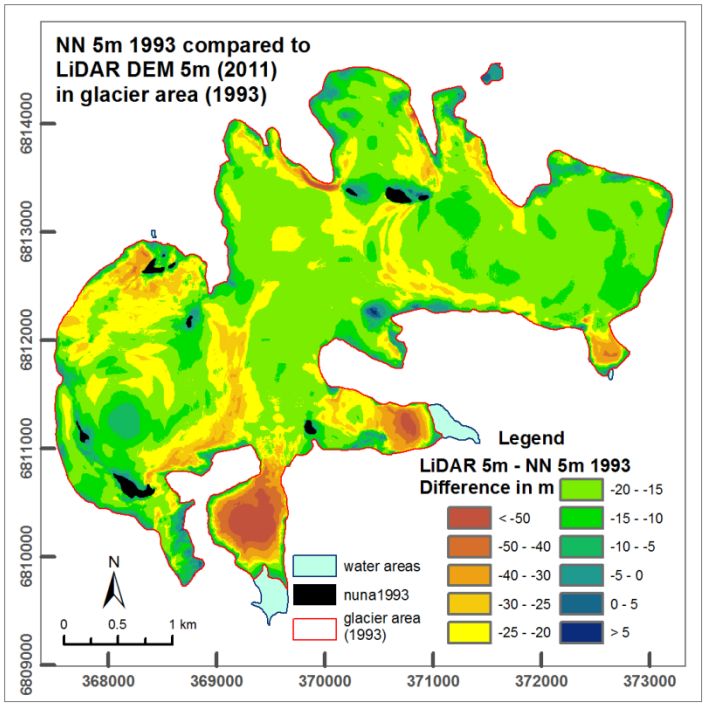

Figure 41. Difference in elevation comparing LiDAR (2011) DEM (resolution 5m) and DEM interpolated from contour lines from 1993 using natural neighbour method (resolution 5m). Surface elevation differences were calculated by subtracting DEMs on a cell-by-cell basis.
Source: Own elaboration
Coordinate System: WGS 1984 UTM Zone 32N

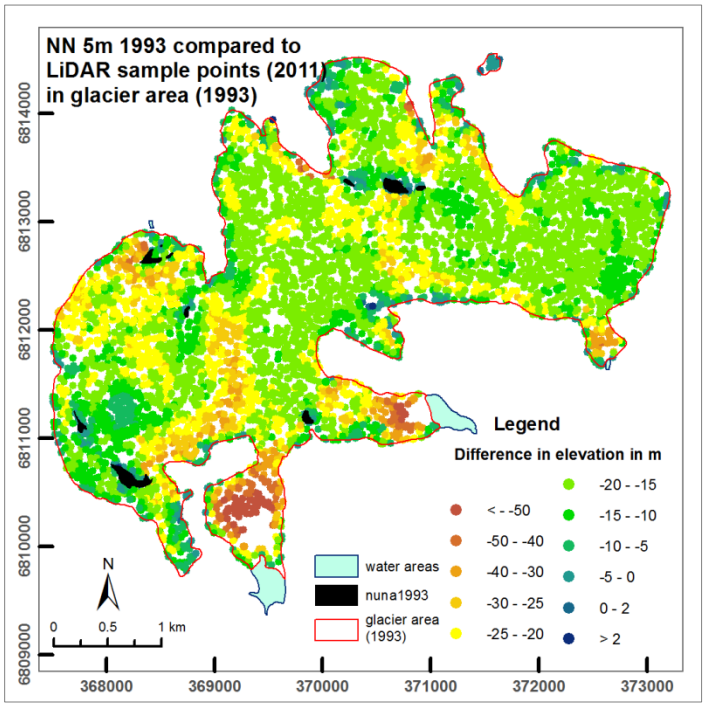

Figure 42. Difference in elevation comparing LiDAR sample points and DEM interpolated from contour lines from 1993 using natural neighbour method (resolution 5m). Surface elevation differences were calculated by extracting the cell values of the interpolated raster based on a set of sample points of LiDAR data (2011).
Source: Own elaboration
Coordinate System: WGS 1984 UTM Zone 32N

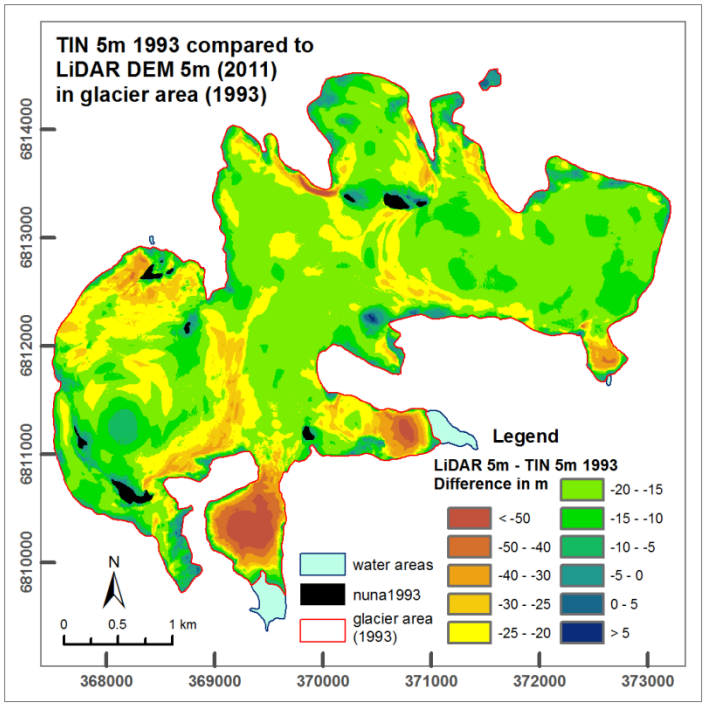

Figure 43. Difference in elevation comparing LiDAR (2011) DEM (resolution 5m) and DEM interpolated from contour lines from 1993 using TIN method (resolution 5m). Surface elevation differences were calculated by subtracting DEMs on a cell-by-cell basis.
Source: Own elaboration
Coordinate System: WGS 1984 UTM Zone 32N

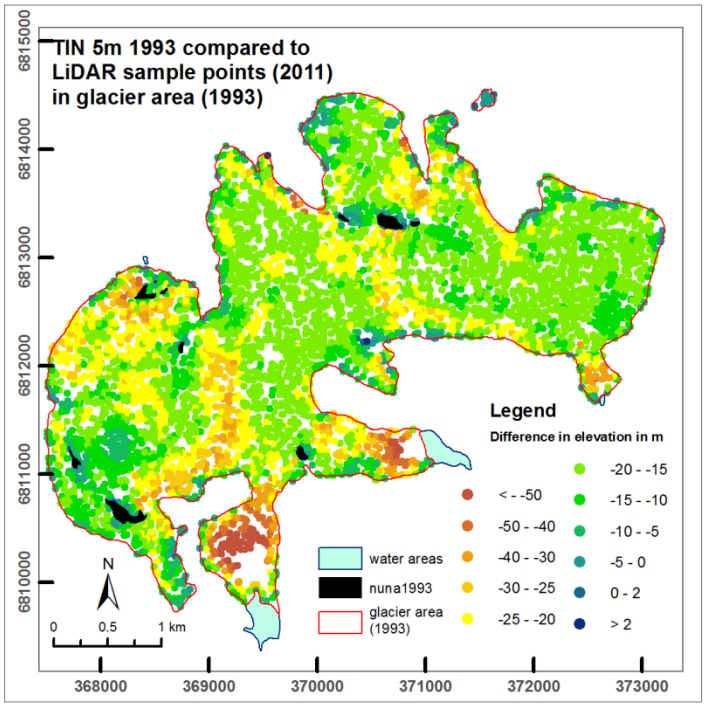

Figure 44. Difference in elevation comparing LiDAR sample points and DEM interpolated from contour lines from 1993 using TIN method (resolution 5m). Surface elevation differences were calculated by extracting the cell values of the interpolated raster based on a set of sample points of LiDAR data (2011).
Source: Own elaboration
Coordinate System: WGS 1984 UTM Zone 32N

The results show the greatest differences at the glacier tongues (Svartevassbreen, Skaddalsbreen). There was a noticeable elevation decrease in the whole area of Jostefonn (from 15 to 25 m decrease).

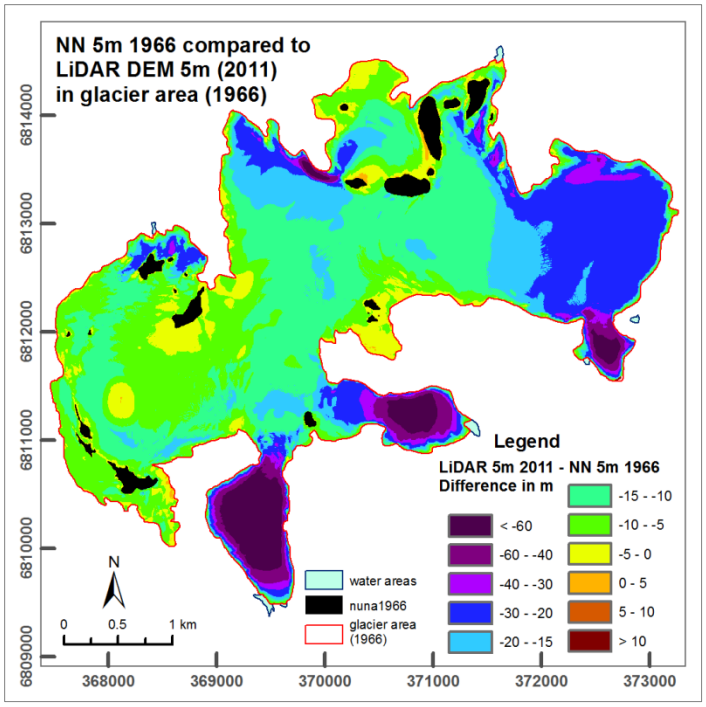

Figure 45. Difference in elevation comparing LiDAR (2011) DEM (resolution 5m) and DEM interpolated from contour lines from 1966 using natural neighbour method (resolution 5m). Surface elevation differences in a glacier free area were calculated by subtracting DEMs on a cell-by-cell basis.
Source: Own elaboration
Coordinate System: WGS 1984 UTM Zone 32N

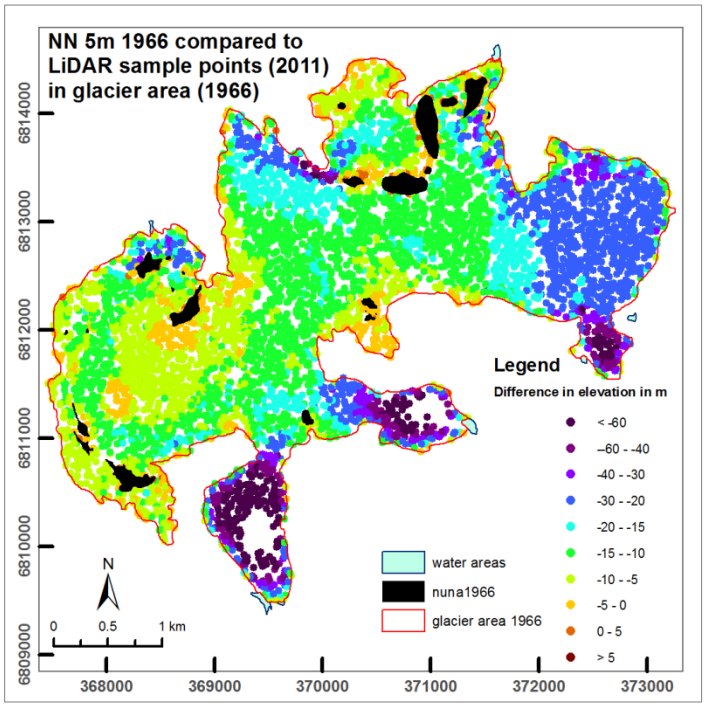

Figure 46. Difference in elevation comparing LiDAR sample points and DEM interpolated from contour lines from 1966 using natural neighbour method (resolution 5m). Surface elevation differences were calculated by extracting the cell values of the interpolated raster based on a set of sample points of LiDAR data (2011).
Source: Own elaboration
Coordinate System: WGS 1984 UTM Zone 32N

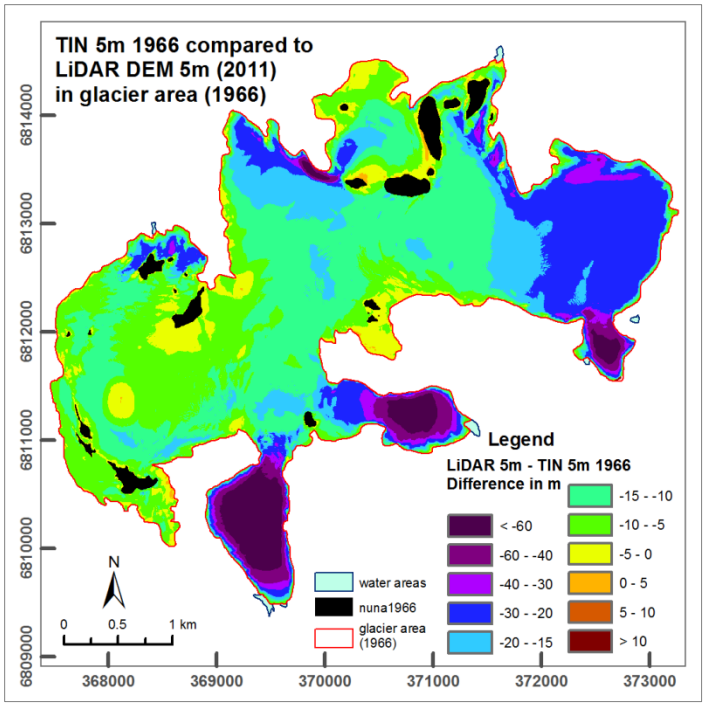

Figure 47. Difference in elevation comparing LiDAR (2011) DEM (resolution 5m) and DEM interpolated from contour lines from 1966 using TIN (resolution 5m). Surface elevation differences in a glacier free area were calculated by subtracting DEMs on a cell-by-cell basis.
Source: Own elaboration
Coordinate System: WGS 1984 UTM Zone 32N

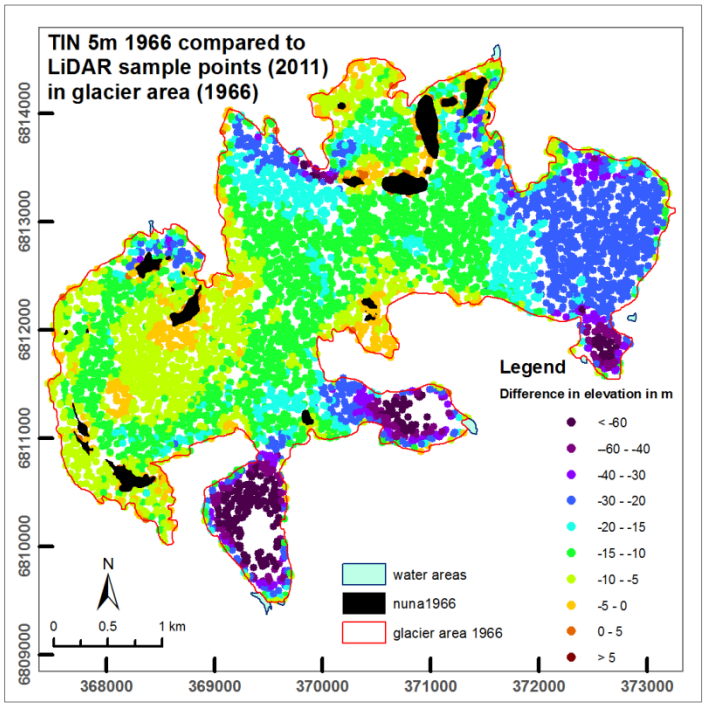

Figure 48. Difference in elevation comparing LiDAR sample points and DEM interpolated from contour lines from 1966 using natural neighbour method (resolution 5m). Surface elevation differences were calculated by extracting the cell values of the interpolated raster based on a set of sample points of LiDAR data (2011).
Source: Own elaboration
Coordinate System: WGS 1984 UTM Zone 32N

The glacier tongues are the places where the greatest decrease in elevation is noticeable comparing data from 1966 and LiDAR data from 2011. The eastern part of Jostefonn glacier (Flatbreen) also decreased in elevation. The highest area of the glacier (Sundfjordbjørnen) did not change considerably.

Table 10 shows how the Jostefonn glacier changed in the period from 1966 to 2011. The greatest changes were observed in the period between 1993 and 2011. There were hardly any changes from 1966 to 1993. Andreassen (1998) in her study also stated that there were small changes in the Jostefonn glacier volume between 1966 and 1993. The upper parts of the glacier have increased in elevation whereas the lower parts have decreased in elevation. Figure 49 shows a very clear picture (elevation increase and decrease) of the glacier situation between 1966 and 1993. The greatest changes have therefore taken place starting in 1993 and that indicates that the Jostefonn glacier has been affected by global warming.

Table 10. Volume change in Jostefonn glacier in the period between 1966 and 2011.

Interpolation method	decrease in volume (x 10^8 m^3)	decrease in volume (x 10^8 m^3)	decrease in volume (x 10^8 m^3)	increase in volume (x 10^8 m^3)
	1966 - 2011	**1993 - 2011**	**1966 -1993**	**1966 -1993**
NN 5	-2.2	-2.3	-0.6	0.7
TIN 5	-2.2	-2.3	-0.5	0.7

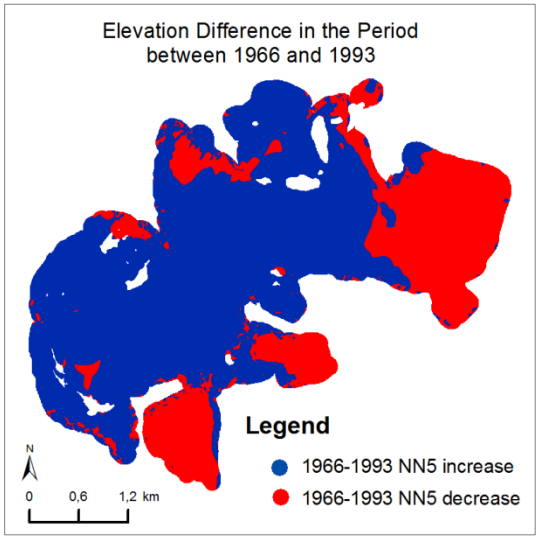

Figure 49. Elevation difference – elevation increase/decrease – in the period between 1966 and 1993. Increase is depicted in blue and decrease – in red.
Source: Own elaboration
Coordinate System: WGS 1984 UTM Zone 32N

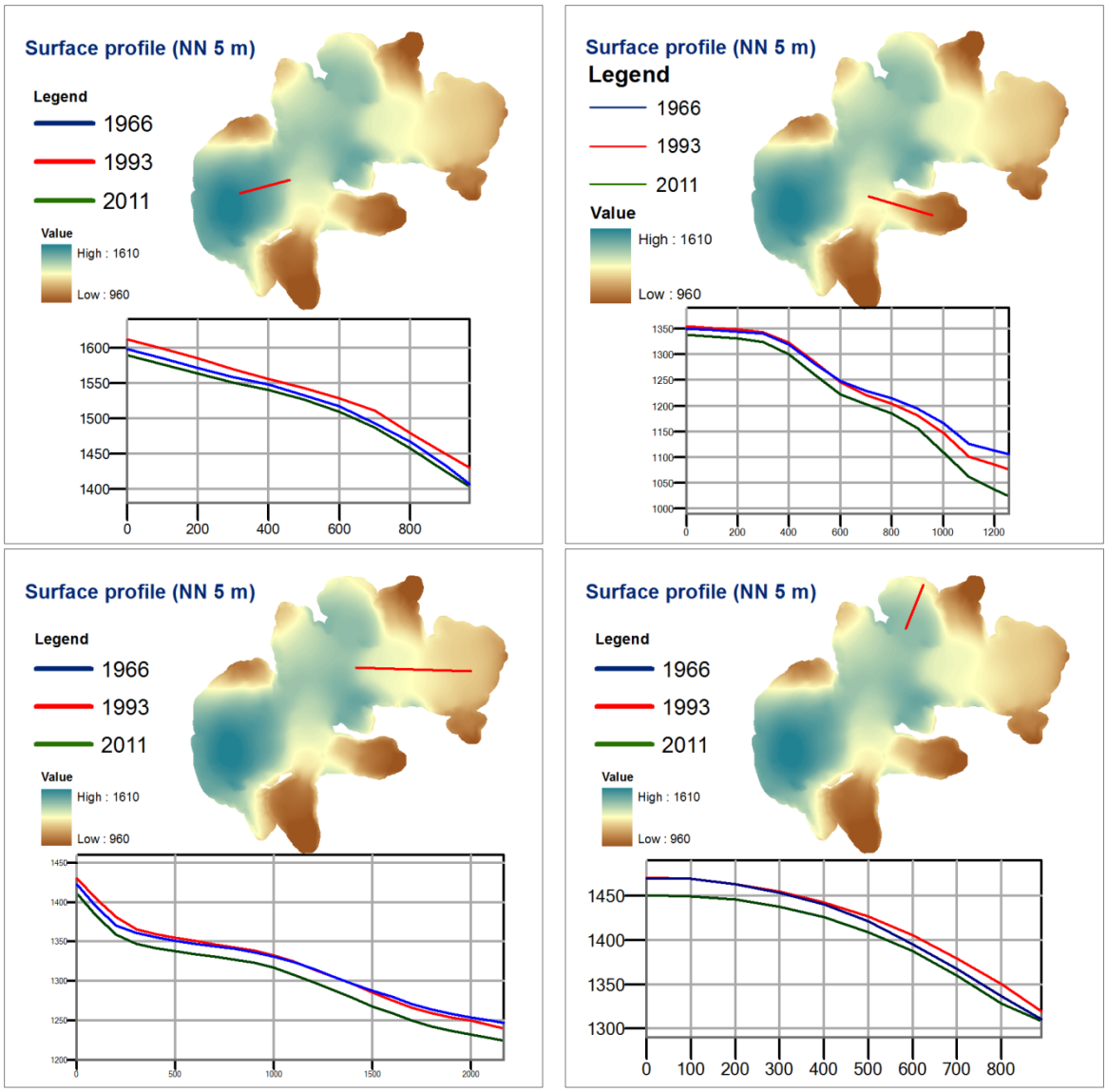

Figure 50. Surface profiles of Jostefonn glacier (NN 5 m, years 1966 – blue, 1993 – red and 2011 – green). X axis shows profile length and Y axis shows elevation.
Source: Own elaboration
Coordinate System: WGS 1984 UTM Zone 32N

The change in elevation of the Jostefonn glacier is presented in four surface profiles in Figure 50 where the elevation of each of the three years (1966, 1993 and 2011) is depicted in three different colours. There is no doubt that the glacier has decreased in elevation over time. The green line in the surface profile corresponding to the elevation in 2011 shows that the elevation has decreased compared to years 1966 and 1993. In the

period between 1966 and 1993 it can be seen that in some places the glacier has increased in elevation, decreased in other areas or remained without changes.

6. Discussion

6.1 Accuracy of DEMs created from contour lines and LiDAR data

The research focuses on assessing the accuracy of DEMs. DEMs were created from contour lines and LiDAR data points. The available contour lines with a contour interval of 10m from the year 1966 and 1993 were used. The terracing effect was observed in the resulting raster data sets. That was observed due to a large concentration of elevation points on the contour lines and no information between the contour lines. The terracing effect might be lessened if contour lines with a smaller contour interval were available. But that refers only to flat or gently sloping terrain. In very steep terrain closer contour lines are observed and that leads to another problem when generating a DEM – one or more elevation points per raster cell depending on the cell size used. In his study Kunqing Xie *et al.* (2003) dealt with steep terrains. The issue of that study was that most interpolations from contour lines failed to address the problem of the multi-value cells (MVCs) and therefore it was difficult to deal with steep slopes. Two or more contour lines could go through one cell because the terrain was steep and the contour line density was very high in those places. They suggested a new approach that involved storing additional information of contour lines that went through the MVCs (Kunqing Xie *et al.*2003). The method suggested by Kunqing Xie *et al.* (2003) was not tested in the current thesis but that could be a solution to the elevation errors in steep terrain. The results of the current thesis and other studies (Droj 2000; Toutin 2002; Kunqing Xie *et al.* 2003; Surazakov & Aizen 2006; Hasan *et al.* 2011) showed that there were larger errors in elevation when the terrain was steep than when it was flat. It was even more obvious when the resolution of the raster was lower (larger cell size). Using a smaller cell size reduced the amount of errors to a certain degree but a larger amount of data was generated and the processing time of the data increased (Kunqing Xie *et al.* 2003).

Ziadat (2007) suggested using different models for each area separately – one model for flat areas and another model for steep areas. His conclusion was that the accuracy for flat areas is different from the accuracy of steep areas and he even suggested using different

contour line spacing and grid cell size for flat and steep areas in order to achieve an optimum accuracy (Ziadat 2007).

Li (1994) in his study came to a conclusion that the accuracy of a DEM created from contour lines could be increased by 40% to 60% if additional feature-specific data (e.g. peats, pits, additional points) were included. Also Burdziej & Kunz (2007) suggested using additional information (extra elevation points, break lines, etc.) in a DEM generation to increase its accuracy. There were not available additional data in the current study. The field measurements (glaciological method) could have been of a great use in accuracy assessment of DEMs.

6.2 Interpolation methods

There are quite a number of studies on interpolation methods for different applications and terrain types. In their study Jing Li and Heap (2011) analysed the performance of 72 methods/sub-methods applied in a total of 53 comparative environmental studies. Inverse Distance Weighing (IDW), ordinary kriging (OK) and ordinary co-kriging (OCK) are the most frequently used methods according to their study. In glaciology, there are also available studies on interpolation techniques applied to construct DEMs either from digitized contour data or from LiDAR point clouds. Four interpolation methods (Tension Spline, IDW, TIN and NN) were tested in the Southern Range, Tasmania, Australia in the study by Zhang *et al* (2004). In this study the best results were achieved by TIN and NN interpolators after performing statistical analysis by calculating quality indicators and histograms of error distributions. In the study by Rivera (2004) three interpolation methods (IDW, TIN and ANUDEM) were tested at the Chico glacier, Southern Patagonia Icefield, Chile. Based upon two criteria (the number of artefacts presented in the resulting DEM and the time and effort of manual interaction needed to produce the DEM), ANUDEM proved to be the best method (Rivera 2004). Racoviteanu *et al* (2007) tested four interpolation methods (ANUDEM, Spline, IDW and TIN) in the Peruvian Andes and the ANUDEM algorithm was found to be superior to other interpolation methods. In the Peruvian Andes study the DEMs were validated against test points in the glacier-free areas. Engh (2013) in his Master's thesis tested five interpolation methods (NN,

ANUDEM, IDW, Kriging and Spline) with NN giving the best results and Spline the worst. Three interpolation methods (IDW, Spline and TIN) were tested by Kamp *et al* (2005) in Cerro Sillajhuay, Andes, Chile/Bolivia where the best results were achieved applying the TIN interpolator. In the study of Peralvo (2003) a total of twelve DEMs were generated using different interpolation methods (ANUDEM, Kriging, IDW and Radial Basis Functions) and parameter settings. ANUDEM outperformed the other methods in the corresponding study. Andreassen (1998, 1999) and Andreassen *et al* (2002) used the TIN interpolater as it proved to be the best method for creating DEMs from contour lines. Racoviteanu *et al* (2007) mentioned in their study that "there is no established interpolation method especially suitable for creating elevation data from topographic maps for accurate representation of glacier terrain".

Table 11. An overview of the interpolation methods used in selected other glacial studies in comparison with the current study. Symbols that are marked red have rendered the best results.

		Interpolation Method						
Study	Year	TIN	NN	Spline	IDW	ANUDEM	Kriging	Radial Basis Functions
Zhang *et al*	2004	X	X	X	X			
Rivera	2004	X			X	X		
Racoviteanu *et al*	2007	X		X	X	X		
Engh	2013		X	X	X	X	X	
Kamp *et al*	2005	X		X	X			
Peralvo	2003				X	X	X	X
Andreassen	1998, 1999	X			X			
Andreassen *et al*	2002	X			X			
Current study	2013	X	X	X	X	X	X	

Table 11 shows an overview of interpolation methods used in glacial studies. According to the given table, the TIN, NN and ANUDEM interpolators rendered the best results compared to other interpolation techniques. This study also showed that the best results were achieved using the TIN and NN interpolators in order to generate DEMs from contour lines. IDW and Spline have been tested in several glaciological studies but in none of these studies have they presented good results. TIN, NN and ANUDEM seem to

be the best interpolators in glaciology when digital elevation models need to be generated from contour maps over the glacier area.

Table 12 shows an overview of interpolation methods used in other studies that are not devoted to glaciology. The same tendency is observed also here, although Spline and Kriging interpolation methods have showed good results in two of the studies.

Table 12. An overview of the interpolation methods used in selected other studies. Symbols that are marked red have rendered the best results.

		Interpolation Method					
Study	**Year**	**TIN**	**NN**	**Spline**	**IDW**	**ANUDEM**	**Kriging**
Sharma *et al*	2009	X		X	X	X	X
Priyakant *et al*	2003	X		X	X		
Mohamed *et al*	2011		X		X		X
Godone&Ganerno	2013		X	X	X		
Arun	2013		X	X	X	X	X

6.3 Cell size (resolution)

Another aspect is the chosen cell size (resolution) in creation of digital elevation models. The current study as well as other studies (Kienzle 2004; Ziadat 2007; Sharma *et al.* 2009) conclude that the accuracy of the DEM decreases progressively as resolution decreases. Ziadat (2007) states that even at the cell size of 10m the accuracy of the DEM has decreased considerably whereas Kienzle (2004) considers that an optimum grid cell size should be between 5m and 20m depending on terrain complexity. Hengl *et al*. (2004) proposes the suitable grid size to be half the average spacing between contour lines. Burdziej & Kunz (2007) conclude that by decreasing the resolution (increasing a cell size of a DEM) a DEM gets generalised and the overall error of a DEM is increased. The current research proved that a DEM with a resolution of 5m and 10m is more accurate than DEMs at a coarse resolution. The cell size of 1m rendered better results on steep terrains although the processing time of a DEM and data volume was increased.

6.4 Methods used assessing DEM accuracy

The accuracy of digital elevation models was tested by statistical methods, visual analyses and comparing the acquired DEMs to a reference source. Podobnikar (2009) considers that visual methods have been neglected and most of the studies rely heavily only on statistical methods. Table 14 shows the opposite as the majority of the selected glaciological studies have used visual analyses as one of the methods to assess the accuracy of digital elevation models.

Table 13 shows an overview of several methods used to access the accuracy of a DEM that covers the area of a glacier or several glaciers.

Table 13. Accuracy assessment in other glacier studies in comparison with the current study.

		Accuracy Assessment			
Study	**Year**	**Visualization**	**RMSE**	**Sources of More Accurate Data**	**Comparison to Glacier-Free Area**
Zhang *et al*	2004	**X**	**X**		
Racoviteanu *et al*	2007	**X**	**X**	**X**	**X**
Engh	2013		**X**	**X**	
Kamp *et al*	2005	**X**	**X**		
Peralvo	2003	**X**	**X**		
Andreassen	1998, 1999				**X**
Andreassen *et al*	2002				**X**
Suzarakov and Aizen	2006	**X**	**X**		**X**
Carlisle	2002	**X**	**X**	**X**	
D'Agata and Zanutta	2006	**X**			**X**
Tenant *et al*	2012				**X**
Current study	2013	**X**	**X**	**X**	**X**

Visualization techniques are considered to be easy to employ and they can give the first impression of the data and that is why they have been used in several studies as well as in the current study (see Table 13). Accuracy measures like the RMSE have been employed

frequently when dealing with the accuracy of a DEM. Nearly every study has used the RMSE as an accuracy measure to find out the best fitting model. Not so many studies have compared the acquired data with a more accurate data source. That may be due to the lack of either precise ground control points or data that can be considered to be the ground truth. Another method that has been used in glaciological studies is to test DEMs on glacier-free areas that are supposed to be constant and without change over years as carried out in this study.

Visual analyses and statistical measures pointed out the best performing interpolation method as well as the optimal resolution in a DEM creation. The further research was accomplished using only the most accurate DEMs instead of all the DEMs created at the beginning of the research. Both visual analysis and statistical approach showed the same results, thus supplementing each other. Podobnikar (2009) suggested the procedure for accuracy assessment of the spatial data sets where statistical and visual methods come after preparing of the data sets, followed by obtaining and analysing results. The current thesis proved the necessity of visual and statistical analyses.

6.5 Correlation between glacier changes and increase in temperature

The greatest changes in the Jostefonn glacier were observed in the period between 1993 and 2011. That can be explained by the average temperature increase over the last century. In their research Winkler *et al.* (2008) stated that over the last century there had been a significant increase in temperatures for almost all parts of Norway, ranging from 0.4 to 1.2^0C. According to Winkler *et al.* (2008) the 1990s had been the warmest decade. Free access weather and climate data from historical to real time observations are available from web portal eKlima provided by the Norwegian Meteorological Institute. Graphs in Figures 51 and 52 showing mean temperature increase are generated in eKlima. Førde is the closest weather station to the Jostefonn glacier. The horizontal axis shows the years when the mean temperatures were measured and the vertical axis shows the temperature deviation from normal (Fig. 51). Mean annual temperature is shown on vertical axis in Figure 52. A continual increase in temperature is observed in the graphs,

which explains the decrease in the Jostefonn glacier volume. There is observed correlation between temperature increase and glacier thinning over the period of time.

According to Nesje *et al*. (2008) the period 1989 – 1995 had heavy winter precipitation in western Norway resulting in glacier increase of up to 80m in a year. There were observed low winter precipitation and large summer melting during the period 2001 -2004 (Nesje *et al*. 2008). That explains the results of this thesis where the greatest changes in glacier elevation were observed after 1993.

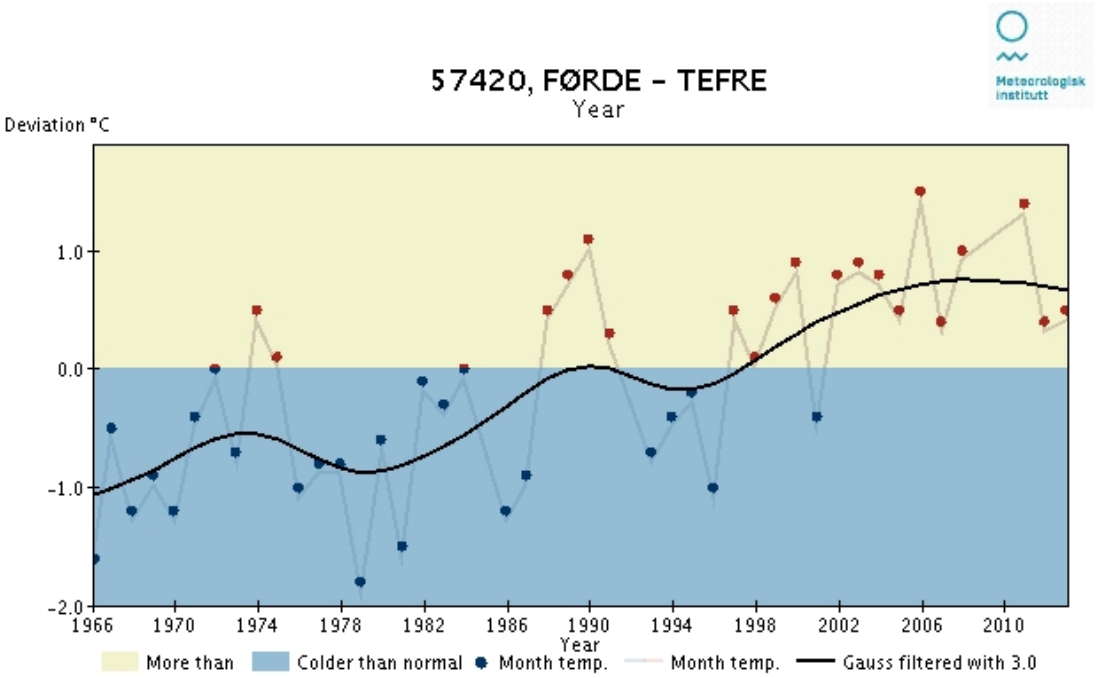

Figure 51. Temperature deviation from normal in the period from 1966 to 2013. A graph generated in eKlima by the Norwegian Meteorological Institute.

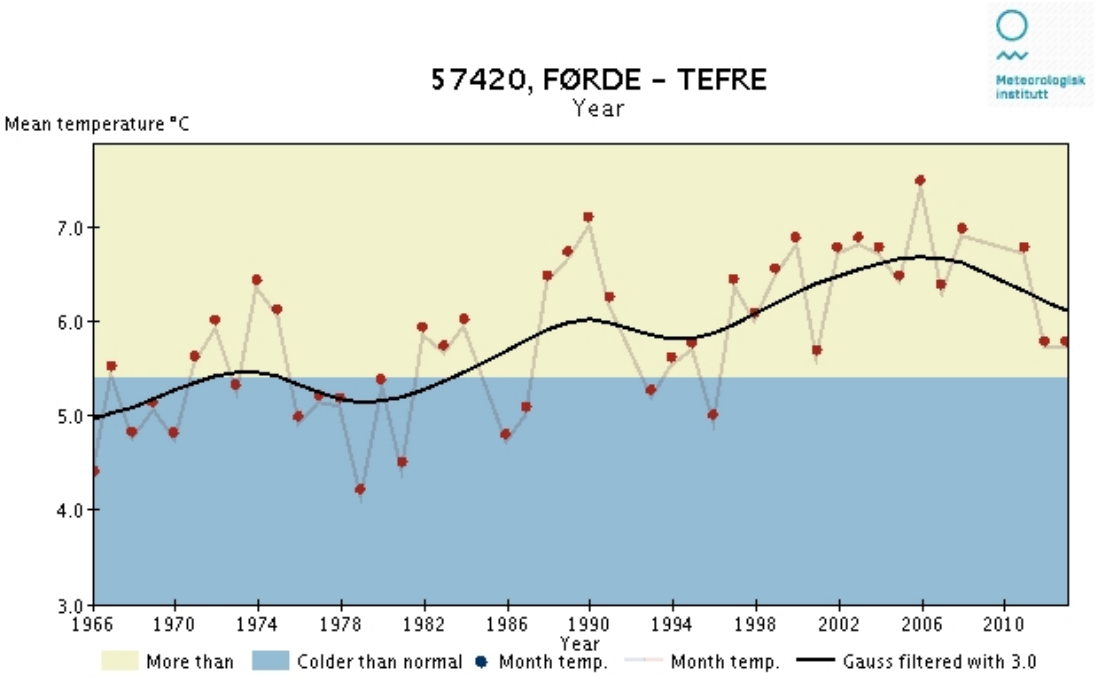

Figure 52. Mean annual temperature in the period from 1966 to 2013. A graph generated in eKlima by the Norwegian Meteorological Institute.

Graphs in Appendix 9.8 show temperature deviation and mean annual temperature in the period from 1940 to 2013.

The results of this research (5.7 and 5.8) showed the greatest elevation change at glacier tongues. According to Winkler *et al*. (2008), any change of the frontal position of a glacier tongue is a dynamic response to change in glacier ice mass. Figure 53 and close up figures of the two biggest tongues of the Jostefonn glacier in Appendix 9.9 visually show how the glacier tongues had changed over years.

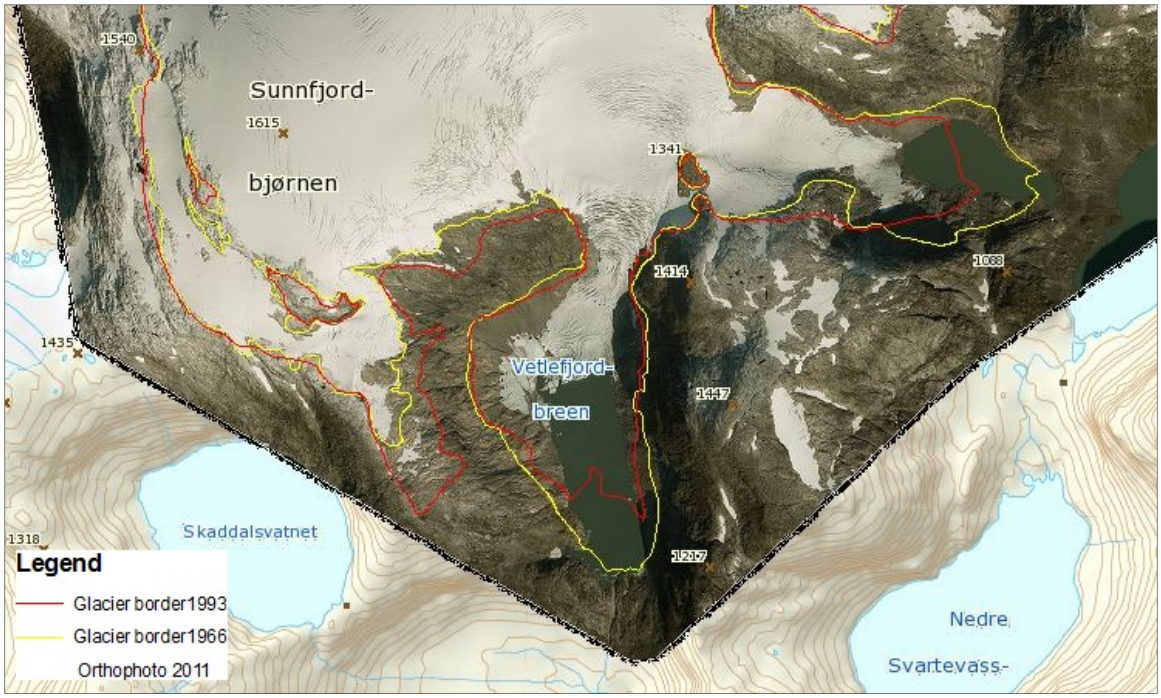

Figure 53. Glacier border in 1966 and 1993 in comparison with orthophoto from 2011.

7. Summary and conclusions

The various methods that were tested in this thesis were carried out in order to access the accuracy of DEMs over the Jostefonn glacier. The current study tested several interpolation methods and visualization techniques, performed statistical analyses as well as data comparison in the glacier-free area to acquire as much information as possible on the accuracy of the data used.

The first research objective was to evaluate the suitability of various interpolation methods to construct DEMs for glaciological studies. According to this study the NN and TIN interpolators were the most suitable in glacier change analysis. Those two interpolators showed the best results both in visual assessment and by statistical analysis. The suitability of the interpolation methods was also tested at different resolutions (5 m, 10 m, 20 m and 50 m). The best results were achieved by choosing a smaller cell size. It was observed that by decreasing the resolution the overall error of the DEM increased.

The second research objective was to assess elevation differences between the DEM from LiDAR data and the DEM from topographic data in the glacier-free area. Two methods were tested: on a cell-by-cell basis and by extracting the elevation at the test points. Both methods rendered very similar results – similar RMSE values and similar elevation differences both outside the glacier area and in glacier areas.

The third research objective was to discuss the methods applied and assess how reliable the results were. The employed methods rendered very similar results and that indicated that the results were reliable.

The fourth research objective was to identify the spatial distribution of elevation differences with respect to the topographic characteristics of slope and aspect. It was concluded in the current thesis that the elevation errors increase with steeper slopes but elevation differences do not depend on slope aspect.

The fifth research objective was to ascertain the factors that affect the accuracy of the DEM. The accuracy of the DEM is affected by how precisely the contour lines (1966 and 1993) for the glacier area are constructed as they depend on snow and ice surface conditions at the time when aerial photographs are taken. The aerial photographs from 1993 had poorer contrast than those from 1966 as the glacier area was partly covered by snow when the 1993 aerial photographs were taken, and this could have led to errors in generating contour lines as well as the glacier border line.

A terracing effect was noticed in the DEMs due to the high density of elevation points on the contour lines and hardly any points between them. Here NN and TIN interpolators also proved to be better than the others with less terracing observed.

The sixth research objective was to suggest methods to improve the quality of the generated DEMs.

Filtering and smoothing of the DEMs can be a solution in order to minimize large error differences that are present in DEMs derived from satellite data.

In order to increase the accuracy of DEMs created from contour lines additional information would be beneficial. For example, elevation information between the existing contour lines and peak points.

The seventh research objective was to observe the changes how the Jostefonn glacier has changed in the period between 1966 and 2011. There were observed changes in Jostefonn glacier, especially in the period between 1996 and 2011. The greatest elevation change was noticed at glacier tongues indicating a change in glacier ice mass. The observed glacier change is correlated with the temperature increase during the last century.

8. References

Aber, J. S., Marzolff, I. and Ries, J., 2010. *Small-Format Aerial Photography: Principles, Techniques and Applications*. Elsevier Science Ltd., Amsterdam, Netherlands.

Aguilar, F.J., Aguilar, M.A., Aguera, F. and Sanchez, J., 2006. The accuracy of grid digital elevation models linearly constructed from scattered sample data. *International Journal of Geographical Information Science*, 20, 169-192.

Andreassen, L.M., 1998. Volumendringer på Jostefonn 1966–93 [Volume change of Jostefonn between 1966 and 1993]. *NVE Rapport*, 3, 1-10.

Andreassen, L.M., 1999. Comparing traditional mass balance measurements with long-term volume change extracted from topographical maps: A case study of Storbreen glacier in Jotunheimen, Norway, for the period 1940–1997. *Annals of Glaciology*, 81 A (4), 467–476.

Andreassen, L.M., Elvehøy, H., Kjøllmoen, B., 2002. Using aerial photography to study glacier changes in Norway. *Annals of Glaciology* 34, 343-348.

Andreassen, L.M., Kjøllmoen, B., Rasmussen, A., Melvold, K. and Nordli, Ø., 2012, Langfjordjøkelen, a rapidly shrinking glacier in northern Norway. *Journal of Glaciology*, Vol. 58, No. 209, 581-593. DOI: 10.3189/2012JoG11J014.

Andreassen, L.M., Winsvold, S.H., Paul, F. and Hausberg, J.E., 2012. *Inventory of Norwegian Glaciers.* Norwegian Water Resources and Energy Directorate (NVE), Oslo, Norway.

Arun, P.V., 2013. A comparative analysis of different DEM interpolation methods. *The Egyptian Journal of Remote Sensing and Space Sciences*, 16, 133–139

Author Unknown, Interpolating raster surfaces. Accessed 8 June, 2013, from http://webapps.fundp.ac.be/geotp/SIG/InterpolMethods.pdf

Bakker, W.H., Janssen, L.L.F., Reeves, C.V., Gorte, B.G.H., Pohl, C., Weir, M.J.C., Horn, J.A., Prakash, A. and Woldai, T., 2001. *Principles of Remote Sensing*, eds. Janssen, L.L.F. and Huurneman, G.C., ITC Educational Textbook Series, International Institute for Geo-Information Science and Earth Observation, Enschede, the Netherlands.

Balan, P. and Mather, P.M., 2010. Evaluation of methods used in assessing the accuracy of InSAR-derived DEMs. *European Space Agency (ESA).* Accessed 16 July, 2013, from http://earth.esa.int/pub/ESA_DOC/gothenburg/

Bamber, J.L. and Kwok, R., 2003. Remote-sensing techniques. In *Mass Balance of the Cryosphere: Observation and modelling of contemporary and future changes*, eds. Bamber, J.L. and Payne, A.J.,Cambridge University Press, Cambridge, UK, 59-113.

Barringer, J.R.F. and Lilburne, L., 1997. An evaluation of digital elevation models for upgrading New Zealand land resource inventory slope data. In *Proceedings of the Second Annual Conference GeoComputation 97, incorporating the Spatial Information Research Centre's 9th Annual Colloquim*, 26-29 April, 1997, ed. Pascoe, R.T., University of Otago, Spatial Information Research Centre, Dunedin, New Zealand, 109-116.

Barringer, J.R.F., Pairman, D. and McNeill, S.J., 2002. Development of a high-resolution digital elevation model for New Zealand. *Landcare Research Contract Report: LC0102/170*, Wellington, New Zealand, 1-31.

Bater, C.W., Coops, N.C., 2009. Evaluating error associated with LiDAR-derived DEM interpolation. *Computers & Geosciences* 35, 289–300.

Bates, J.K. 2007. *An evaluation of digital elevation models and geotechnical properties of the glacial deposits in Franklin County, Ohio, using a geographic information system.* PhD diss. Ohio State University, USA.

Bell, A.D.F., 2012. Creating DEMs from survey data: interpolation methods and determination of accuracy. British Society of Geomorphology. *Geomorphological Techniques*, Ch.2, Sec. 3.1, 1-9.

Berrand, N.E., Murray, T., James, T.D., Barr, S.L. and Mills, J.P., 2009. Optimizing photogrammetric DEMs for glacier volume change assessment using laser-scanning derived ground-control points, *Journal of Glaciology*, 55 (189), 106-116.

Borisov, M., Bankovic, R. and Drobnjak, S., 2009. Modelling the uncertainty of digital elevation models with geostatistical simulation and application on spatially distribution of soil nitrogen. *Scientific Technical Review*, LIX (3-4), 54-59.

Boslaugh S. and Watters P.A., 2008. *Statistics in a Nutshell.* O'Reilly Media, Inc.

Burdziej, J. and Kunz, M., 2007. Effect of digital terrain model resolution on topographic parameters calculation and spatial distributions of errors. In *New Developments and Challenges in Remote Sensing*, ed. Bochenek, A., Millpress, Rotterdam, Netherlands, 615-626.

Carlisle, B.H., 2002. *Digital elevation model quality and uncertainty in DEM-based spatial modelling.* PhD diss. University of Greenwich, London, UK.

Carlisle, B.H., 2005. Modelling the spatial distribution of DEM error. *Transactions in GIS*, 9, 521-540.

Carrara, A., Bitelli, G. and Carla, R., 1997. Comparison of techniques for generating digital terrain models from contour lines. *International Journal of Geographical Information Science*, 11 (5), 451-473.

Commitee on Himalayan Glaciers, Hydrology, Climate Change, and Implications for Water Security, 2012. *Himalayan Glaciers: Climate Change, Water Resources, and Water Security*. The National Academies Press, Washington DC, USA.

Congalton, R.G. and Green, K., 1999. *Assessing the Accuracy of Remotely Sensed Data: Principles and Practices*, Lewis Publishers, USA.

D'Agata, C. and Zanutta, A., 2007. Reconstruction of the recent changes of a debris-covered glacier (Brenva Glacier, Mont Blanc Massif, Italy) using indirect sources: Methods, results and validation. *Global and Planetary Change*, 56, 57–68.

Daix, N., 2008. Interpolating raster surface, FUNDP, University of Namur, Belgium. Accessed 18 January, 2014, from http://webapps.fundp.ac.be/geotp/SIG/InterpolMethods.pdf

Davis, O., 2012. Processing and working with LiDAR data in ArcGIS: a practical guide for archaeologists. *The Royal Commission on the Ancient and Historical Monuments of Wales*, 1-23

Desmet, P.J.J., 1997. Effects of interpolation errors on the analysis of DEM. *Earth Surface Processes and Landforms,* 22, 563–580.

Droj, G., 2000. Improving the accuracy of digital terrain models. *Studia Universitatis Babes-Bolyai, Informatica,* XLV (1), 1-8.

Dyurgerov, M.B., 2010. Reanalysis of glacier changes: from the IGY to the IPY, 1960—2008. *Data of Glaciological Studies,* Publication 108, 1-116.

Engh, S., 2013. *Potensiale for anvendelse av LiDAR-data i glasiologi* [Potential of application of LiDAR data in glaciology]. MS diss. University of Oslo, Faculty of Mathematics, Natural Science and Technology, Oslo, Norway.

Erdogan, S., 2009. A comparision of interpolation methods for producing digital elevation models at the field scale. *Earth Surface Processes and Landforms,* 34, 366–376, DOI: 10.1002/esp.1731.

ESRI, 2008. ArcGIS Webhelp, Geostatistical Analyst, Performing Validation. Accessed 17 July, 2013, from http://webhelp.esri.com/arcgisdesktop/9.3/index.cfm?TopicName=Performing_validation_on_a_geostatistical_layer_created_from_a_subset

ESRI, 2009a. ArcGIS Desktop: Release 9.3.1. Environmental Systems Research Institute, Redlands, California, USA.

ESRI, 2009b. ArcGIS Webhelp, Natural Neighbour Interpolation. Accessed 26 July, 2013, from http://webhelp.esri.com/arcgisdesktop/9.3/index.cfm?TopicName=Natural%20Neighbor%20Interpolation

ESRI, 2009c. ArcGIS Webhelp, Spatial Analyst, Interpolation. Accessed 23 May, 2013, from http://webhelp.esri.com/arcgisdesktop/9.3/index.cfm?TopicName=welcome

ESRI, 2009d. ArcGIS Webhelp, Terrains. Accessed 8 June, 2013, from http://webhelp.esri.com/arcgisdesktop/9.3/index.cfm?TopicName=An_overview_of_terrain_datasets

ESRI, 2010. ArcGIS Resources, Understanding curvature rasters. Accessed 2 August, 2013, from http://blogs.esri.com/esri/arcgis/2010/10/27/understanding-curvature-rasters/.

ESRI, 2011a. ArcGIS Resources, Generalization Toolset. Accessed 19 January, 2014, from http://help.arcgis.com/en/arcgisdesktop/10.0/help/index.html#//007000000012000000

ESRI, 2011b. ArcUser Online, Terrain Data sets, The top 10 reasons to use them by Colin Childs, Esri Writer. Accessed 8 June, 2013, from http://www.esri.com/news/arcuser/0311/terrain-datasets.html

ESRI, 2011c. ArcGIS Webhelp, Spatial Analyst, Surface Analysis. Accessed 2 August, 2013, from http://webhelp.esri.com/arcgisdesktop/9.3/index.cfm?TopicName=An_overview_of_the_Surface_tools.

ESRI, 2011d. ArcGIS, Geomorphometry. Accessed 7 August, 2013, from http://www.arcgis.com/home/group.html?owner=reuter&title=geomorphometry

ESRI, 2012. ArcGIS Resources, Fundamentals of Creating TIN Surfaces. Accessed 20 July, 2013, from

http://resources.arcgis.com/en/help/main/10.1/index.html#/Fundamentals_of_creating_TIN_surfaces/006000000010000000/

ESRI, 2013a. ArcGIS Desktop: Release 10.2. Environmental Systems Research Institute, Redlands, California, USA.

ESRI, 2013b. ArcGIS Resources, Data types, LAS data set, Fundamentals about LiDAR. Accessed 17 April, 2013, from http://resources.arcgis.com/en/help/main/10.1/index.html#/What_is_lidar/015w00000041000000/

ESRI, 2013c. ArcGIS Resources, Data types, LAS data set, LiDAR support in ArcGIS, LiDAR solutions in ArcGIS. Accessed 8 June, 2013, from http://resources.arcgis.com/en/help/main/10.1/index.html#/Creating_raster_DEMs_and_DSMs_from_large_lidar_point_collections/015w0000004q000000/

ET Spatial Techniques, 2004a. ET Surface Tools for ArcGIS. Available at: http://www.ian-ko.com/.

ET Spatial Techniques, 2004b. Triangulated Irregular Network (TIN) from Spatial Techniques. Accessed 20 July, 2013, from http://www.ian-ko.com/resources/triangulated_irregular_network.htm

Etzelmüller, B., 2000. On the quantification of surface changes using grid-based digital elevation models (DEMs). *Transactions in GIS*, 4(2), 129–143.

Findlay, D., 2005. Working with digital elevation models. University of Waterloo, Accessed 2 August, 2013, from http://www.lib.uwaterloo.ca/locations/umd/documents/.

Fisher, P.F. and Tate, N.J., 2006. Causes and consequences of error in digital elevation models. *Progress in Physical Geography*, 30(4), 467-489, DOI: 10.1191/0309133306pp492ra.

Fox, A.J. and Nuttall, A.M., 1997. Photogrammetry as a research tool for glaciology. *Photogrammetric Record*, 15 (89), 725-797.

Frey, H., 2011. *Compilation and applications of glacier inventories using satellite data and digital terrain information.* PhD diss. Department of Geography, University of Zurich, Switzerland.

Gens, R., 1999. Quality assessment of interferometrically derived digital elevation models. *International Journal of Applied Earth Observation and Geoinformation*, 1 (2), 102-108.

Geomaps Tanzania Limited. Accessed 17 April, 2013, from http://www.geomaps.co.tz/index.php/services/aerial_lidar

Godone, D. and Garnero, G., 2013. The role of morphometric parameters in Digital Terrain Models interpolation accuracy: a case study. *European Journal of Remote Sensing*, 46, 198-214, DOI: 10.5721/EuJRS20134611.

Gonga-Saholiariliva, N., Gunnell, Y., Petit, C. and Mering, C., 2011. Techniques for quantifying the accuracy of gridded elevation models and for mapping uncertainty in digital terrain analysis. *Progress in Physical Geography*, 35(6), 739–764, DOI: 10.1177/0309133311409086.

Haakensen, N., 1986. Glacier mapping to confirm results from mass-balance measurements. *Annals of Glaciology*, 8, 73-77.

Hagg, W. J., Braun, L. N., Uvarov, V. N. and Makarevich, K. G., 2004. A comparison of three methods of mass-balance determination in the Tuyuksu glacier region, Tien Shan, Central Asia. *Journal of Glaciology*, 50 (171), 505-510.

Hasan, A., Pilesjo, P., and Persson, A., 2011. The use of LIDAR as a data source for digital elevation models – a study of the relationship between the accuracy of digital elevation models and topographical attributes in northern peatlands. Hydrol. *Hydrology and Earth System Sciences Discussions*, 8, 5497–5522, DOI:10.5194/hessd-8-5497-2011.

Hengl, T. and Evans, I.S., 2009. Mathematical and digital models of the land surface. In *Geomorphometry: Concepts, Software, Applications*, eds. Hengl, T. and Reuter H.I., Developments in Soil Science, Elsevier Science Publishing Co Inc., Amsterdam, the Netherlands, 33, 31-63, DOI: 10.1016/S0166-2481(08)00002-0.

Hengl, T. and Reuter, H.I. (eds), 2009. *Geomorphometry: Concepts, Software, Applications***.** Developments in Soil Science, Elsevier Science Publishing Co Inc**.,** Amsterdam, the Netherlands, 33, 772 pp.

Hengl, T., Gruber, S. and Shrestha, D.P., 2004. Reduction of errors in digital terrain parameters used in soil-landscape modeling. *International Journal of Applied Observation and Geoinformation*, 5, 97-112.

Hirt, C., Filmer, M.S. and Featherstone, W.E., 2010. Comparison and validation of the recent freely available ASTER-GDEM ver1, SRTM ver4.1 and GEODATA DEM-9S ver3 digital elevation models over Australia. *Australian Journal of Earth Sciences: An International Geoscience Journal of the Geological Society of Australia*, 57(3), 337-347, DOI: 10.1080/08120091003677553.

Hugentobler, M., 2004. *Terrain modelling with triangle based free-form surfaces*. PhD diss. Faculty of Mathematics and Natural Sciences, University of Zurich, Switzerland.

Höhle, J. and Potuckova, M., 2011. Assessment of the Quality of Digital Terrain Models. *European Spatial Data Research (EuroSDR)*, 60, 1-91.

Jenness, J. 2013. DEM Surface Tools for ArcGIS (surface_area.exe). Jenness Enterprises. Available at: http://www.jennessent.com/arcgis/surface_area.htm.

Jin Li and Heap, A.D., 2011. A review of comparative studies of spatial interpolation methods in environmental sciences: Performance and impact factors. *Ecological Informatics*, 6, 228–241.

Joerg, P.C., Morsdorf, F. and Zemp, M., 2012. Uncertainty assessment of multi-temporal airborne laser scanning data: a case study on an Alpine glacier. *Remote Sensing of Environment*, 127, 118–129.

Johnston, K., Hoef, J.M.V., Krivoruchko, K. and Lucas, N., 2004. *ArcGIS 9: Using ArcGIS Geostatistical Analyst*. ESRI Press.

Junfeng Wei, Shiyin Liu, Junli Xu and Wanqin Guo, 2012. Evaluating the accuracy of ASTER GDEM for glaciological application: an example from the Irtysh Basin, China, 21st IAHR International Symposium on Ice. In *Ice Research for a Sustainable Environment*, eds. Zhijun Li and Peng Lu Dalian, Dalian University of Technology Press, Dalian, China, 734-745.

Kamp, U., Bolch, T. and Olsenholler, J., 2005. Geomorphometry of Cerro Sillajhuay (Andes, Chile/Bolivia): comparison of digital elevation models (DEMs) from ASTER remote sensing data and contour maps, *Geocarto International*, 20 (1), 23-33.

Kienzle, S.W., 2004. The effect of DEM raster resolution on first order, second order and compound terrain derivatives. *Transactions in GIS*, 8(1), 83–111.

Kraus, K., 2007. *Photogrammetry: Geometry from Images and Laser Scans*. Walter de Gruyter & Co, Berlin, Germany.

Kyaruzi, J.K., 2005. *Quality assessment of DEM from radargrammetry data. Quality aseessment from the user perspective*. MS diss. International Institute for Geo-information and Earth Observation, Enschede, the Netherlands.

La Frenierre, J., 2009. Measuring the mass balance of mountain glaciers: a review of techniques and recent investigations. GEOG 3720: Mountain Environments and Sustainability, University of Denver, 1-23.

Lam, N. S, 1980. *Methods and problems of areal interpolation*. PhD Diss, University of Western Ontario, Canada.

Lam, N.S., 2009. Spatial interpolation. In *International Encyclopedia of Human Geography*, eds. Kitchin, R. and Thrift, N., Elsevier, Oxford, UK, 10, 369-376.

LAStools, accessed 19 July, 2013 from http://rapidlasso.com/

Lawrence, K., Hutchinson, M. and McKenney, D., 2008. Multi-scale Digital Elevation Models for Canada. *Frontline, Forestry Research Applications*, Technical note 109, Canadian Forestry Service, Great Lakes Forestry Centre, Sault Ste. Marie, Ontario, Canada.

Lemke, P., Ren, J., Alley, R.B., Allison, I., Carrasco, J., Flato, G., Fujii, Y., Kaser, G., Mote, P., Thomas, R.H. and Zhang, T., 2007. Observations: Changes in Snow, Ice and Frozen Ground. In *Climate Change 2007: The Physical Science Basis. Contribution of Working Group I to the Fourth Assessment Report of the Intergovernmental Panel on Climate Change*, eds. Solomon, S., D., Manning, Qin, M., Chen, Z., Marquis, M., Averyt, K.B., Tignor, M. and Miller, H.L., Cambridge University Press, Cambridge, United Kingdom and New York, NY, USA.

Li, Z., 1994. A comparative study of the accuracy of digital terrain models (DTMs) based on various data models, *ISPRS Journal Of Photogrammetry And Remote Sensing*, 49(1), 2-11.

Li, Z., Zhu, Q. and Gold, C., 2005. *Digital Terrain Modeling Principles and Methodology*. CRC Press, New York, USA.

LiDAR UK by Bluesky International Limited. Accessed 17 April, 2013, from http://www.lidar-uk.com/

Mangoua, F.H. and Goita, K., 2008. A comparison between Canadian digital elevation data (CDED) and SRTM data of Mount Carleton in New Brunswick (Canada). In *International Archives of Photogrammetry Remote Sensing and Spatial Information Sciences*, International Society for Photogrammetry and Remote Sensing, Congress, 21st, 37(3), 1423-1430.

Maroju, S., 2007. *Evaluation of five GIS based interpolation techniques for estimating the rtadon concentration for unmeasured zip codes in the State of Ohio*.MS diss. Department of Civil Engeneering, University of Toledo, Ohio, United States of America.

Maune D.F. et al., 2007. *Digital Elevation Model Technologies and Applications: The DEM Users Manual*. American Society for Photogrammetry and Remote Sensing, Bethesda, USA.

Melini, D., 2013. A spatial model for sporadic tree species distribution in support of tree oriented silviculture. *Annals of Silvicultural Research*, 37(1), 64-68.

Mennis, J.I. and Fountain, A.O., 2001. A spatio-temporal GIS database for monitoring Alpine glacier change. *Photogrammetric Engineering and Remote Sensing*, 67(8), 967-975.

National Park Service, U.S. Department of the Interior, Monitoring Glaciers. Accessed 24 July, 2013, from http://www.nature.nps.gov/views/KCs/Glaciers/HTML/ET_Monitoring.htm

Natural Resources Canada, Radar Basics, Accessed 26 July, 2013 from www.nrcan.gc.ca.

Nelson, A., Reuter, H.I. and Gessler, P., 2009. DEM production methods and sources. In *Geomorphometry: Concepts, Software, Applications*, eds. Hengl, T. and Reuter H.I., Developments in Soil Science, Elsevier Science Publishing Co Inc., Amsterdam, the Netherlands, 33, 65-85, DOI: 10.1016/S0166-2481(08)00003-2.

Nesje, A., Bakke, J., Dahl, S.O., Lie, Ø. and Matthews, J.A., 2008. Norwegian mountain glaciers in the past, present and future. *Global and Planetary Change*, 60, 10–27.

Nuth, C. and Kääb, A., 2011. Co-registration and bias corrections of satellite elevation data sets for quantifying glacier thickness change. *The Cryosphere*, 5, 271–290.

Organization of American States, Remote Sensing in Natural Hazard Assessments, Radar. Accessed 26 July, 2013, from http://www.oas.org/DSD/publications/Unit/oea66e/ch04.htm#2.%20radar

Østrem, G., 1986. Repeated glacier mapping for hydrological purposes: water power planning. *Annals of Glaciology*, 8, 135-140.

PCI Geomatics, Tutorials, Extracting Elevation from Air Photos. Accessed 23 May, 2013, from http://www.pcigeomatics.com/pdf/extracting_DEM_from_stereo_photos.pdf

Pellikka, P. and Rees, W. G., 2009. *Remote Sensing of Glaciers. Techniques for Topographic, Spatial and Thematic Mapping of Glaciers*. Taylor & Francis, London, UK.

Peralvo, M., 2003. Influence of DEM interpolation methods in Drainage Analysis. *GIS Hydro 2004 Preconference Seminar Website*, GIS in Water Resources Term Projects. Accessed 17 July, 2013, from http://www.crwr.utexas.edu/gis/gishydro04/

Podobnikar, T., 2009. Methods for visual quality assessment of a digital terrain model. *SAPIENS*, 2 , 2, Special issue, 1-9.

Pope, A., Murray, T. and Luckman, A., 2007. DEM quality assessment for quantification of glacier surface change. *Annals of Glaciology*, 46, 189-194.

Pringle, D., 2010. The aspects of geographical information science module web site, GIS lecture notes, Lecture 9: Spatial interpolation techniques. Accessed 18 January, 2014, from http://www.nuim.ie/staff/dpringle/gis/gis09.pdf

Priyakant, N.K.V, Rao, L.I.M. and Singh, A.N., 2003. Surface approximation of point data using different interpolation techniques – a GIS approach. Accessed 25 January, 2014, from http://gisdevelopment.net/technology/survey/techgp0009pf.htm

Raber, B. R. and Cannistra, J., 2005. *LiDAR Guidebook: Concepts, Project Design, and Practical Applications*. The Urban and Regional Information Systems Association (URISA), USA.

Racoviteanu, A.E., Manley, W.F., Arnaud, Y., Williams, M.W., 2007. Evaluating digital elevation models for glaciologic applications: An example from Nevado Coropuna, Peruvian Andes. *Global and Planetary Change*, 59, 110–125. DOI: 10.1016/j.gloplacha.2006.11.036.

Rampal, K. K., 1999. *Handbook of Aerial Photography and Interpretation.* Concept Publishing Company, New Delhi, India.

Ravibabu, M.V. and Jain, K., 2008. Digital Elevation Model Accuracy Aspects. *Journal of Applied Sciences*, 8(1), 134-139.

Reuter, H.I., Hengl, T., Gessler, P. and Soille, P., 2009. Preparation of DEMs for geomorphometric analysis. In *Geomorphometry: Concepts, Software, Applications,* eds. Hengl, T. and Reuter H.I., Developments in Soil Science, Elsevier Science Publishing Co Inc., Amsterdam, the Netherlands, 33, 87-120, DOI: 10.1016/S0166-2481(08)00004-4.

Rivera, A., 2004. *Mass balance investigations at glacier Chico, Southern Patagonia, Icefield, Chile.* PhD diss. Faculty of Science, School of Geographical Sciences, University of Bristol, UK.

Robson, B.A., 2012. *A remote sensing investigation into the evolution of Folgefonna glacier over the last 150 years.* MS diss. Department of Earth Science, University of Bergen, Norway.

Rolstad, C., Haug, T. and Denby, B., 2009. Spatially integrated geodetic glacier mass balance and its uncertainty based on geostatistical analysis: application to the western Svartisen ice cap, Norway. *Journal of Glaciology*, 55(192), 666-680.

Rye, C.J., Willis, I.C., Arnold, N.S., and Kohler, J., 2012. On the need for automated multiobjective optimization and uncertainty estimation of glacier mass balance models. *Journal of Geophysical Research*, 117, 1-21.

Sharma, A., Tiwari, K.N. and Bhadoria, P.B.S., 2009. Measuring the accuracy of contour interpolated digital elevation models. *Journal of the Indian Society of Remote Sensing*, 37, 139–146.

Sindayihebura, A., Meirvenne, M.V. and Nsabimana, S., 2006. Comparison of methods for deriving a digital elevation model from contours and modelling of the associated uncertainty. 7th International Symposium on Spatial Accuracy Assessment in Natural Resources and Environmental Sciences, in *Accuracy 2006*,

eds. Caetano, M. and Painho, M., Lisbon, Portugal, 181-190. Accessed 16 July, 2013, from http://www.spatial-accuracy.org/History

Surazakov, A.B. and Aizen, V.B., 2006. Estimating volume change of mountain glaciers using SRTM and map-based topogrpahic data, *IEEE Transactions on Geoscience and Remote Sensing*, 44 (10), 2991-2995.

Tate, E., 1998. Remote sensing with digital orthophotos. Accessed 14 August, 2013, from http://www.ce.utexas.edu/prof/maidment/grad/tate/research/orthophotos.html.

Tennant, C., Menounos, B., Ainslie, B., Shea, J. and Jackson, P., 2012. Comparison of modeled and geodetically-derived glacier mass balance for Tiedemann and Klinaklini glaciers, southern Coast Mountains, British Columbia, Canada. *Global and Planetary Change*, 82-83, 74–85.

Thomas, J., 2009. *Volume change of the Tasman glacier using remote sensing.* MS diss. Department of Geography, University of Canterbury, New Zealand.

Toutin, T., 2002. Impact on terrain slope and aspect on radargrammetric DEM accuracy. *ISPRS Journal of Photogrammetry & Remote Sensing*, 57, 228– 240.

Wang, D., Laffan, S.W., Yu Liu and Lun Wu, 2010. Morphometric characterisation of landform from DEMs. *International Journal of Geographical Information Science*, 24 (2), 305-326, DOI: 10.1080/13658810802467969.

Wechsler, S.P., 1999. Digital elevation model (DEM) uncertainty: evaluation and effect on topographic parameters. ESRI User Conference.

Wechsler, S.P., 2003. Perceptions of digital elevation model uncertainty by DEM users. *URISA Journal*, 15(2), 57-64.

Wenzhong Shi, 2010. Sources of uncertainty in spatial data and spatial analysis. In *Principles of Modelling Uncertainties in Spatial Data and Spatial Analysis*, ed. Wenzhong Shi, CRC Press, Taylor and Francis Group, Boca Raton, Florida, USA.

Wilson, J.P., 2012. Digital terrain modeling. Geomorphology, 137, 107–121.

Winkler, S., Elvehøy, H. and Nesje, A., 2009. Glacier fluctuations of Jostedalsbreen, western Norway, during the past 20 years: the sensitive response of maritime mountain glaciers. *The Holocene*, 19 (3), 395–414.

Wood, J. D. and Fisher, P. F., 1993. Assessing interpolation accuracy in elevation models. *IEEE Computer Graphics and Applications*, 13, 48-56.

Wood, J., 1996. *The geomorphological characterisation of digital elevation models*. PhD diss. University of Leicester, UK. Accessed 2 August, 2013, from http://www.soi.city.ac.uk/~jwo/phd/

Xiaohang Liu, 2009. On the accuracy of digital elevation models. *Proceedings of the 24th International Cartographic Conference*, Santiago, Chile, 15–21 November, 2009, 1-10. Accessed 17 July, 2013, from http://icaci.org/icc2009/

Zhang, S., Peterson, J. and Shan, J., 2004. High quality 3D visualization for glacial cirque terrain, *Journal of Spatial Science*, 49 (2), 75-86.

Ziadat, F.M., 2007. Effect of contour intervals and grid cell size on the accuracy of DEMs and slope derivatives. *Transactions in GIS*, 11, 67-81.

The highest point (Sunnfjordbjørnen) of Jostefonn glacier seen from the air (to your right in the picture).

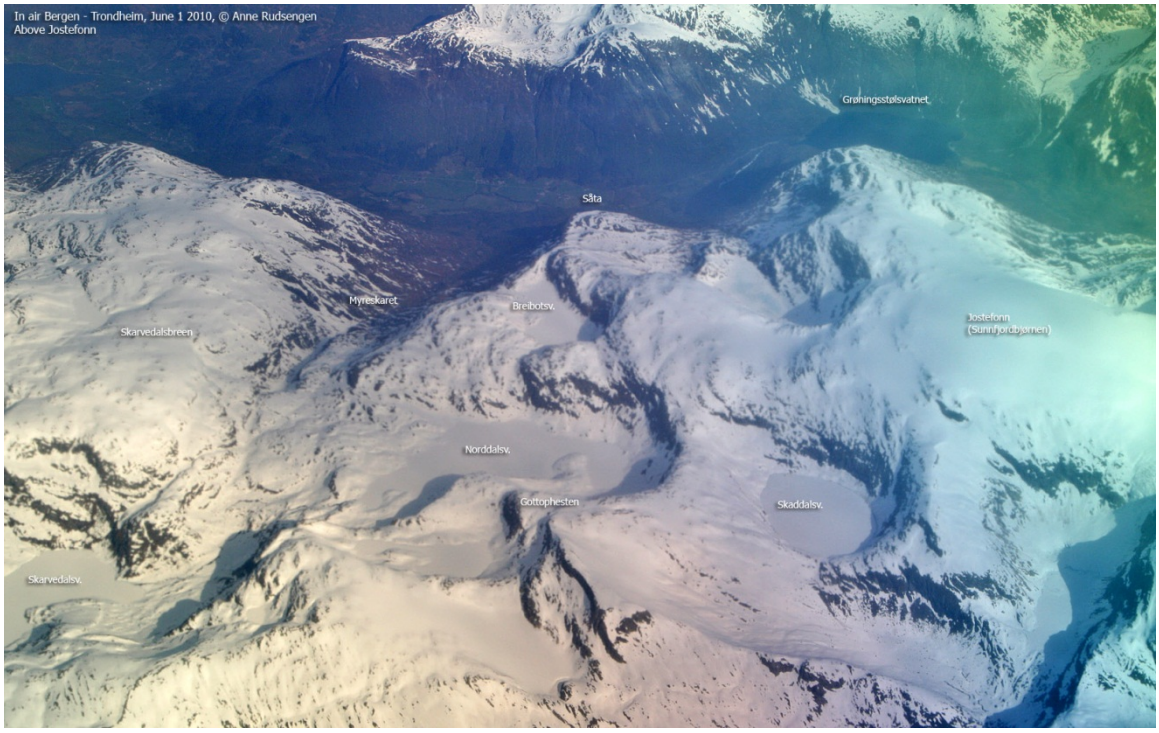

(Source: http://www.westcoastpeaks.com/Peaks/meneseggi.html)

9. Appendix

9.1 Histograms of interpolated surfaces

	Histograms of DEMs		
	1966	**1993**	**2011**
IDW 5m	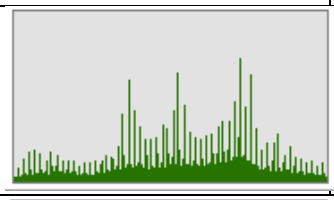	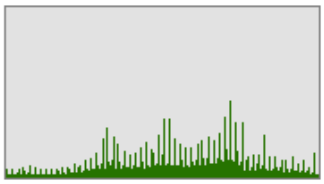	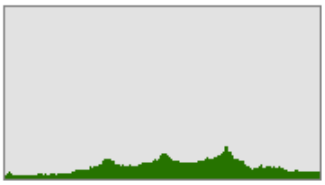
IDW 10m	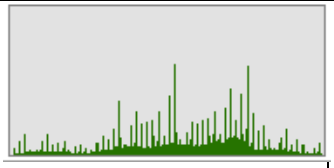	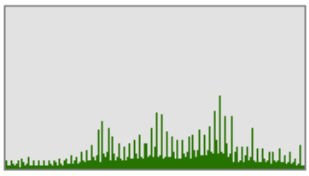	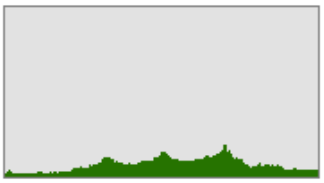
IDW 20m	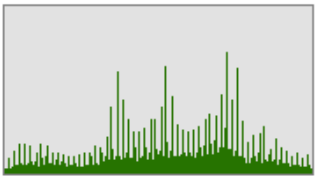	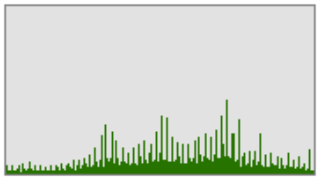	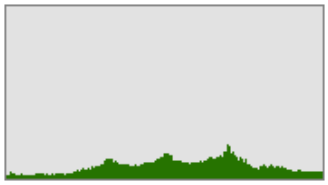
IDW 50m	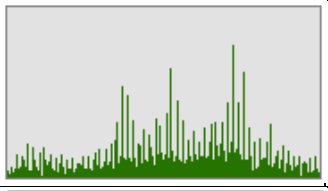	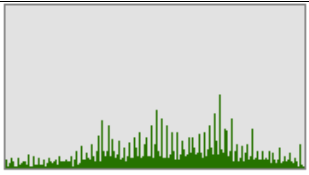	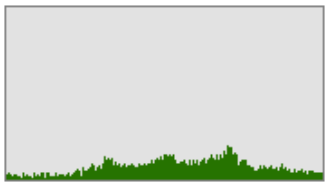
Kriging 5m	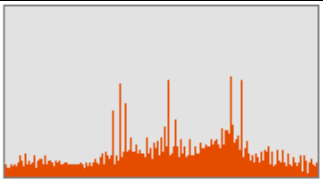	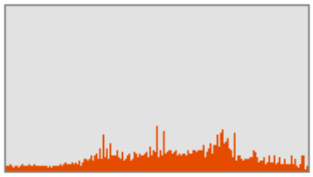	
Kriging 10m	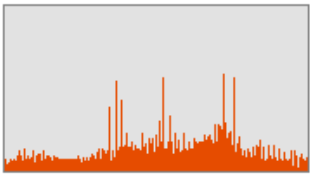	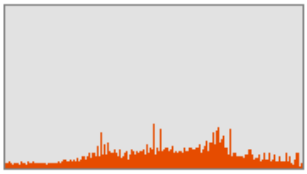	
Kriging 20m	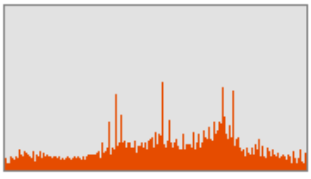	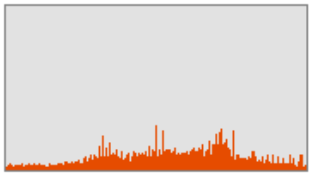	
Kriging 50m	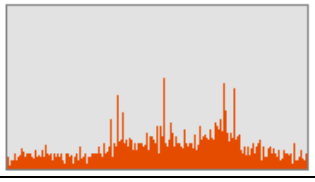	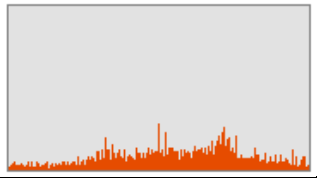	

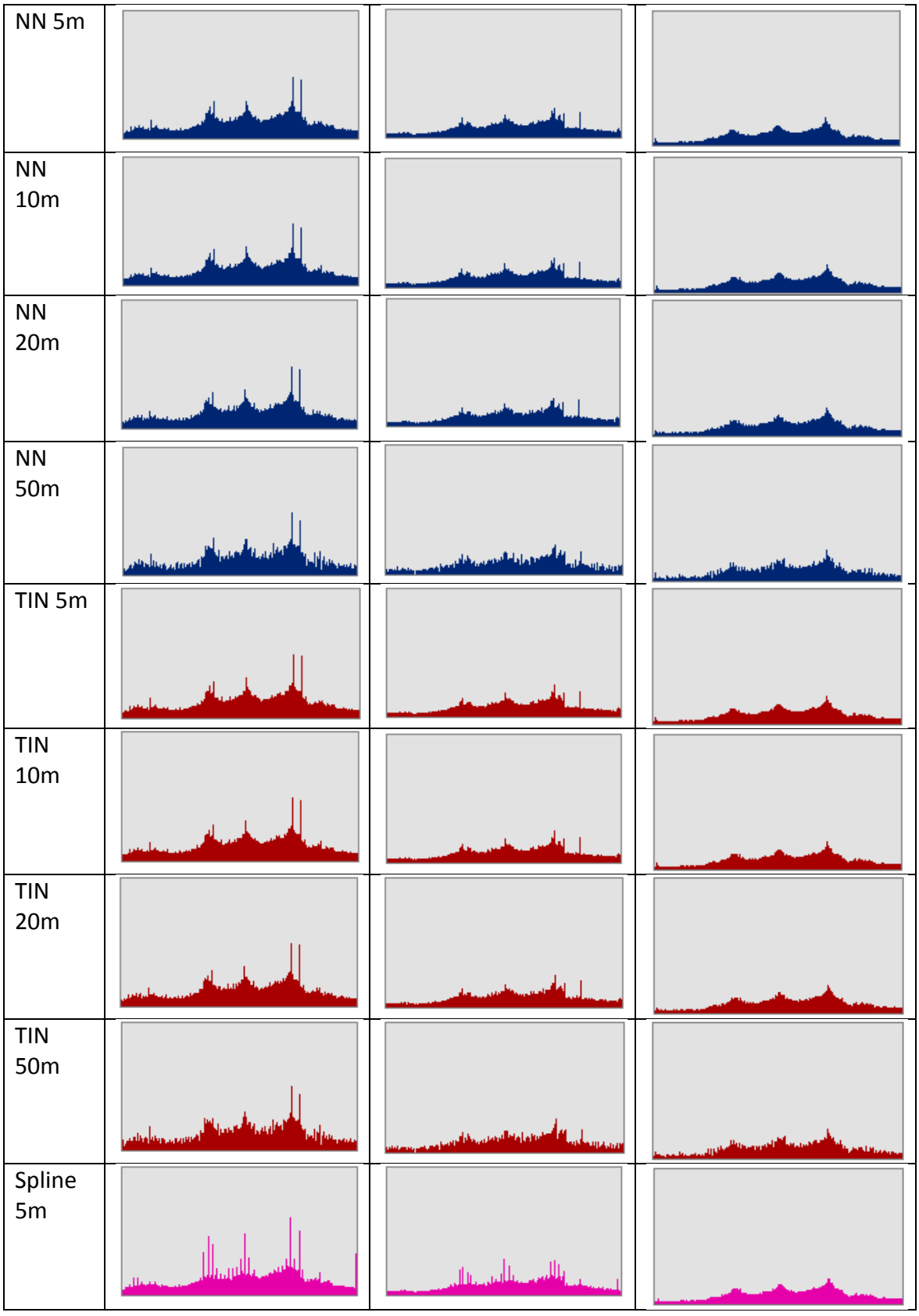
NN 5m
NN 10m
NN 20m
NN 50m
TIN 5m
TIN 10m
TIN 20m
TIN 50m
Spline 5m

Spline 10m	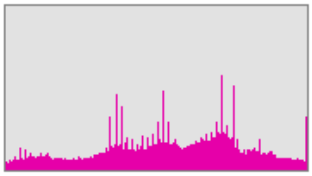	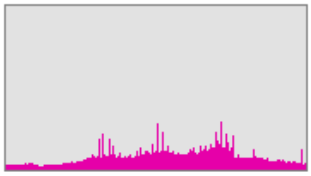	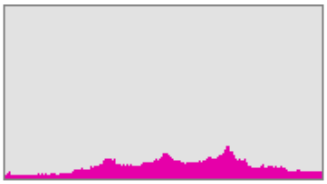
Spline 20m	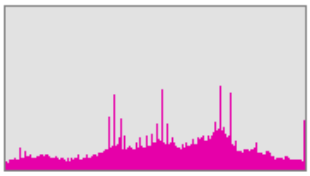	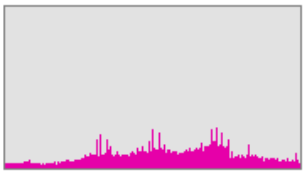	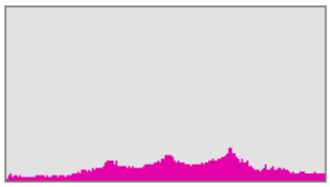
Spline 50m	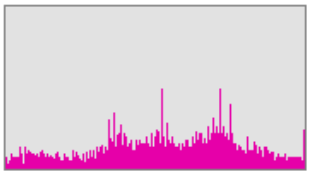	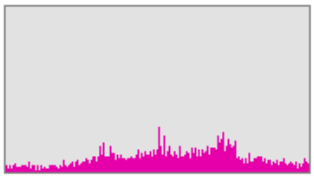	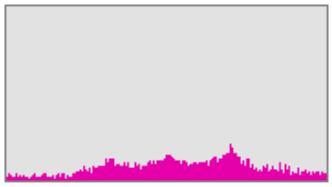
ANUDEM 5m	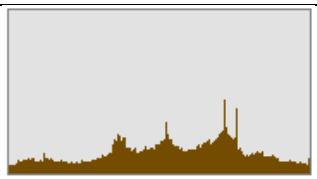	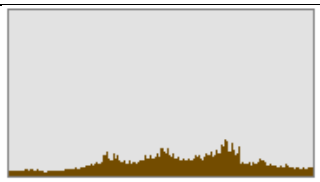	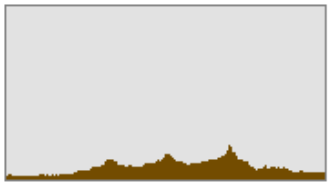
ANUDEM 10m	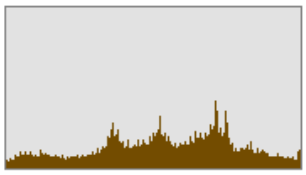	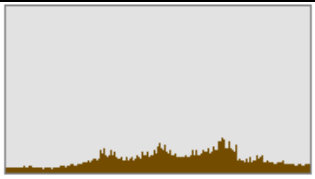	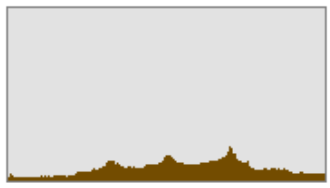
ANUDEM 20m	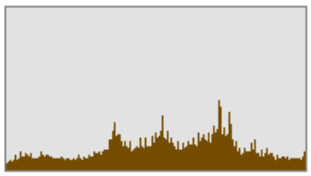	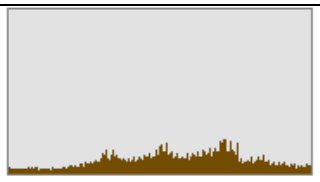	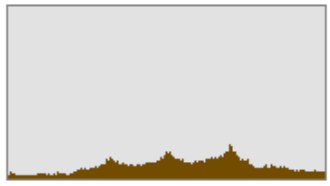
ANUDEM 50m	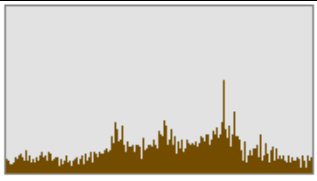	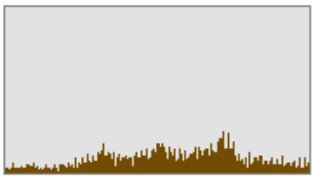	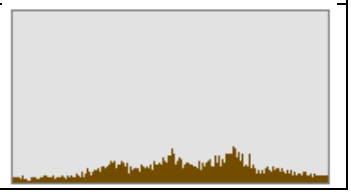

9.2. Visual comparison of interpolation methods

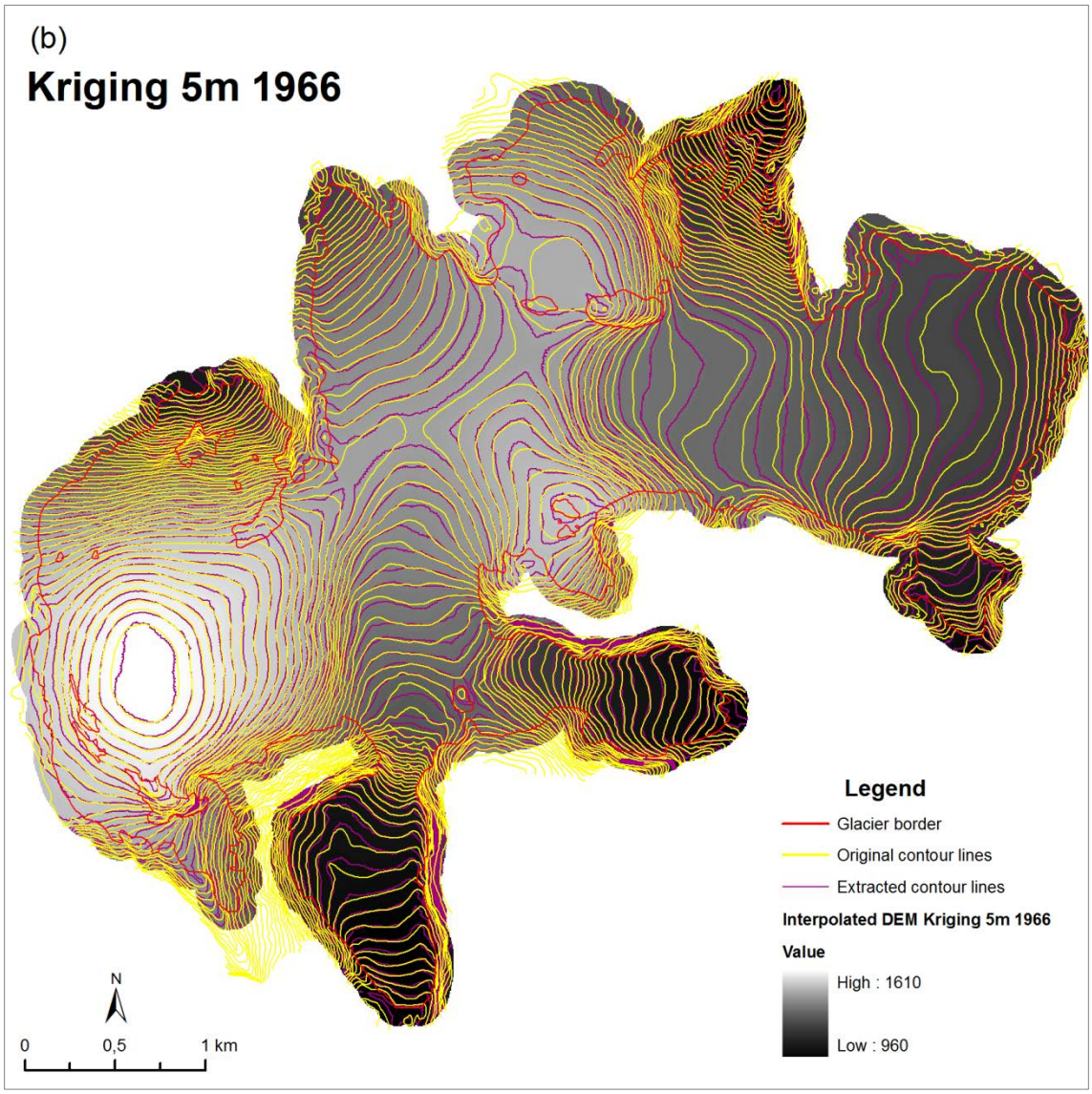

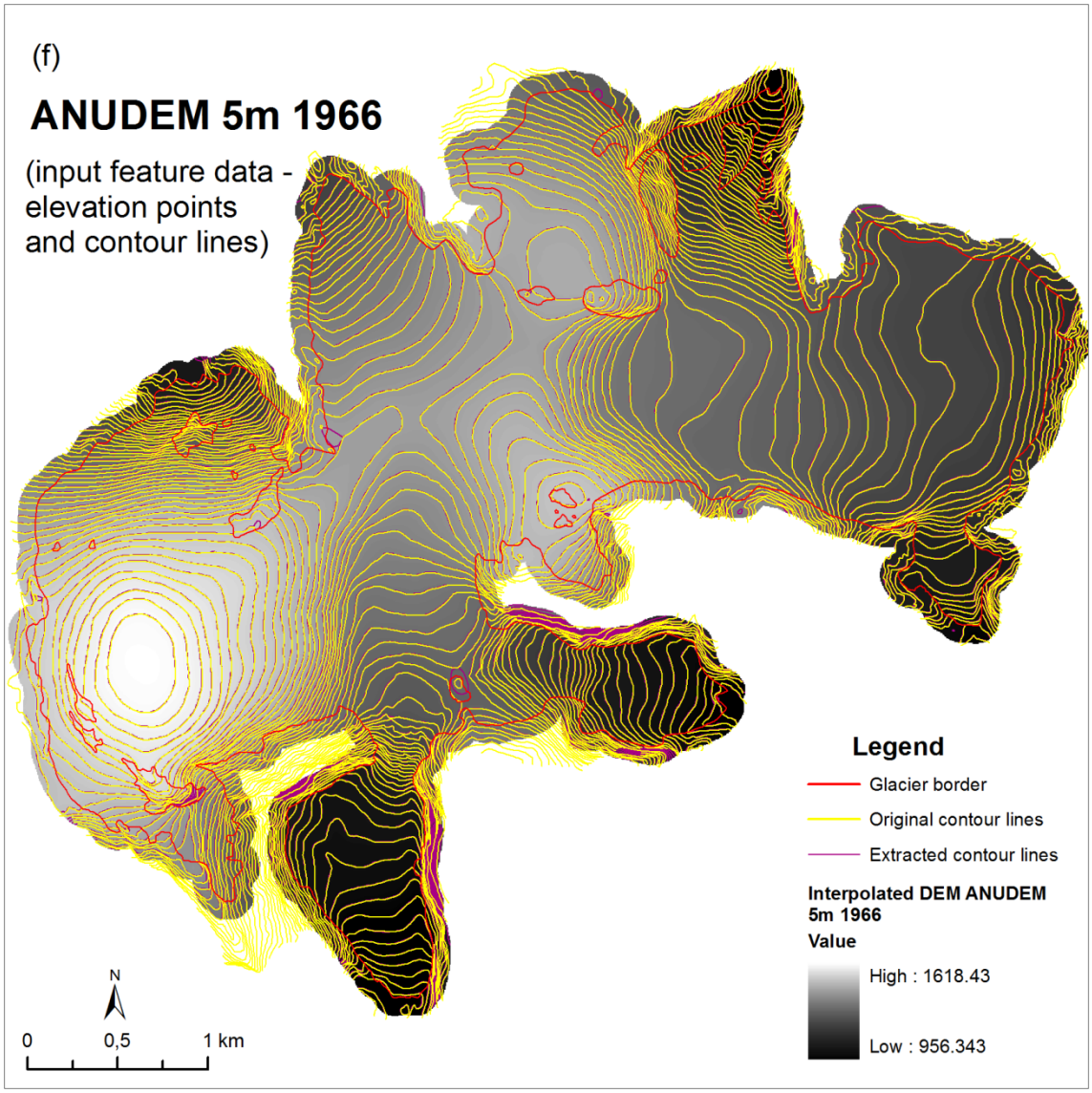
(f)
ANUDEM 5m 1966
(input feature data - elevation points and contour lines)
Legend
Glacier border
Original contour lines
Extracted contour lines
Interpolated DEM ANUDEM 5m 1966
Value
High : 1618.43
Low : 956.343
N
0
0,5
1 km

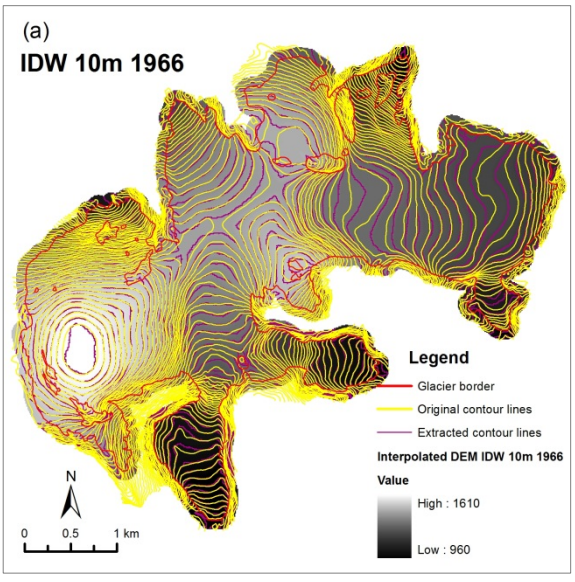
(a)
IDW 10m 1966
Legend
Glacier border
Original contour lines
Extracted contour lines
Interpolated DEM IDW 10m 1966
Value
High : 1610
Low : 960
N
0
0.5
1 km

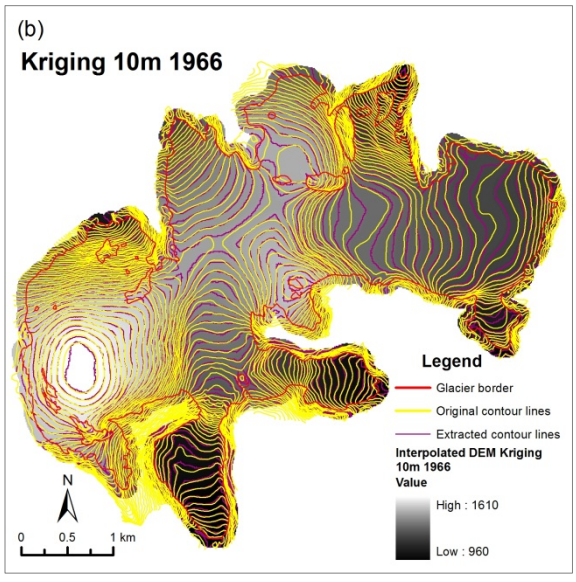
(b)
Kriging 10m 1966
Legend
Glacier border
Original contour lines
Extracted contour lines
Interpolated DEM Kriging 10m 1966
Value
High : 1610
Low : 960
N
0
0.5
1 km

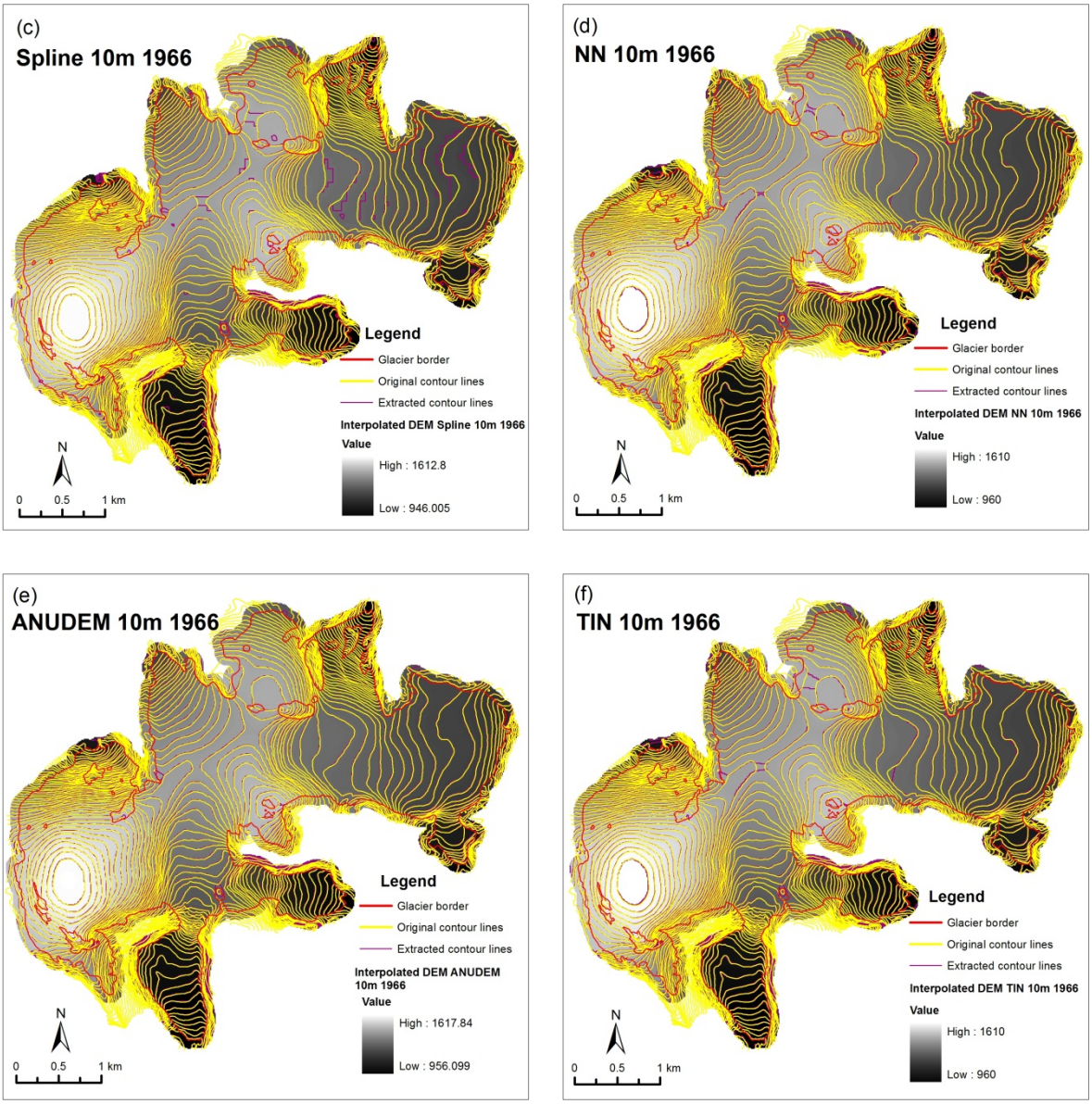

A comparison between the modelled and the reference contour lines for (a) IDW, (b) Kriging, (c) Spline, (d) Natural Neighbours, (e) ANUDEM, (f) TIN for the year of 1966. The extracted contour lines are shown in purple and the original contour lines are depicted in yellow. The cell size for all the maps is 10 m.
Source: Own elaboration
Coordinate System: WGS 1984 UTM Zone 32N

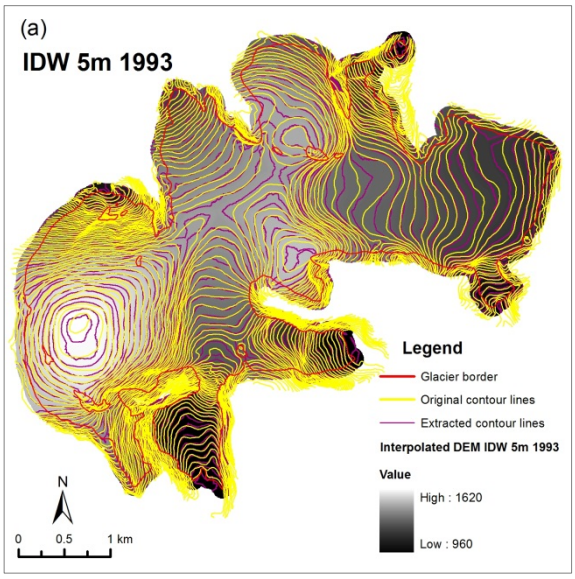
(a)
IDW 5m 1993
Legend
Glacier border
Original contour lines
Extracted contour lines
Interpolated DEM IDW 5m 1993
Value
High : 1620
Low : 960
N
0
0.5
1 km

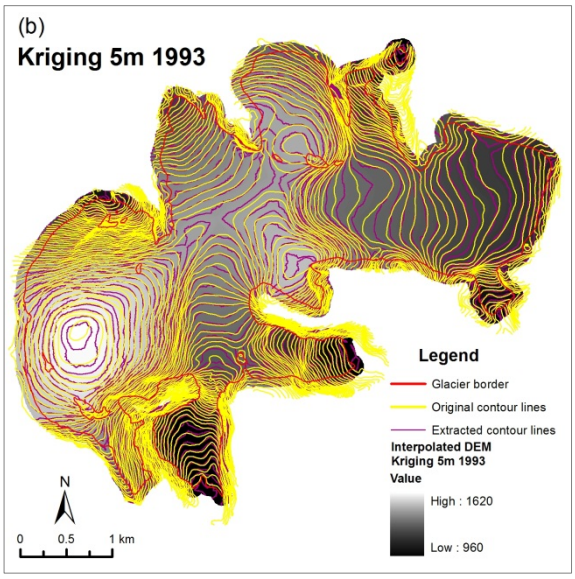
(b)
Kriging 5m 1993
Legend
Glacier border
Original contour lines
Extracted contour lines
Interpolated DEM
Kriging 5m 1993
Value
High : 1620
Low : 960
N
0
0.5
1 km

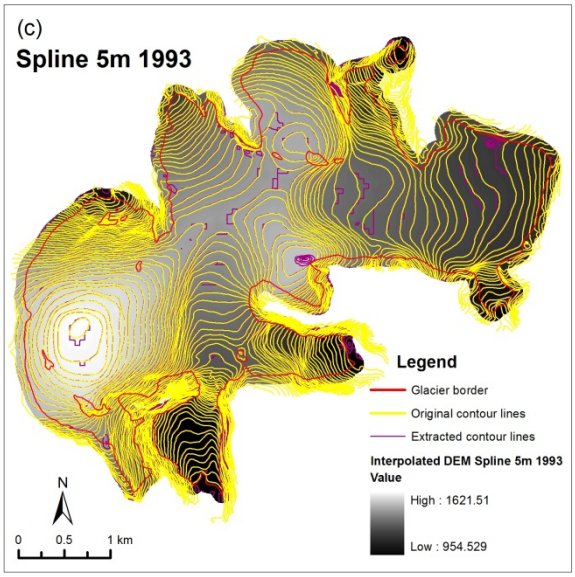
(c)
Spline 5m 1993
Legend
Glacier border
Original contour lines
Extracted contour lines
Interpolated DEM Spline 5m 1993
Value
High : 1621.51
Low : 954.529
N
0
0.5
1 km

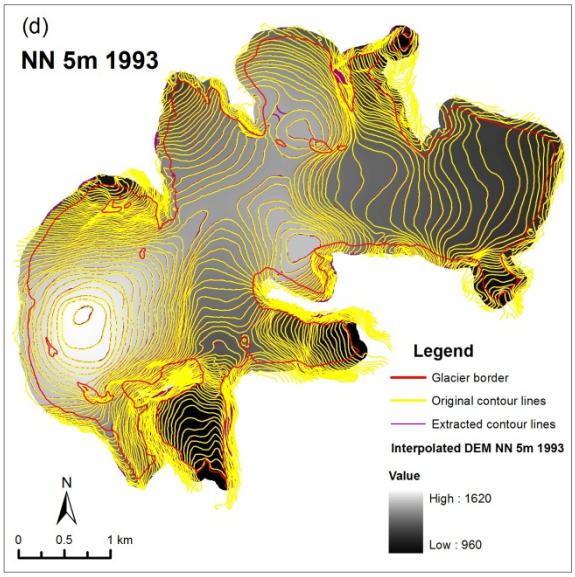
(d)
NN 5m 1993
Legend
Glacier border
Original contour lines
Extracted contour lines
Interpolated DEM NN 5m 1993
Value
High : 1620
Low : 960
N
0
0.5
1 km

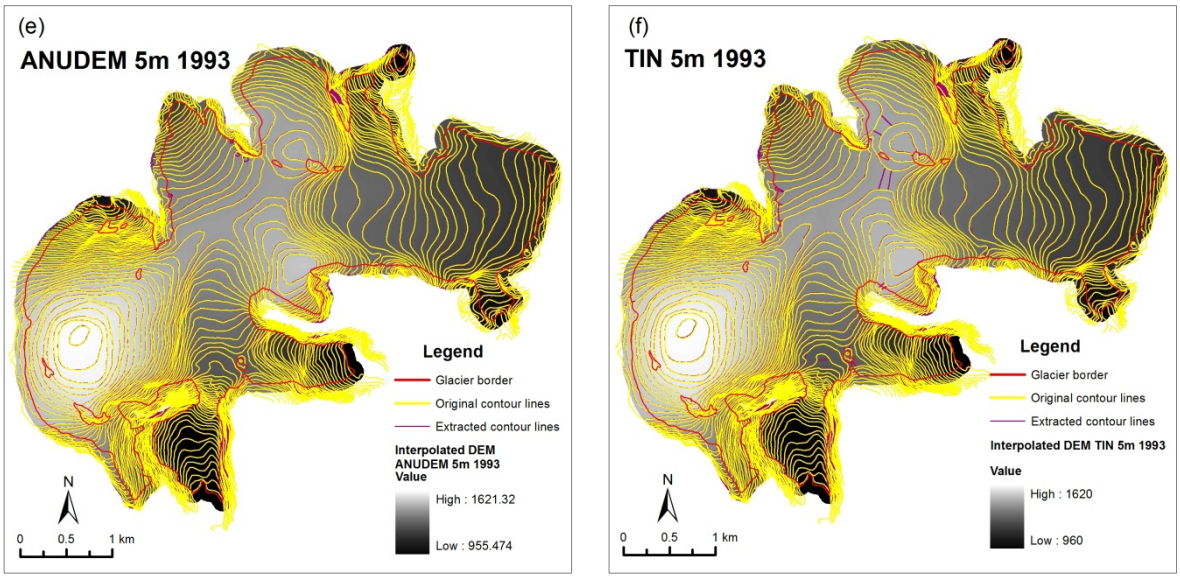

A comparison between the modelled and the reference contour lines for (a) IDW, (b) Kriging, (c) Spline, (d) Natural Neighbours, (e) ANUDEM, (f) TIN for the year of 1993. The extracted contour lines are shown in purple and the original contour lines are depicted in yellow. The cell size for all the maps is 5 m.
Source: Own elaboration
Coordinate System: WGS 1984 UTM Zone 32N

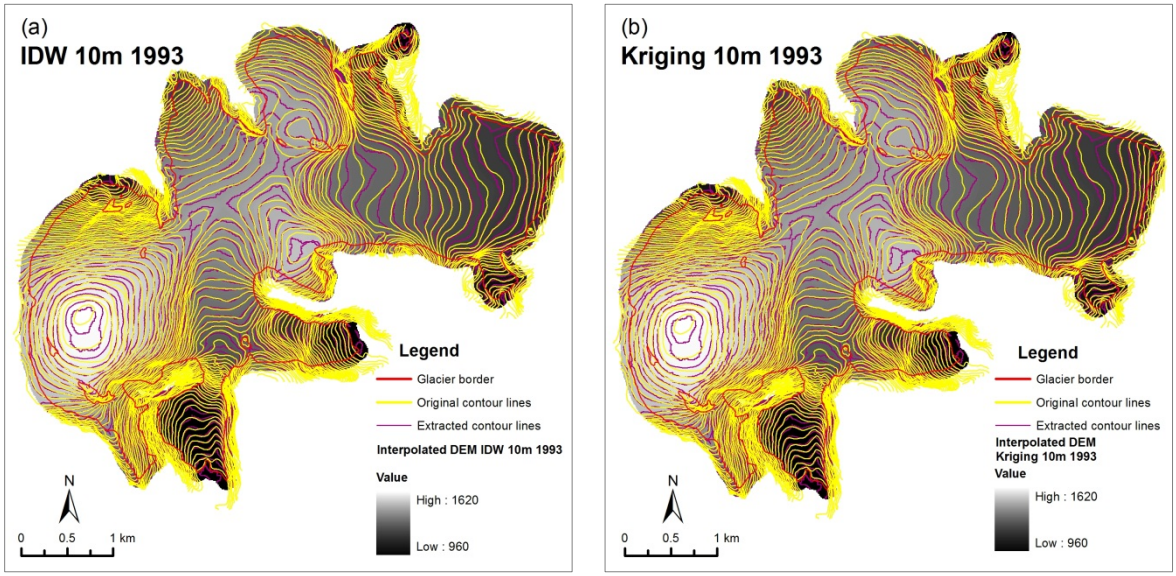

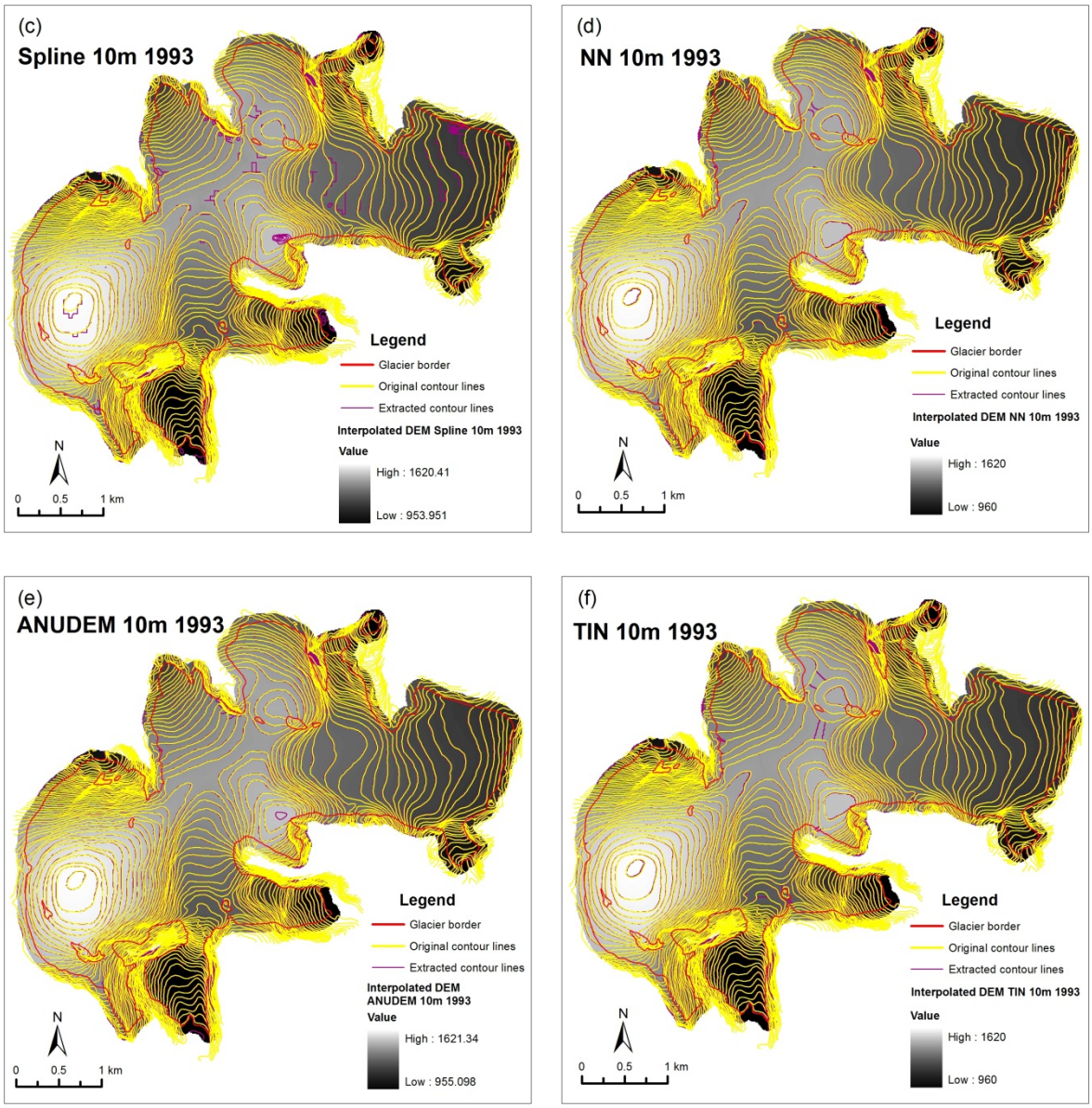

A comparison between the modelled and the reference contour lines for (a) IDW, (b) Kriging, (c) Spline, (d) Natural Neighbours, (e) ANUDEM, (f) TIN for the year of 1993. The extracted contour lines are shown in purple and the original contour lines are depicted in yellow. The cell size for all the maps is 10 m.
Source: Own elaboration
Coordinate System: WGS 1984 UTM Zone 32N

9.3 Frequency distribution (difference between the values in a DEM and test points)

	Frequency Distribution (Difference between the Values in a DEM and Test Points)		
	1966	**1993**	**2011**
IDW 5m	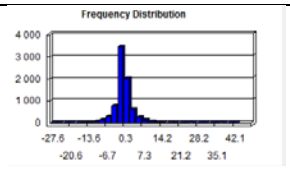	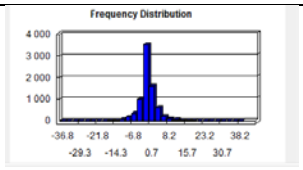	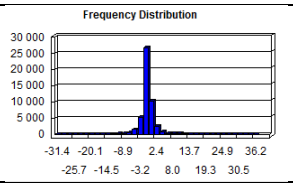
IDW 10m	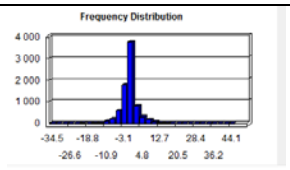	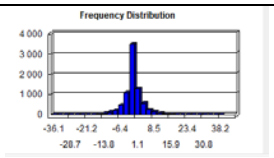	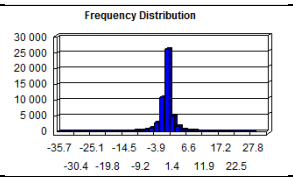
IDW 20m	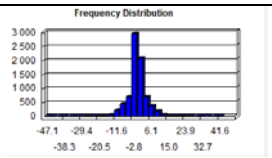	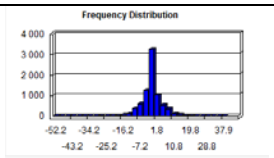	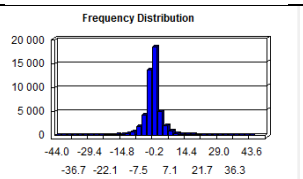
IDW 50m	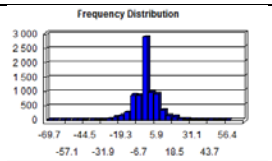	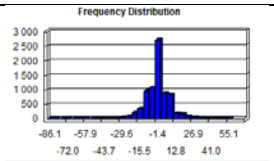	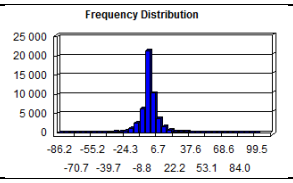
Kriging 5m	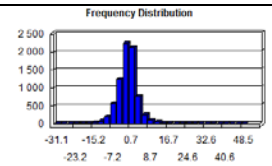	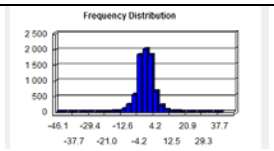	
Kriging 10m	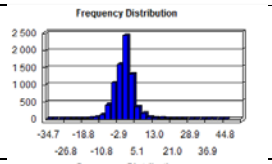	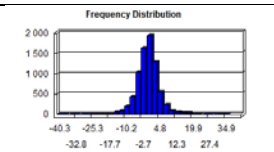	
Kriging 20m	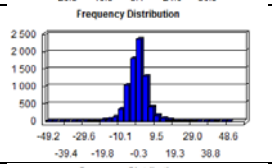	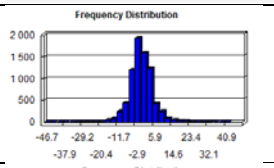	
Kriging 50m	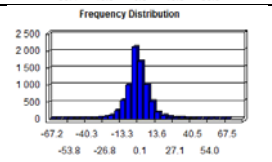	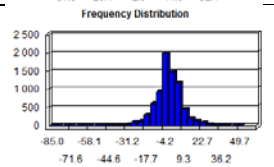	

NN 5m	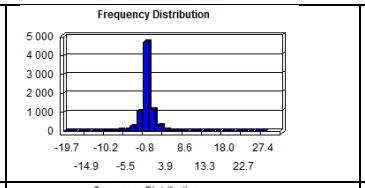	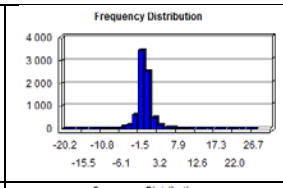	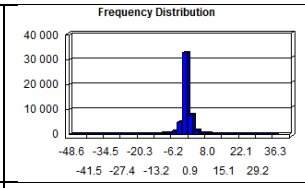
NN 10m	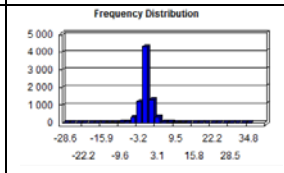	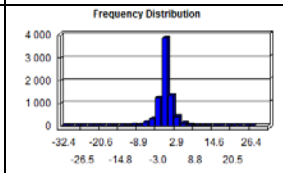	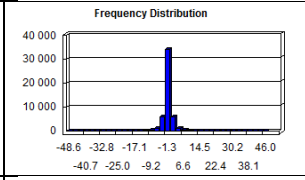
NN 20m	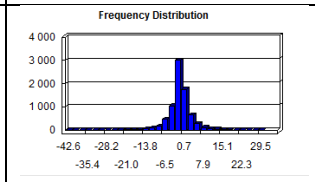	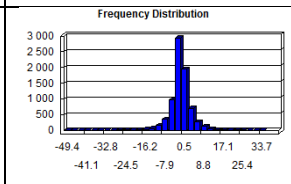	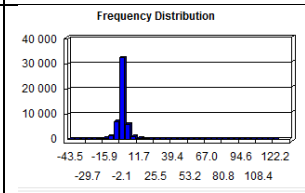
NN 50m	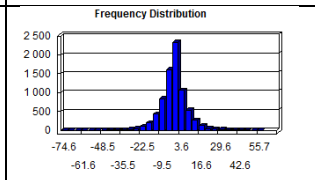	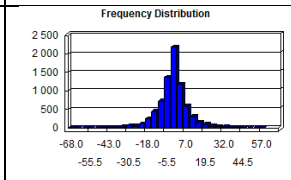	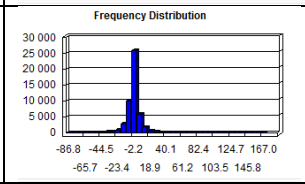
TIN 5m	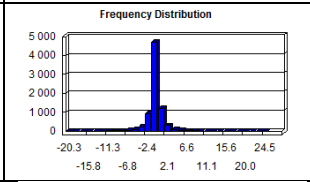	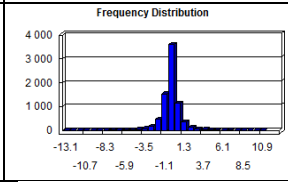	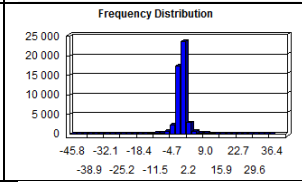
TIN 10m	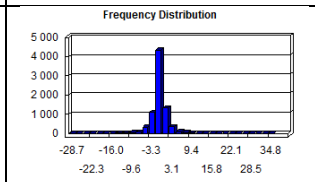	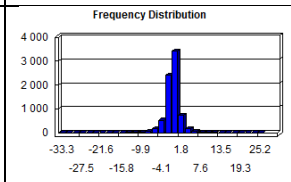	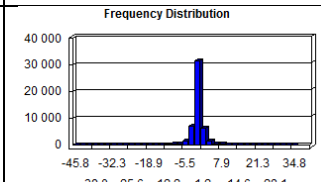
TIN 20m	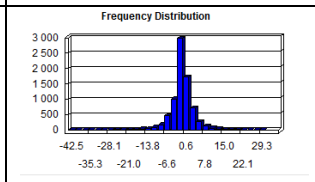	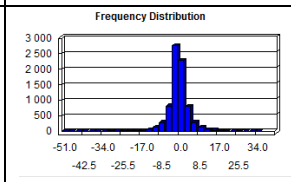	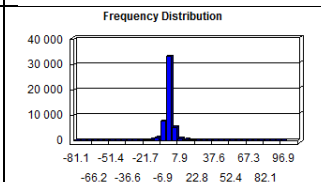
TIN 50m	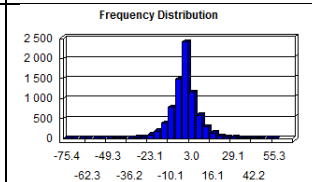	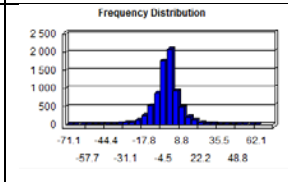	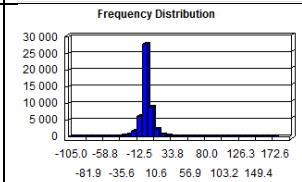
Spline 5m	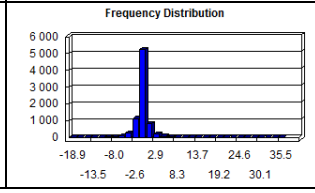	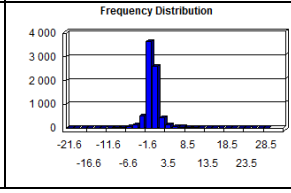	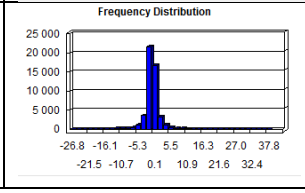

Spline 10m	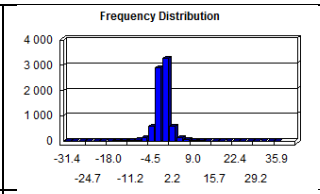	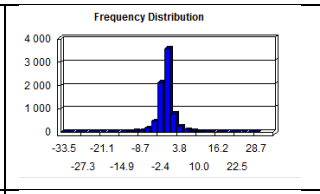	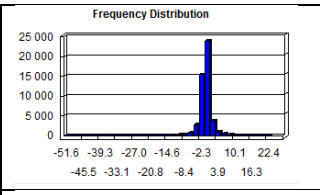
Spline 20m	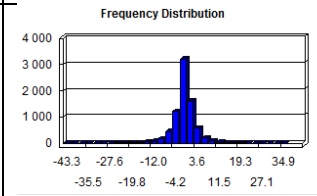	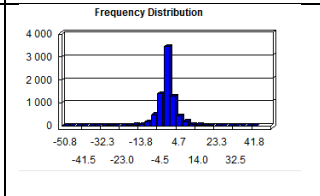	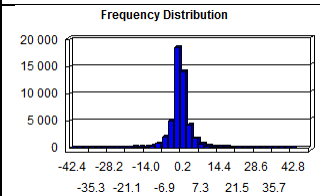
Spline 50m	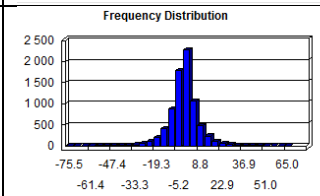	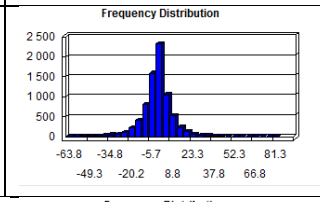	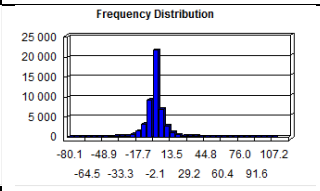
ANUDEM 5m	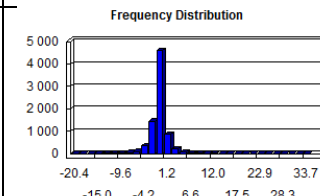	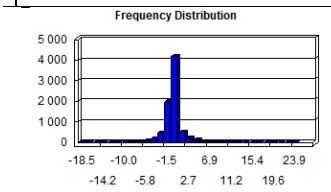	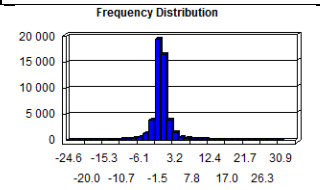
ANUDEM 10m	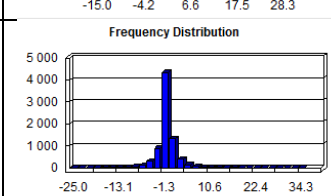	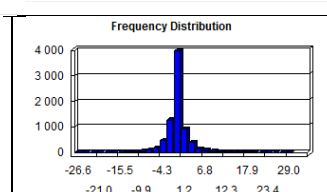	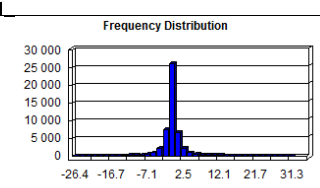
ANUDEM 20m	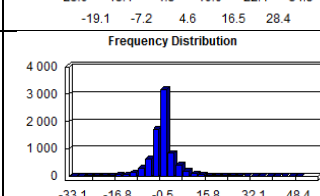	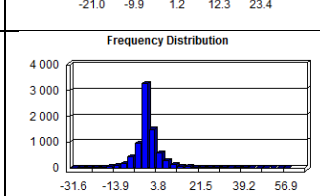	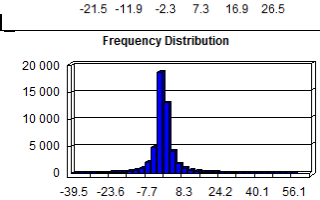
ANUDEM 50m	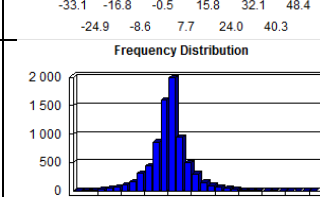	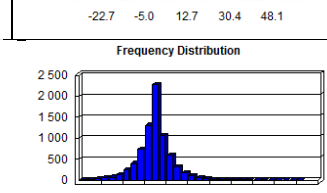	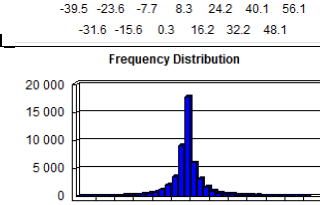

9.4 Comparison of accuracy measures

Statistical Parameters of Error (Minimum Error (Min), Maximum Error (Max), Standard Deviation (SD), Root Mean Square Error (RMSE), Mean Error (ME), Mean Absolute Error (MAE), 95% Confidence Interval)

Year	1966						95% confidence interval
	Min	Max	SD	RMSE	ME	MAE	
IDW 5m	-27.563	43.857	3.269	3.270	0.107	1.986	6.410
IDW 10m	-34.506	46.088	3.597	3.598	0.105	2.193	7.052
IDW 20m	-47.128	43.857	4.740	4.740	0.074	2.998	9.291
IDW 50m	-69.723	59.524	8.900	8.900	0.079	5.957	17.445
Kriging 5m	-31.125	50.536	4.691	4.692	0.121	3.167	9.197
Kriging 10m	-34.707	46.838	4.839	4.841	0.125	3.295	9.488
Kriging 20m	-49.155	51.033	5.602	5.604	0.120	3.877	10.983
Kriging 50m	-67.240	70.881	9.116	9.116	0.067	6.453	17.868
NN 5m	-19.652	28.552	1.725	1.726	-0.033	1.002	3.382
NN 10m	-28.574	36.417	2.450	2.450	-0.016	1.488	4.802
NN 20m	-42.591	31.299	4.031	4.031	-0.023	2.621	7.901
NN 50m	-74.583	58.888	8.969	8.970	0.030	6.108	17.580
TIN 5m	-20.295	25.647	1.750	1.750	-0.023	0.990	3.431
TIN 10m	-28.670	36.418	2.462	2.462	-0.012	1.486	4.825
TIN 20m	-42.504	31.115	4.059	4.059	-0.016	2.631	7.956
TIN 50m	-75.410	58.492	8.968	8.968	0.042	6.102	17.577
Spl 5m	-18.897	36.860	1.647	1.647	-0.005	0.933	3.228
Spl 10m	-31.444	37.577	2.450	2.450	0.008	1.478	4.801
Spl 20m	-43.284	36.898	4.096	4.096	0.007	2.664	8.027
Spl 50m	-75.455	68.532	9.692	9.693	-0.151	6.502	18.999
ANUDEM 5m	-20.446	35.058	2.208	2.208	0.041	1.192	4.328
ANUDEM 10m	-24.992	35.779	2.873	2.874	0.063	1.553	5.632
ANUDEM 20m	-33.070	50.490	5.169	5.169	0.067	3.108	10.132
ANUDEM 50m	-53.469	82.623	11.393	11.393	-0.049	7.681	22.331

Year	1993						95% confidence interval
	Min	Max	SD	RMSE	ME	MAE	
IDW 5m	-36.768	39.976	3.482	3.482	0.072	2.234	6.826
IDW 10m	-36.099	39.976	3.911	3.912	0.082	2.503	7.668

IDW 20m	-52.189	39.976	5.018	5.020	0.127	3.302	9.839
IDW 50m	-86.099	58.475	9.703	9.704	-0.048	6.578	19.019
Kriging 5m	-46.119	39.660	4.674	4.674	0.076	3.351	9.161
Kriging 10m	-40.296	36.679	4.895	4.895	0.067	3.509	9.595
Kriging 20m	-46.668	42.942	5.699	5.700	0.103	4.111	11.172
Kriging 50m	-85.043	52.846	9.791	9.791	-0.028	6.991	19.191
NN 5m	-20.210	27.790	1.857	1.857	0.022	1.088	3.639
NN 10m	-32.393	27.790	2.624	2.624	0.000	1.619	5.143
NN 20m	-49.414	35.646	4.388	4.388	0.048	2.834	8.600
NN 50m	-67.973	59.896	9.634	9.635	-0.149	6.594	18.884
TIN 5m	-13.133	11.457	1.239	1.239	0.002	0.730	2.429
TIN 10m	-33.307	26.543	2.381	2.381	-0.015	1.443	4.666
TIN 20m	-50.961	36.035	4.343	4.343	0.043	2.774	8.512
TIN 50m	-71.064	65.213	9.676	9.678	-0.151	6.594	18.968
Spl 5m	-21.572	29.659	1.842	1.843	0.049	1.043	3.612
Spl 10m	-33.534	30.141	2.635	2.635	0.027	1.615	5.165
Spl 20m	-50.801	43.969	4.493	4.494	0.066	2.883	8.807
Spl 50m	-63.789	84.776	10.281	10.286	-0.324	6.964	20.161
ANUDEM 5m	-18.462	24.860	1.934	1.936	0.088	0.938	3.794
ANUDEM 10m	-26.557	30.288	3.130	3.134	0.151	1.712	6.142
ANUDEM 20m	-31.581	59.019	5.637	5.646	0.319	3.374	11.067
ANUDEM 50m	-51.490	101.450	12.259	12.259	0.074	8.196	24.027

Year	**2011**						**95% confidence interval**
	Min	**Max**	**SD**	**RMSE**	**ME**	**MAE**	
IDW 5m	-31.358	37.702	2.202	2.202	0.003	1.309	4.317
IDW 10m	-35.705	29.279	2.104	2.104	-0.013	1.246	4.124
IDW 20m	-44.033	45.621	3.810	3.810	0.019	2.373	7.467
IDW 50m	-86.152	103.766	7.678	7.678	-0.019	4.962	15.048
Kriging 5m							
Kriging 10m							
Kriging 20m							

Kriging 50m							
NN 5m	-48.613	38.228	2.019	2.019	0.013	1.156	3.958
NN 10m	-48.613	48.163	1.993	1.993	0.006	1.171	3.906
NN 20m	-43.476	125.931	3.717	3.717	0.008	2.246	7.286
NN 50m	-86.809	172.681	7.920	7.920	-0.005	4.943	15.523
TIN 5m	-45.760	38.294	2.060	2.060	0.011	1.184	4.037
TIN 10m	-45.760	36.598	2.003	2.003	0.005	1.192	3.926
TIN 20m	-81.052	100.963	3.707	3.707	-0.001	2.255	7.265
TIN 50m	-105.047	178.782	7.875	7.875	-0.012	4.944	15.434
Spl 5m	-26.836	39.280	2.076	2.076	0.007	1.216	4.068
Spl 10m	-51.649	24.137	1.997	1.997	0.001	1.221	3.914
Spl 20m	-42.361	44.733	3.675	3.675	-0.004	2.283	7.203
Spl 50m	-80.133	111.518	8.032	8.032	-0.029	5.152	15.742
ANUDEM 5m	-24.587	32.191	2.124	2.126	0.089	1.237	4.166
ANUDEM 10m	-26.352	32.660	2.430	2.431	0.070	1.356	4.765
ANUDEM 20m	-39.545	58.276	4.852	4.852	0.063	2.891	9.510
ANUDEM 50m	-81.008	91.315	10.692	10.693	0.127	6.696	20.958

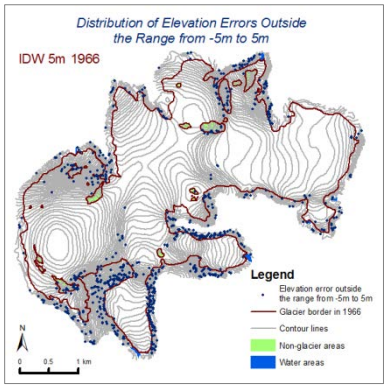

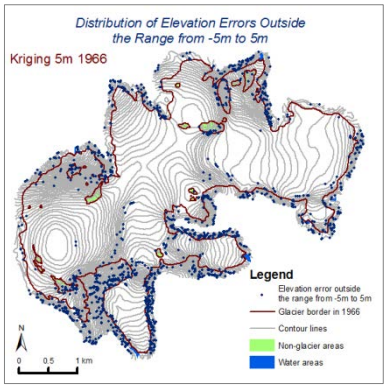

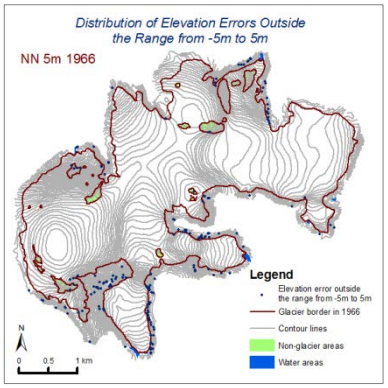

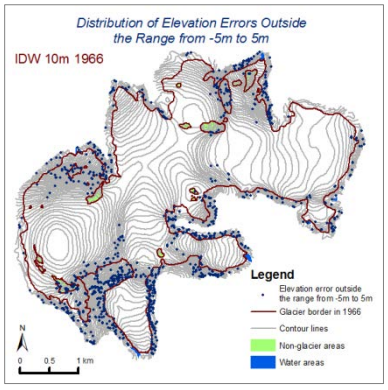

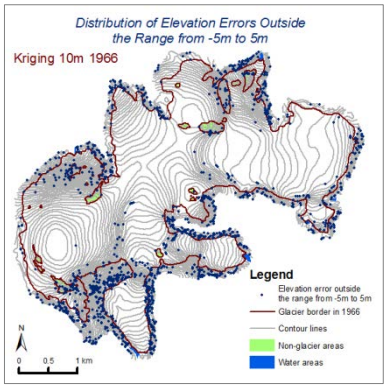

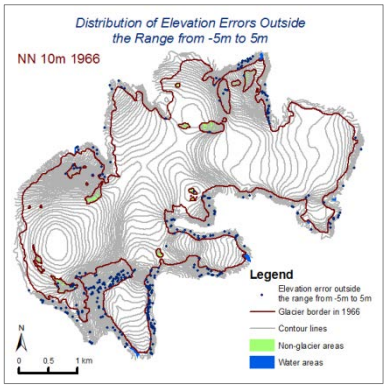

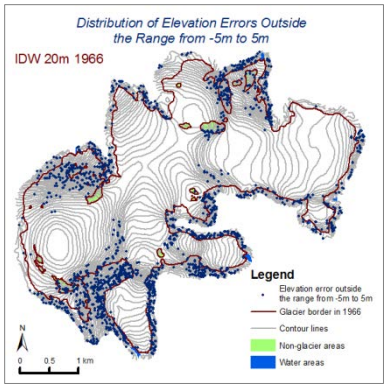
Distribution of Elevation Errors Outside the Range from -5m to 5m
IDW 20m 1966
Legend
Elevation error outside the range from -5m to 5m
Glacier border in 1966
Contour lines
Non-glacier areas
Water areas
N
0 0.5 1 km

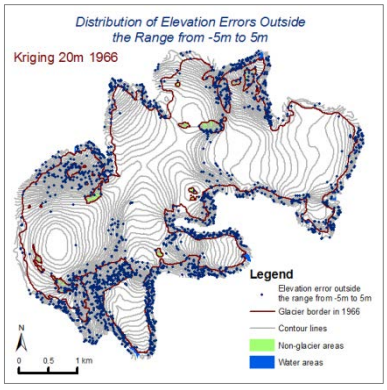
Distribution of Elevation Errors Outside the Range from -5m to 5m
Kriging 20m 1966
Legend
Elevation error outside the range from -5m to 5m
Glacier border in 1966
Contour lines
Non-glacier areas
Water areas
N
0 0.5 1 km

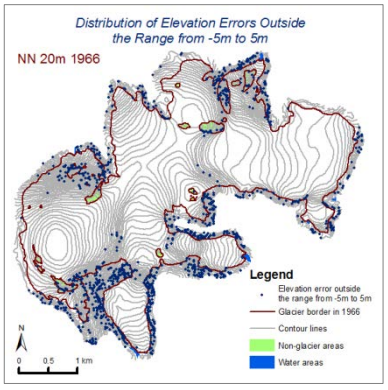
Distribution of Elevation Errors Outside the Range from -5m to 5m
NN 20m 1966
Legend
Elevation error outside the range from -5m to 5m
Glacier border in 1966
Contour lines
Non-glacier areas
Water areas
N
0 0.5 1 km

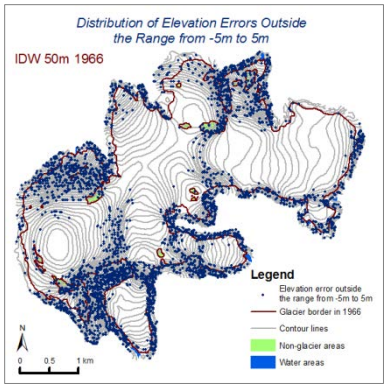
Distribution of Elevation Errors Outside the Range from -5m to 5m
IDW 50m 1966
Legend
Elevation error outside the range from -5m to 5m
Glacier border in 1966
Contour lines
Non-glacier areas
Water areas
N
0 0.5 1 km

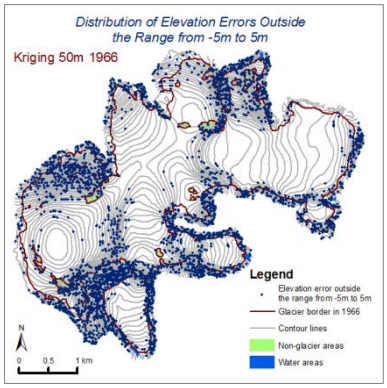
Distribution of Elevation Errors Outside the Range from -5m to 5m
Kriging 50m 1966
Legend
Elevation error outside the range from -5m to 5m
Glacier border in 1966
Contour lines
Non-glacier areas
Water areas
N
0 0.5 1 km

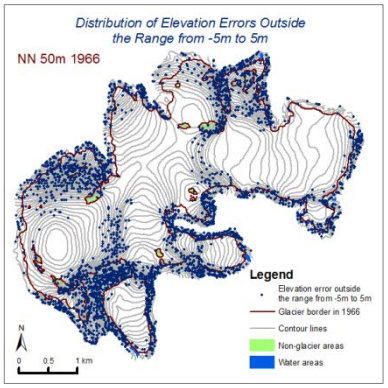
Distribution of Elevation Errors Outside the Range from -5m to 5m
NN 50m 1966
Legend
Elevation error outside the range from -5m to 5m
Glacier border in 1966
Contour lines
Non-glacier areas
Water areas
N
0 0.5 1 km

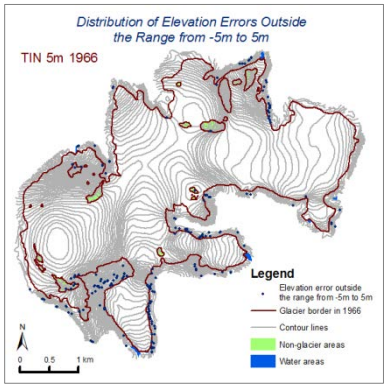
Distribution of Elevation Errors Outside the Range from -5m to 5m
TIN 5m 1966
Legend
Elevation error outside the range from -5m to 5m
Glacier border in 1966
Contour lines
Non-glacier areas
Water areas
N
0 0.5 1 km

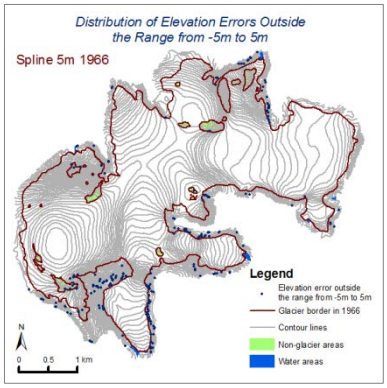
Distribution of Elevation Errors Outside the Range from -5m to 5m
Spline 5m 1966
Legend
Elevation error outside the range from -5m to 5m
Glacier border in 1966
Contour lines
Non-glacier areas
Water areas
N
0 0.5 1 km

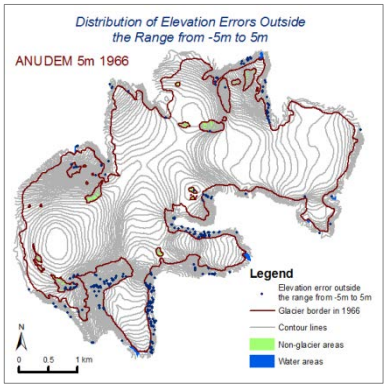
Distribution of Elevation Errors Outside the Range from -5m to 5m
ANUDEM 5m 1966
Legend
Elevation error outside the range from -5m to 5m
Glacier border in 1966
Contour lines
Non-glacier areas
Water areas
N
0 0.5 1 km

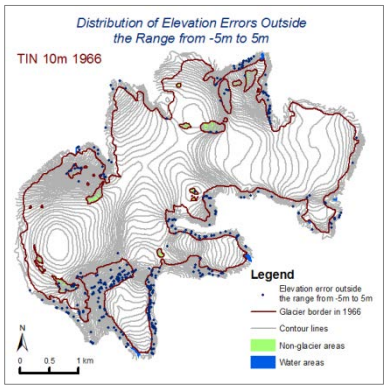
Distribution of Elevation Errors Outside the Range from -5m to 5m
TIN 10m 1966
Legend
Elevation error outside the range from -5m to 5m
Glacier border in 1966
Contour lines
Non-glacier areas
Water areas
N
0 0.5 1 km

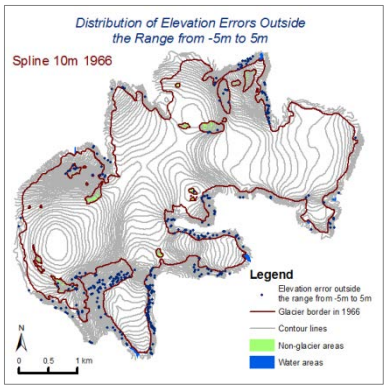
Distribution of Elevation Errors Outside the Range from -5m to 5m
Spline 10m 1966
Legend
Elevation error outside the range from -5m to 5m
Glacier border in 1966
Contour lines
Non-glacier areas
Water areas
N
0 0.5 1 km

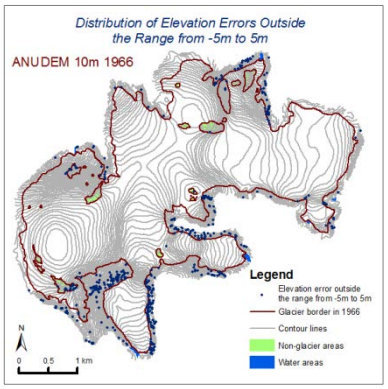
Distribution of Elevation Errors Outside the Range from -5m to 5m
ANUDEM 10m 1966
Legend
Elevation error outside the range from -5m to 5m
Glacier border in 1966
Contour lines
Non-glacier areas
Water areas
N
0 0.5 1 km

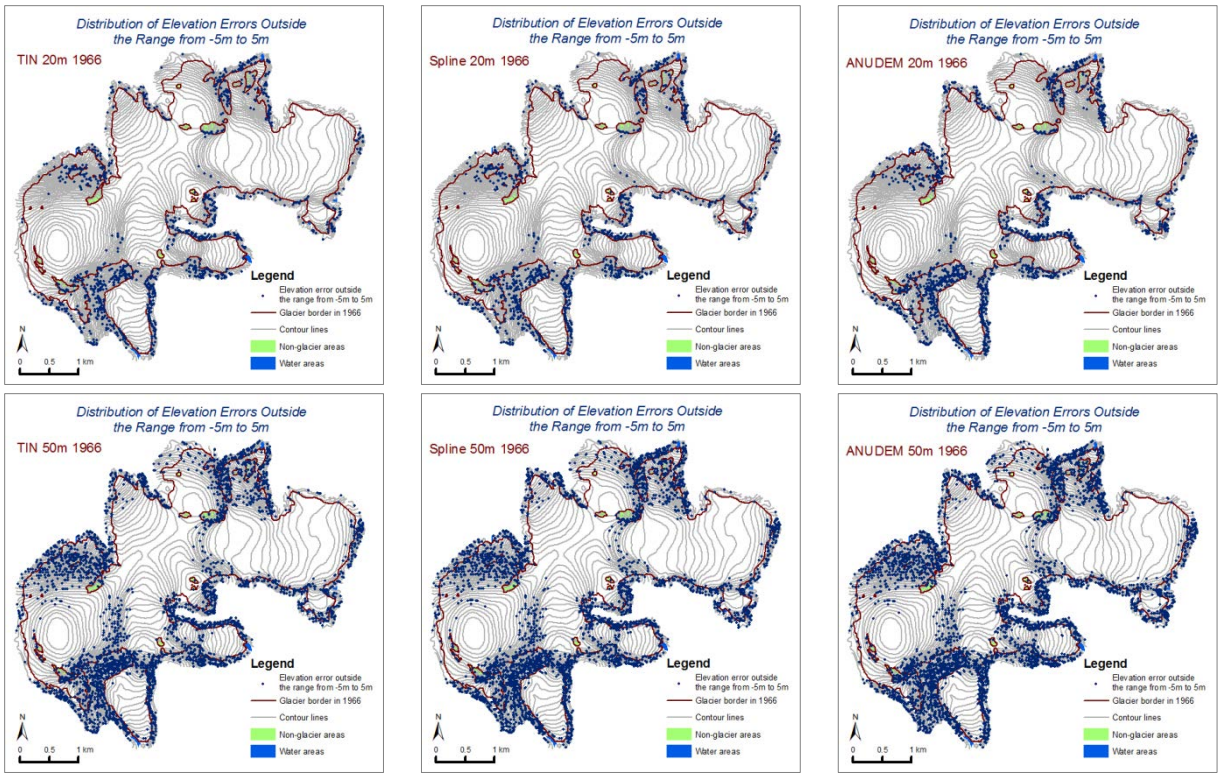

Distribution of elevation errors outside the range from -5m to 5m (1966).

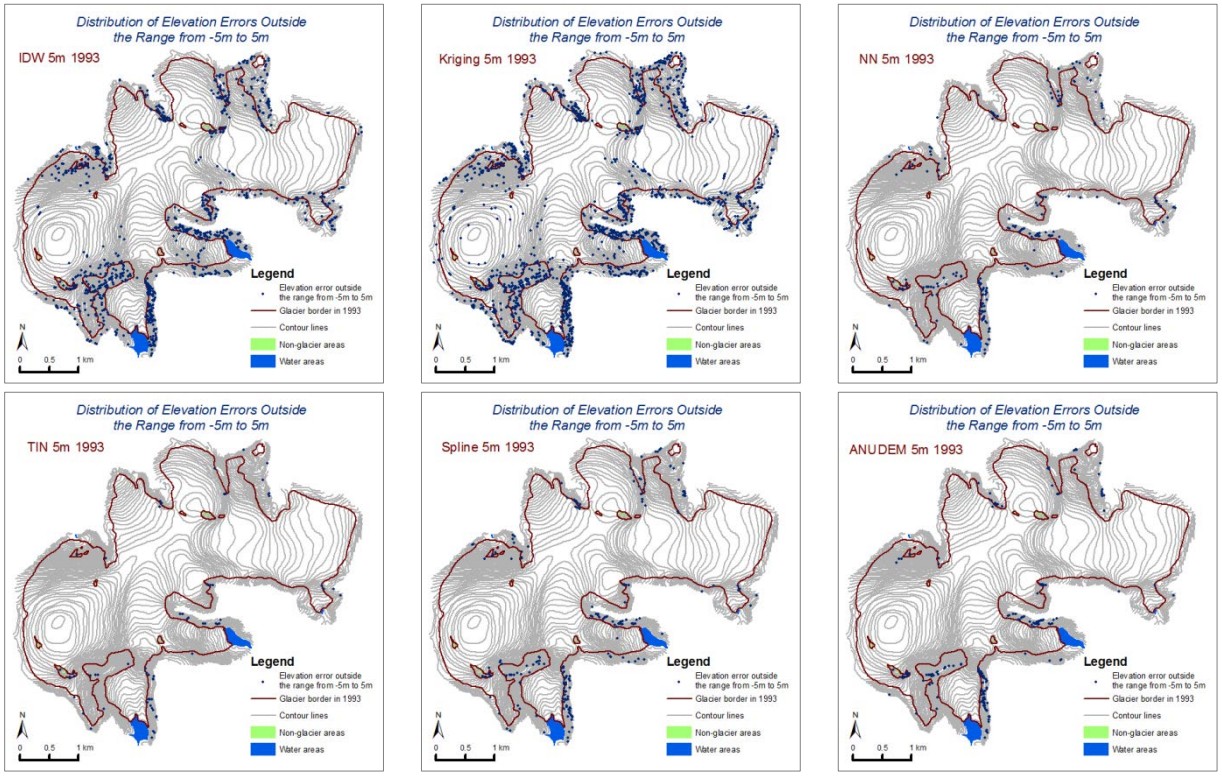

Distribution of elevation errors outside the range from -5m to 5m (1993). Only cell size 5m is used.

9.5 Accuracy of the DEM for terrain on different slopes

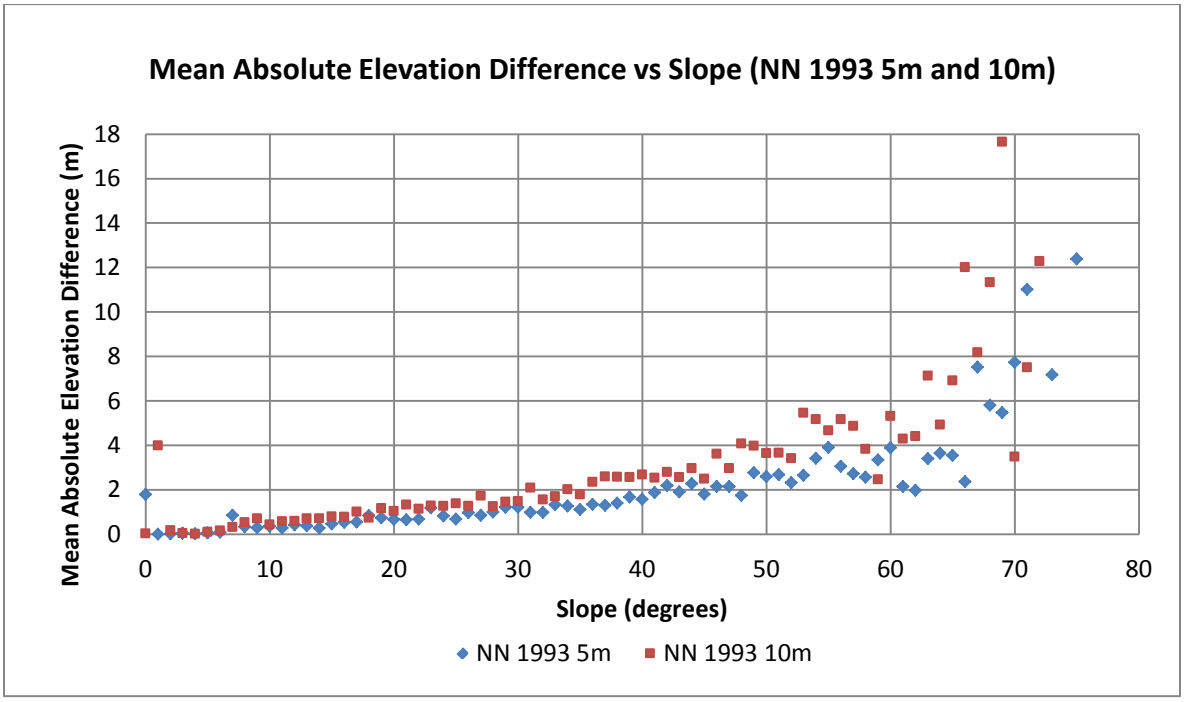

Mean absolute elevation differences plotted against slope (DEM NN 1993 5m and 10m).

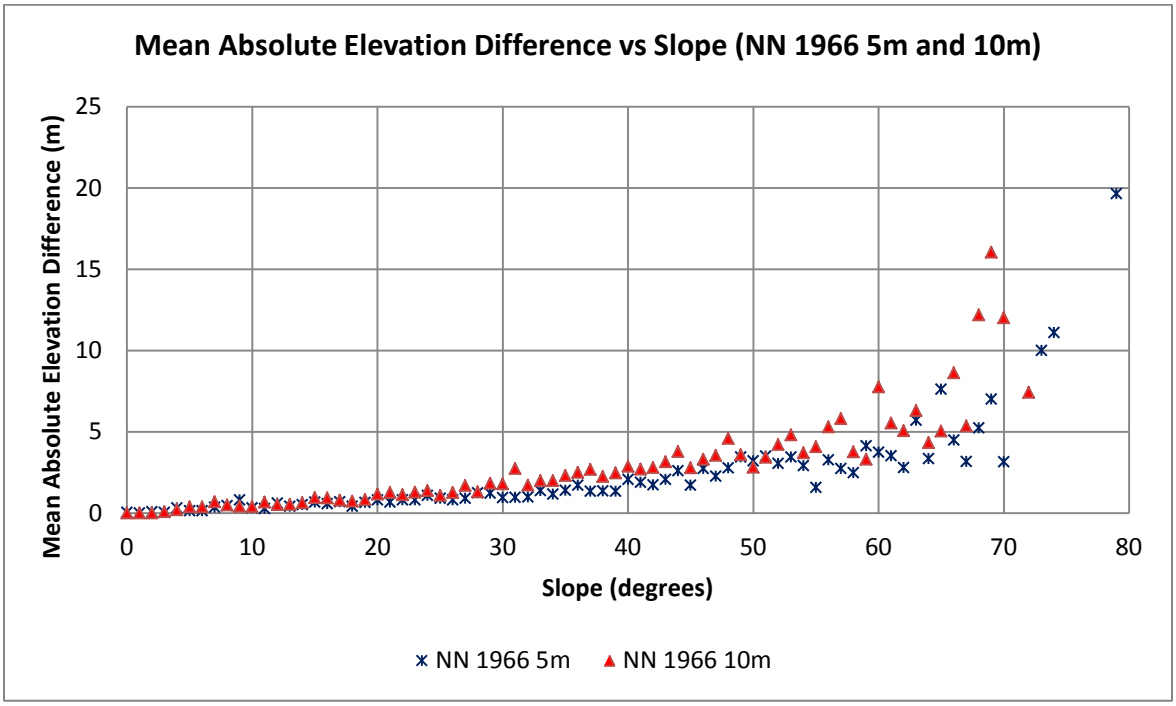

Mean absolute elevation differences plotted against slope (DEM NN 1966 5m and 10m).

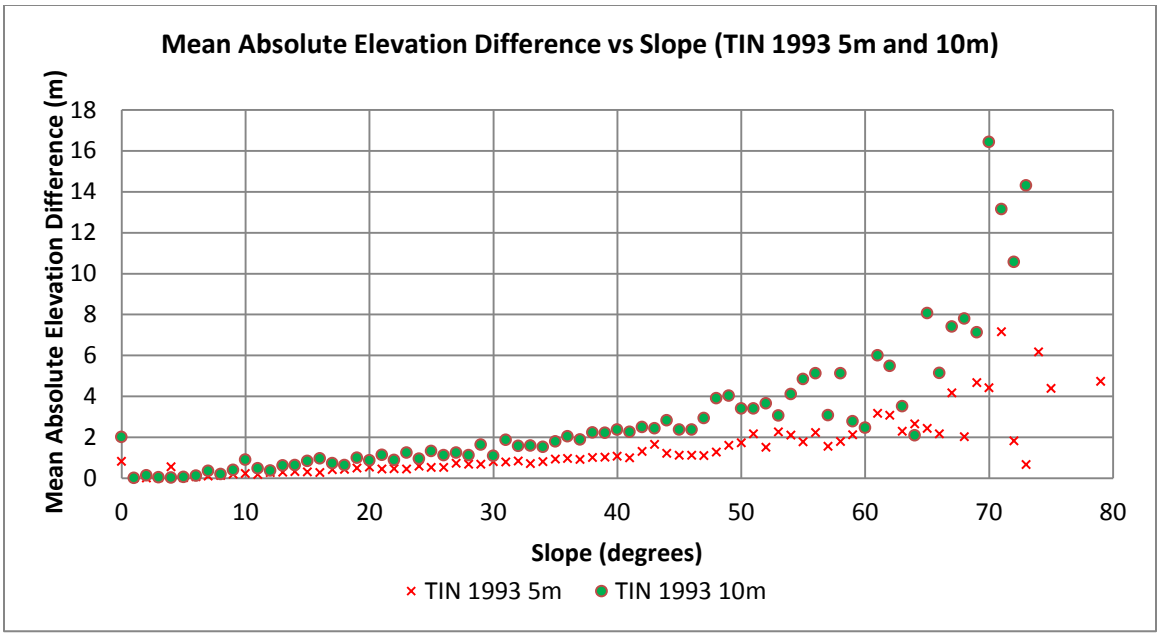

Mean absolute elevation differences plotted against slope (DEM TIN 1993 5m and 10m).

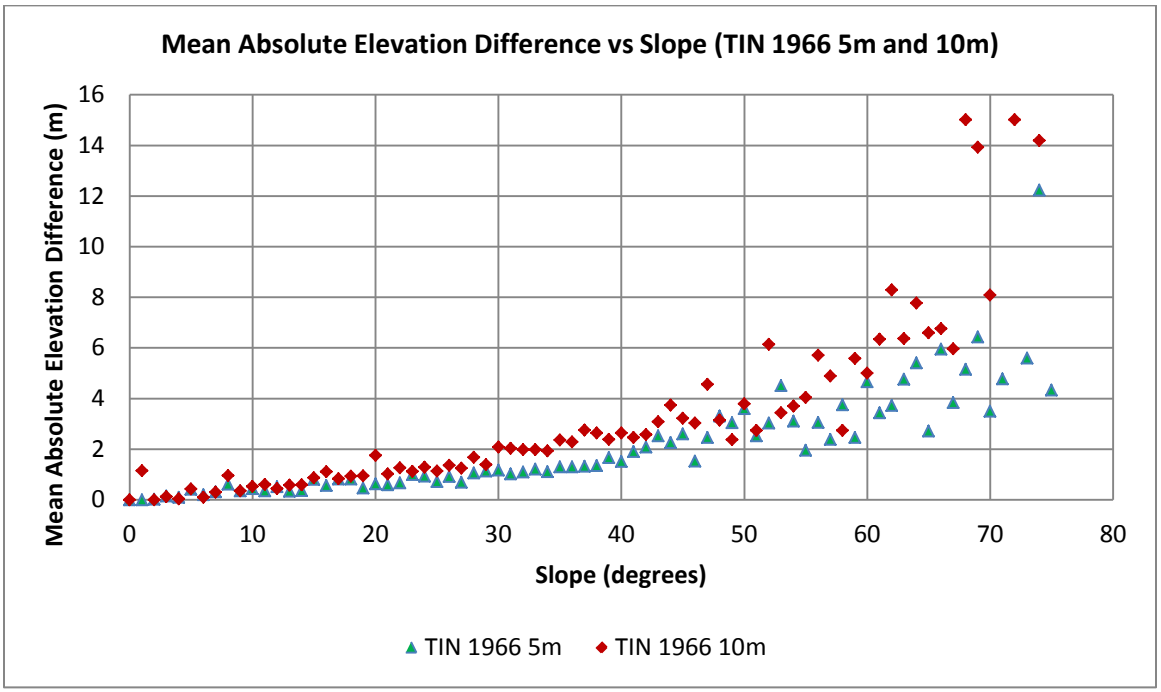

Mean absolute elevation differences plotted against slope (DEM TIN 1966 5m and 10m).

9.6 DEM comparison with LiDAR data in non-glacier areas

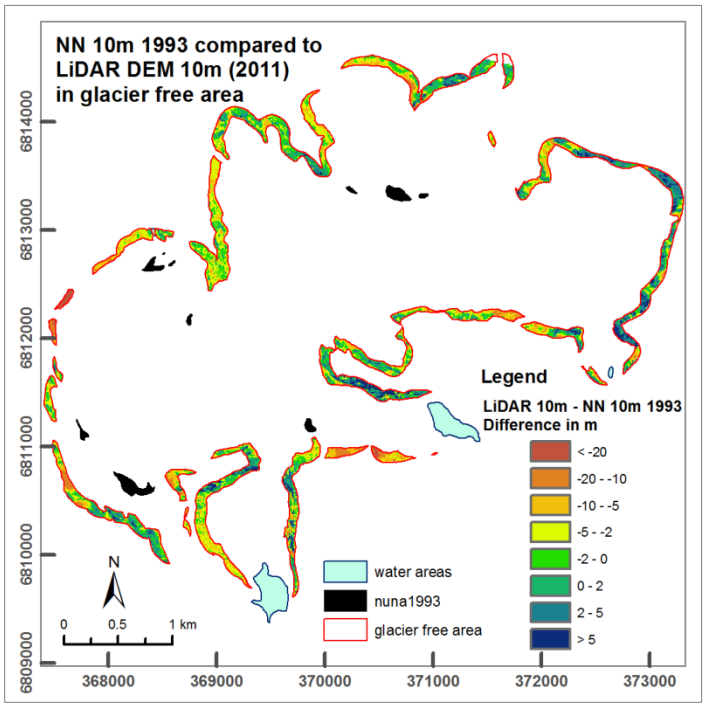

Difference in elevation comparing LiDAR DEM (resolution 10m) and DEM interpolated from contour lines from 1993 using natural neighbour method (resolution 10m). Surface elevation differences were calculated by subtracting DEMs on a cell-by-cell basis.

Source: Own elaboration
Coordinate System: WGS 1984 UTM Zone 32N

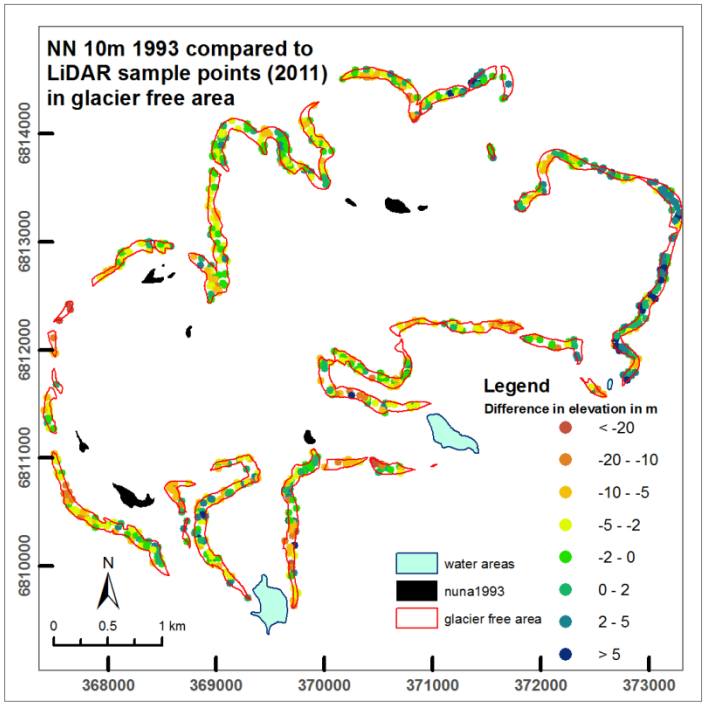

Difference in elevation comparing LiDAR sample points and DEM interpolated from contour lines from 1993 using natural neighbour method (resolution 10m). Surface elevation differences were calculated by extracting the cell values of the interpolated raster based on a set of sample points of LiDAR data (2011).

Source: Own elaboration
Coordinate System: WGS 1984 UTM Zone 32N

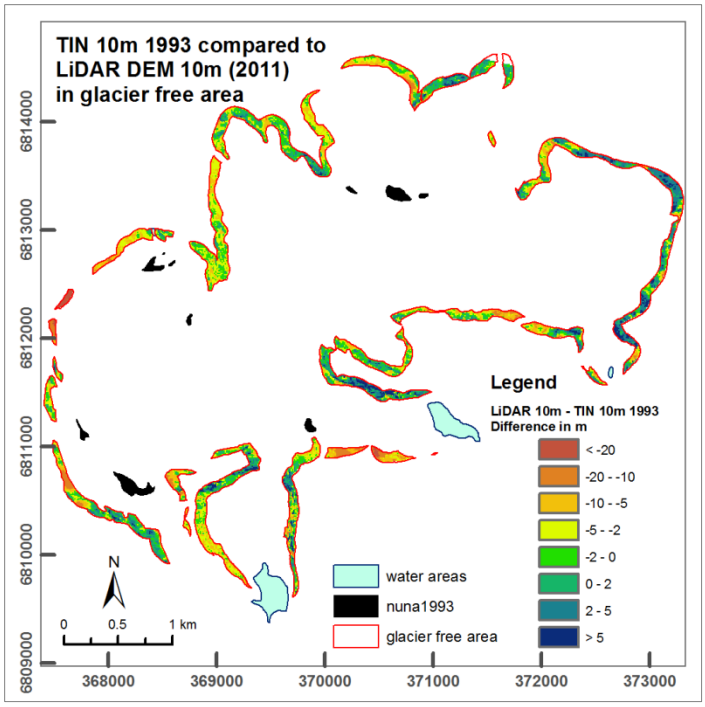

Difference in elevation comparing LiDAR 2011 DEM (resolution 10m) and DEM interpolated from contour lines from 1993 using TIN method (resolution 10m). Surface elevation differences were calculated by subtracting DEMs on a cell-by-cell basis.

Source: Own elaboration
Coordinate System: WGS 1984 UTM Zone 32N

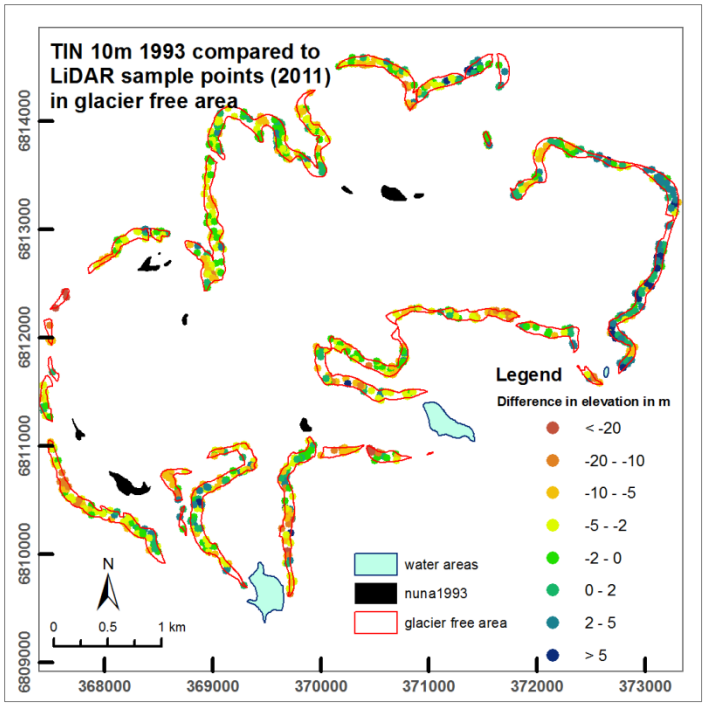

Difference in elevation comparing LiDAR sample points and DEM interpolated from contour lines from 1993 using TIN method (resolution 10m). Surface elevation differences were calculated by extracting the cell values of the interpolated raster based on a set of sample points of LiDAR data (2011).

Source: Own elaboration
Coordinate System: WGS 1984 UTM Zone 32N

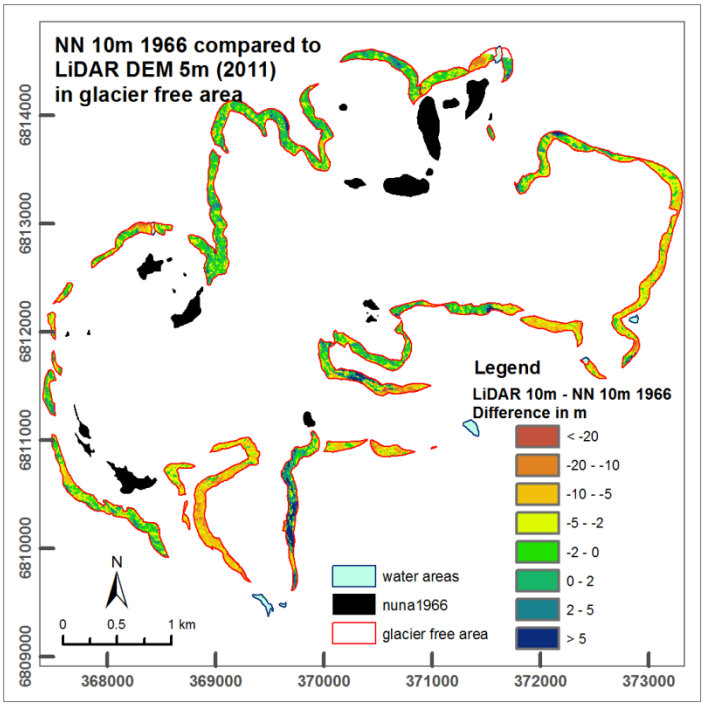

Difference in elevation comparing LiDAR (2011) DEM (resolution 10m) and DEM interpolated from contour lines from 1966 using natural neighbour method (resolution 10m). Surface elevation differences in a glacier free area were calculated by subtracting DEMs on a cell-by-cell basis.

Source: Own elaboration
Coordinate System: WGS 1984 UTM Zone 32N

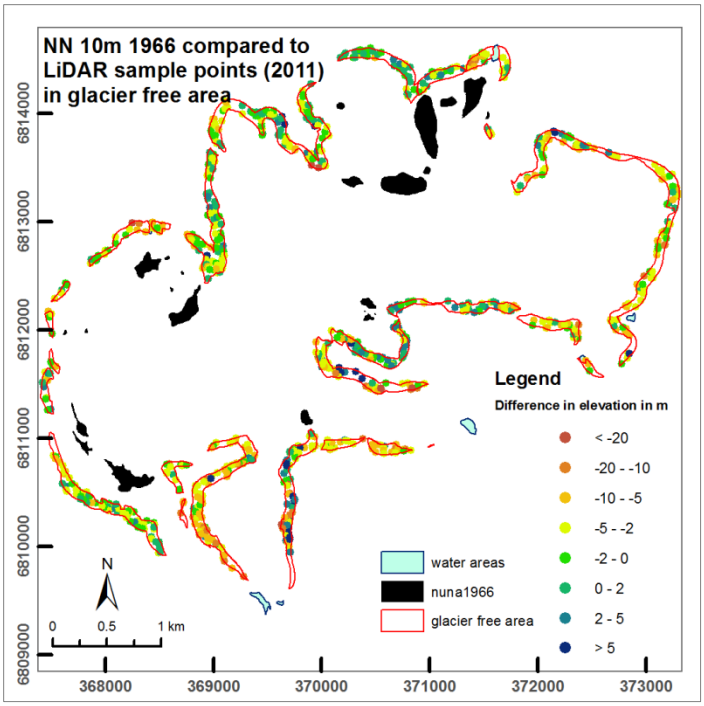

Difference in elevation comparing LiDAR sample points and DEM interpolated from contour lines from 1966 using natural neighbour method (resolution 10m). Surface elevation differences were calculated by extracting the cell values of the interpolated raster based on a set of sample points of LiDAR data (2011).

Source: Own elaboration
Coordinate System: WGS 1984 UTM Zone 32N

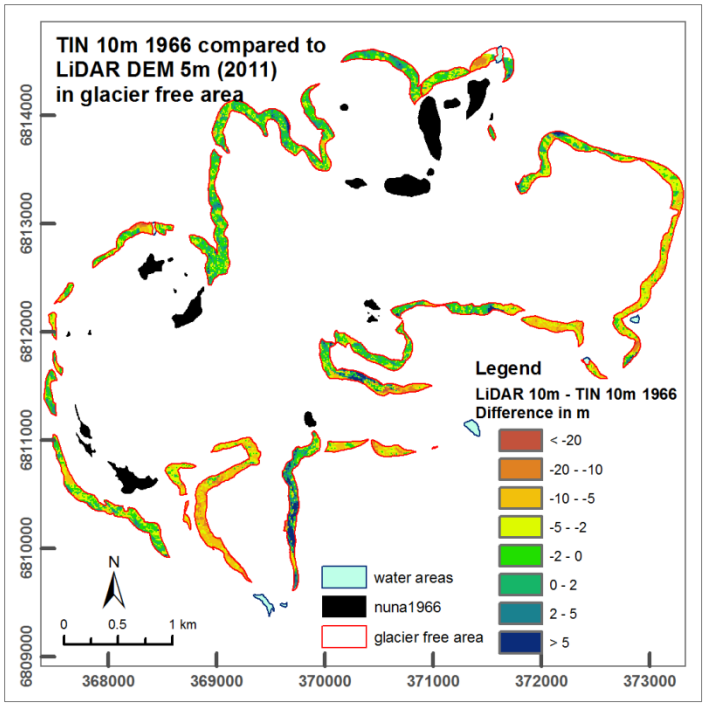

Difference in elevation comparing LiDAR (2011) DEM (resolution 10m) and DEM interpolated from contour lines from 1966 using TIN (resolution 10m). Surface elevation differences in a glacier free area were calculated by subtracting DEMs on a cell-by-cell basis.

Source: Own elaboration
Coordinate System: WGS 1984 UTM Zone 32N

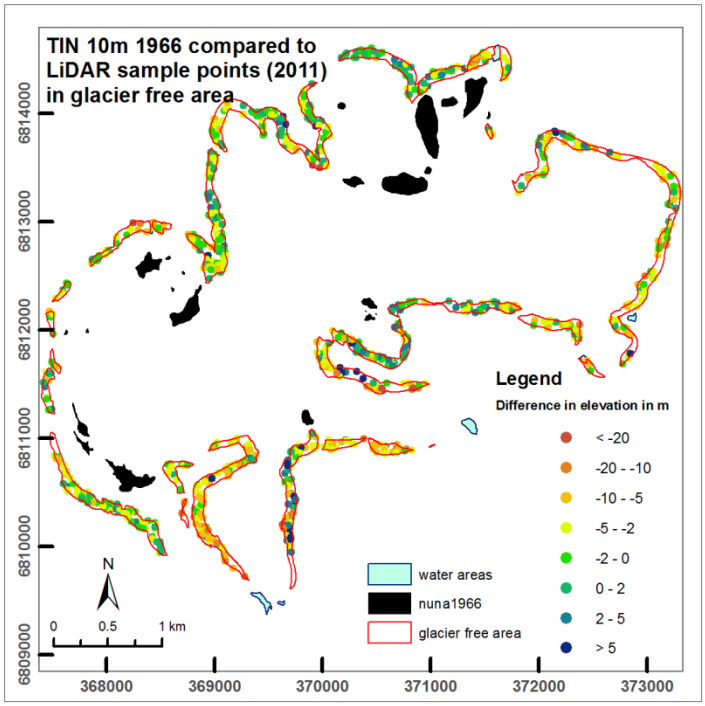

Difference in elevation comparing LiDAR sample points and DEM interpolated from contour lines from 1966 using natural neighbour method (resolution 10m). Surface elevation differences were calculated by extracting the cell values of the interpolated raster based on a set of sample points of LiDAR data (2011).

Source: Own elaboration
Coordinate System: WGS 1984 UTM Zone 32N

9.7 DEM comparison with LiDAR data in glacier areas

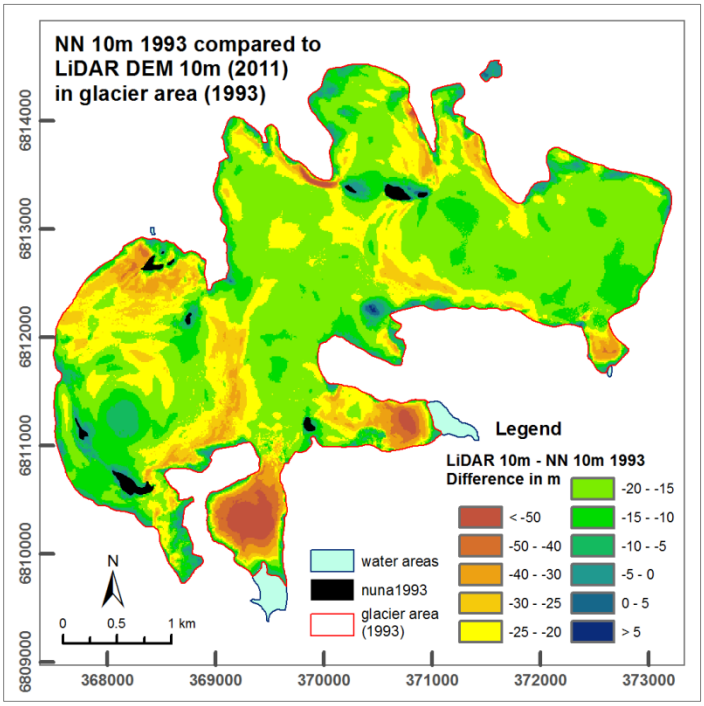

Difference in elevation comparing LiDAR DEM (resolution 10m) and DEM interpolated from contour lines from 1993 using natural neighbour method (resolution 10m). Surface elevation differences were calculated by subtracting DEMs on a cell-by-cell basis.

Source: Own elaboration
Coordinate System: WGS 1984 UTM Zone 32N

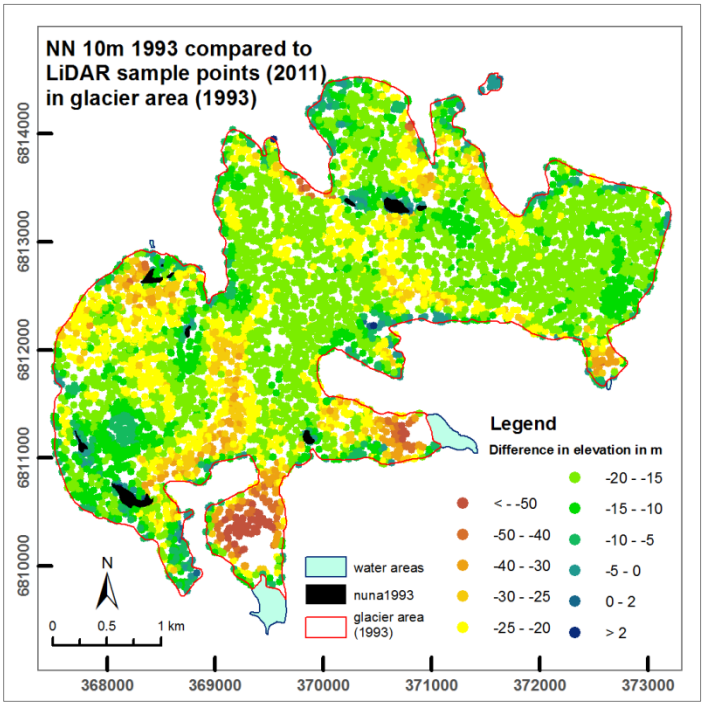

Difference in elevation comparing LiDAR sample points and DEM interpolated from contour lines from 1993 using natural neighbour method (resolution 10m). Surface elevation differences were calculated by extracting the cell values of the interpolated raster based on a set of sample points of LiDAR data (2011).

Source: Own elaboration
Coordinate System: WGS 1984 UTM Zone 32N

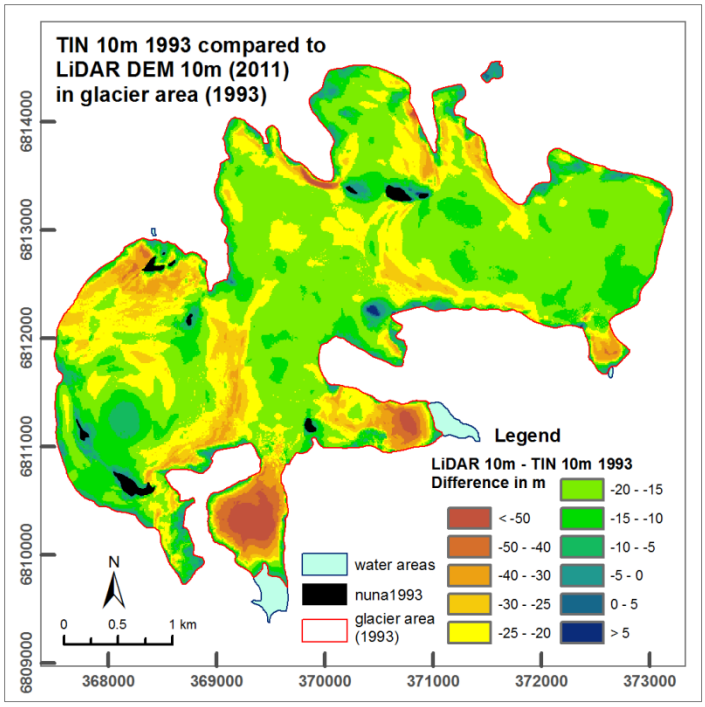

Difference in elevation comparing LiDAR 2011 DEM (resolution 10m) and DEM interpolated from contour lines from 1993 using TIN method (resolution 10m). Surface elevation differences were calculated by subtracting DEMs on a cell-by-cell basis.

Source: Own elaboration
Coordinate System: WGS 1984 UTM Zone 32N

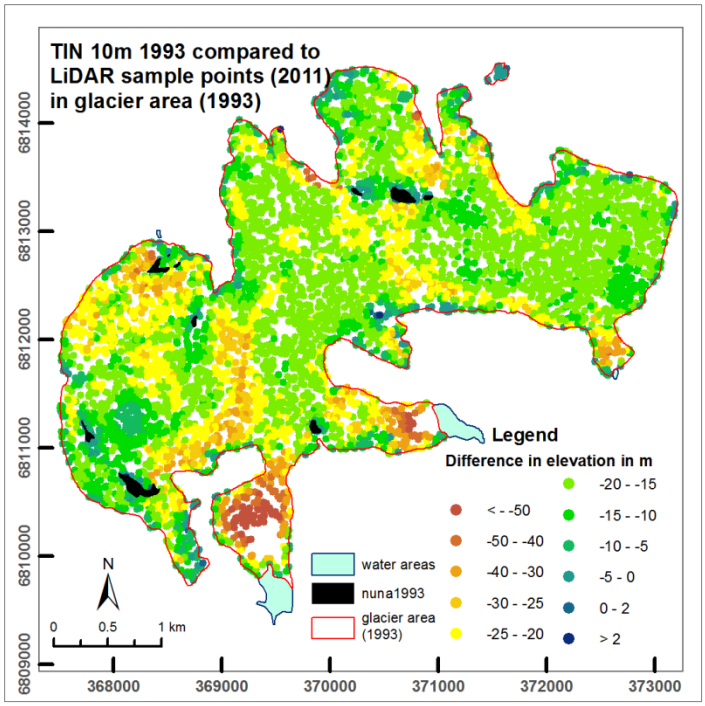

Difference in elevation comparing LiDAR sample points and DEM interpolated from contour lines from 1993 using TIN method (resolution 10m). Surface elevation differences were calculated by extracting the cell values of the interpolated raster based on a set of sample points of LiDAR data (2011).

Source: Own elaboration
Coordinate System: WGS 1984 UTM Zone 32N

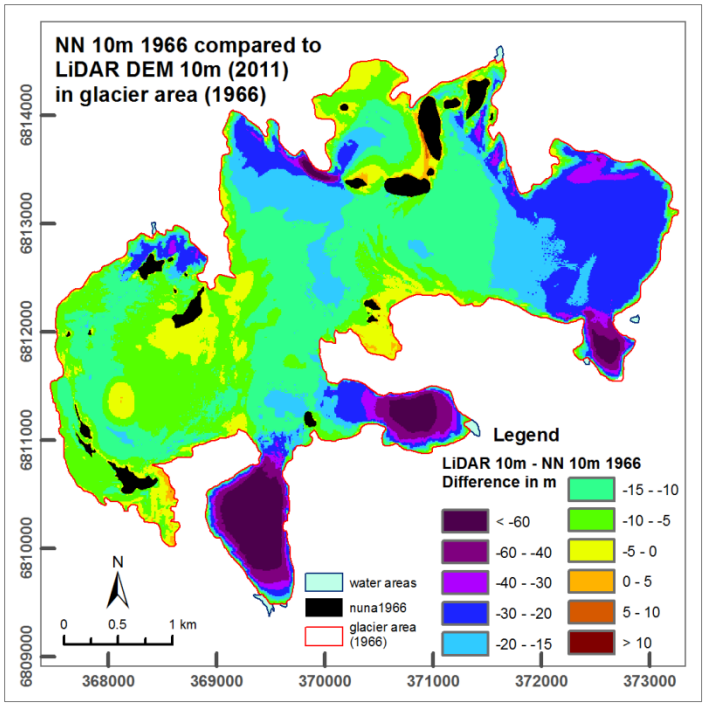

Difference in elevation comparing LiDAR (2011) DEM (resolution 10m) and DEM interpolated from contour lines from 1966 using natural neighbour method (resolution 10m). Surface elevation differences in a glacier free area were calculated by subtracting DEMs on a cell-by-cell basis.

Source: Own elaboration
Coordinate System: WGS 1984 UTM Zone 32N

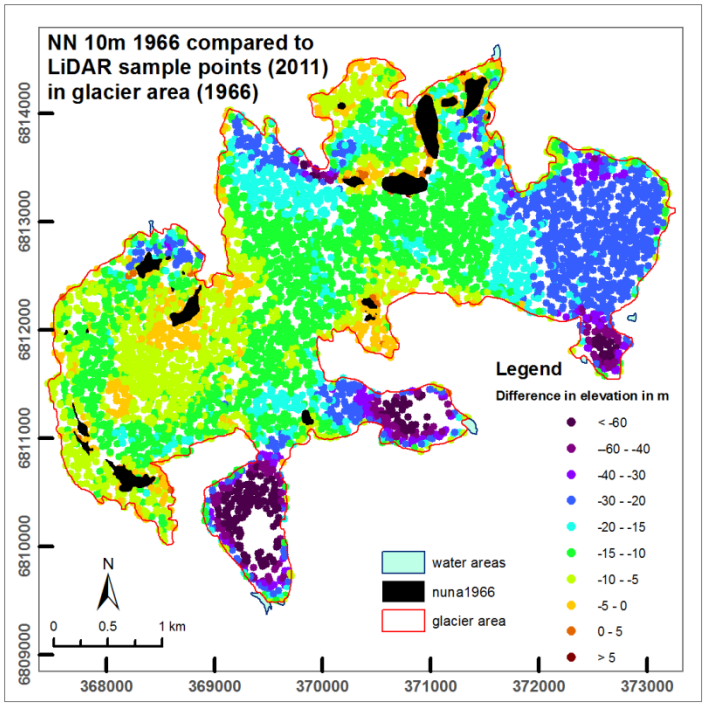

Difference in elevation comparing LiDAR sample points and DEM interpolated from contour lines from 1966 using natural neighbour method (resolution 10m). Surface elevation differences were calculated by extracting the cell values of the interpolated raster based on a set of sample points of LiDAR data (2011).

Source: Own elaboration
Coordinate System: WGS 1984 UTM Zone 32N

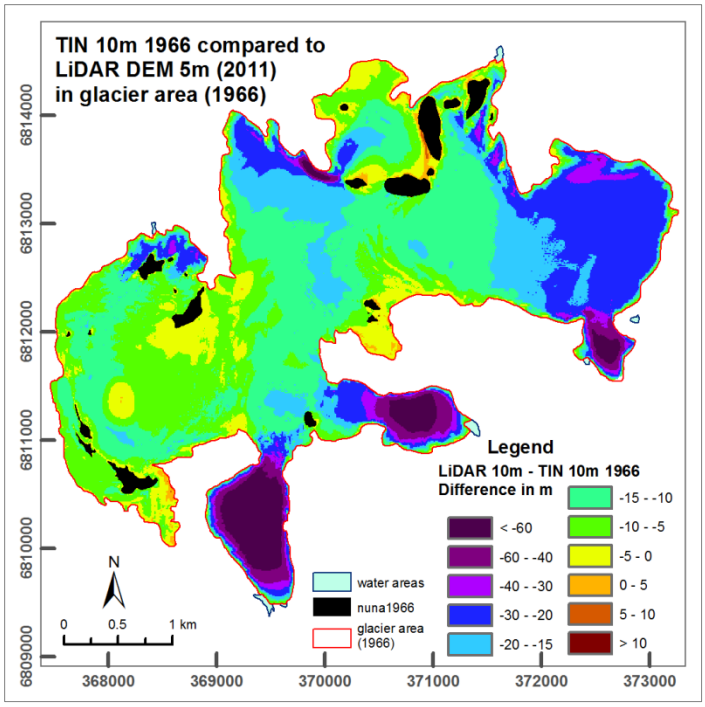

Difference in elevation comparing LiDAR (2011) DEM (resolution 10m) and DEM interpolated from contour lines from 1966 using TIN (resolution 10m). Surface elevation differences in a glacier free area were calculated by subtracting DEMs on a cell-by-cell basis.

Source: Own elaboration
Coordinate System: WGS 1984 UTM Zone 32N

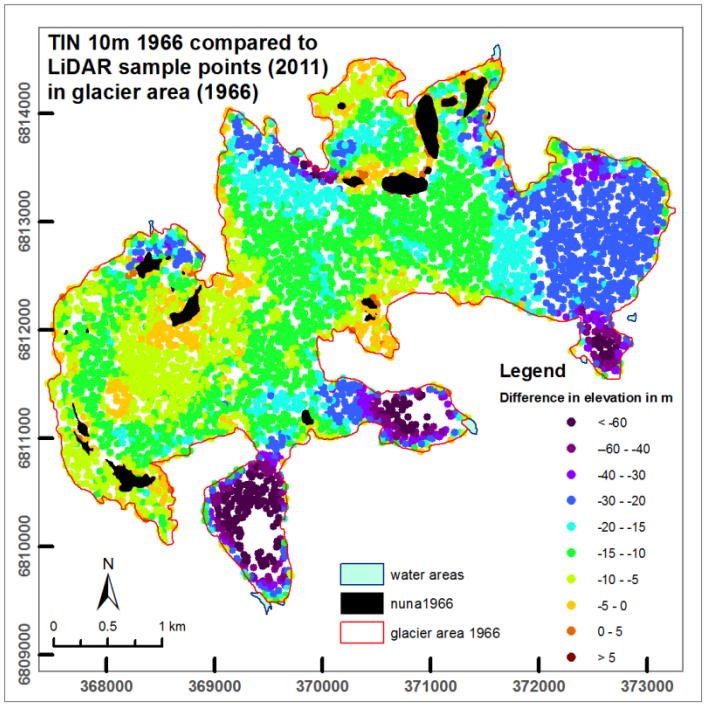

Difference in elevation comparing LiDAR sample points and DEM interpolated from contour lines from 1966 using natural neighbour method (resolution 10m). Surface elevation differences were calculated by extracting the cell values of the interpolated raster based on a set of sample points of LiDAR data (2011).

Source: Own elaboration
Coordinate System: WGS 1984 UTM Zone 32N

9.8 Temperature increase graphics

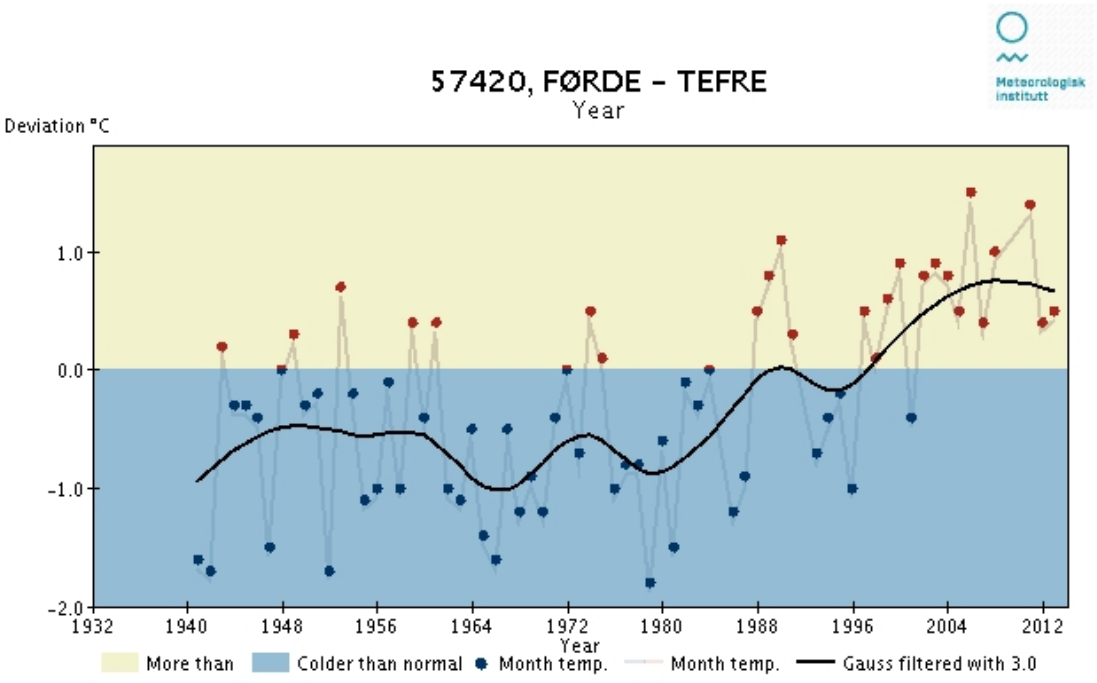

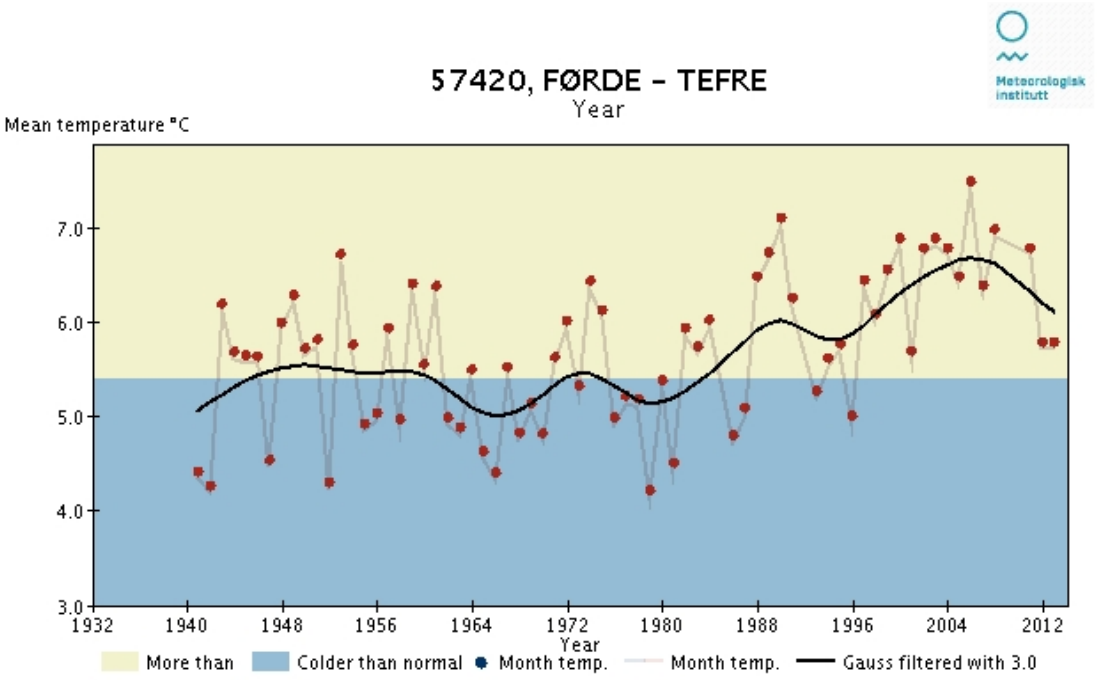

9.9 The two biggest tongues of the Jostefonn

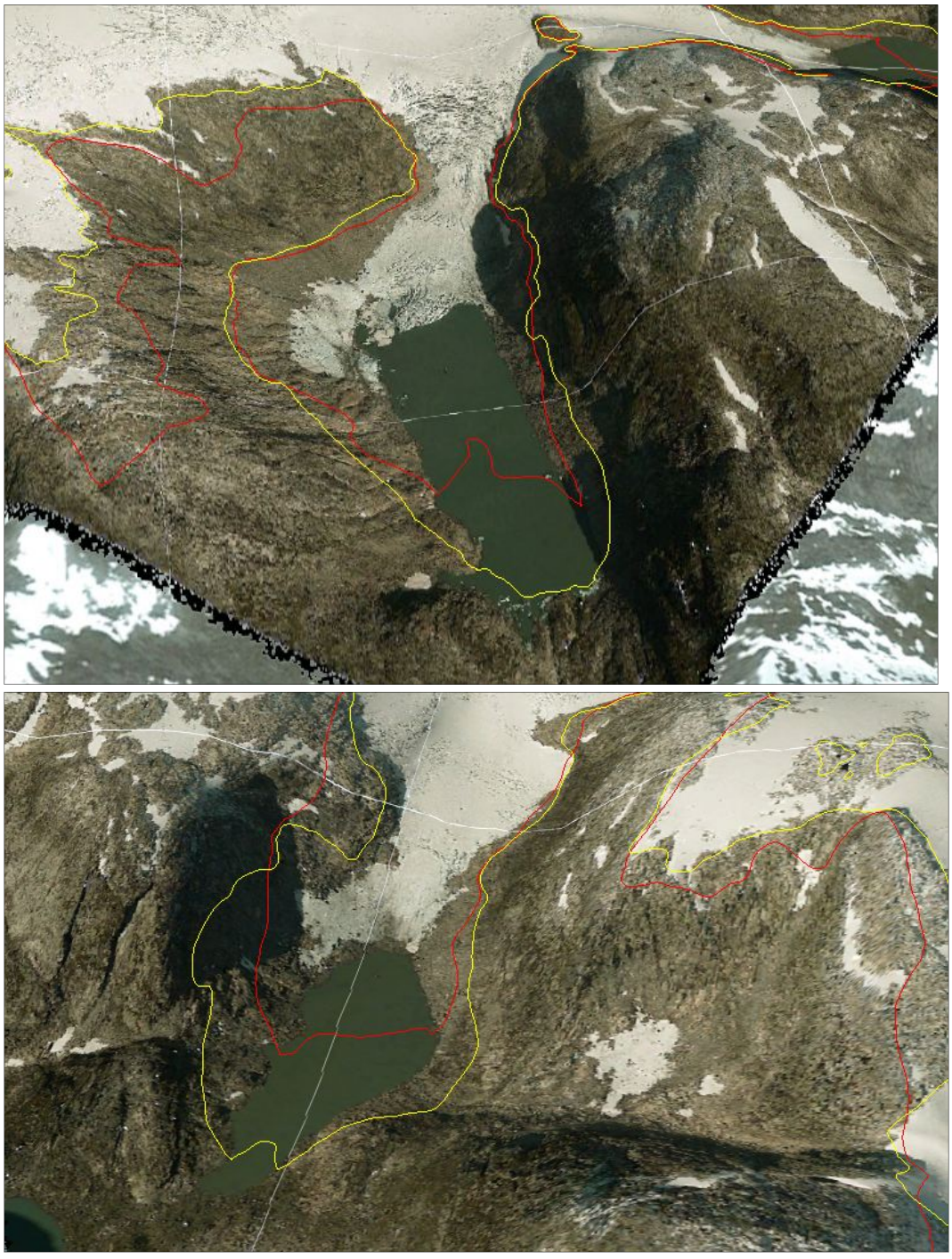

The two biggest tongues of the Jostefonn glacier showing the border of the glacier: 1966 border – yellow, 1993 – red, orthophoto from 2011. The three layers are visually shown in Google Earth.

Series from Lund University
Department of Physical Geography and Ecosystem Science

Master Thesis in Geographical Information Science (LUMA-GIS)

1. *Anthony Lawther:* The application of GIS-based binary logistic regression for slope failure susceptibility mapping in the Western Grampian Mountains, Scotland. (2008).
2. *Rickard Hansen:* Daily mobility in Grenoble Metropolitan Region, France. Applied GIS methods in time geographical research. (2008).
3. *Emil Bayramov:* Environmental monitoring of bio-restoration activities using GIS and Remote Sensing. (2009).
4. *Rafael Villarreal Pacheco:* Applications of Geographic Information Systems as an analytical and visualization tool for mass real estate valuation: a case study of Fontibon District, Bogota, Columbia. (2009).
5. *Siri Oestreich Waage:* a case study of route solving for oversized transport: The use of GIS functionalities in transport of transformers, as part of maintaining a reliable power infrastructure (2010).
6. *Edgar Pimiento:* Shallow landslide susceptibility – Modelling and validation (2010).
7. *Martina Schäfer:* Near real-time mapping of floodwater mosquito breeding sites using aerial photographs (2010)
8. *August Pieter van Waarden-Nagel:* Land use evaluation to assess the outcome of the programme of rehabilitation measures for the river Rhine in the Netherlands (2010)
9. *Samira Muhammad:* Development and implementation of air quality data mart for Ontario, Canada: A case study of air quality in Ontario using OLAP tool. (2010)
10. *Fredros Oketch Okumu*: Using remotely sensed data to explore spatial and temporal relationships between photosynthetic productivity of vegetation and malaria transmission intensities in selected parts of Africa (2011)
11. *Svajunas Plunge:* Advanced decision support methods for solving diffuse water pollution problems (2011)
12. *Jonathan Higgins:* Monitoring urban growth in greater Lagos: A case study using GIS to monitor the urban growth of Lagos 1990 - 2008 and produce future growth prospects for the city (2011).
13. *Mårten Karlberg:* Mobile Map Client API: Design and Implementation for Android (2011).
14. *Jeanette McBride:* Mapping Chicago area urban tree canopy using color infrared imagery (2011)
15. *Andrew Farina:* Exploring the relationship between land surface temperature and vegetation abundance for urban heat island mitigation in Seville, Spain (2011)
16. *David Kanyari*: Nairobi City Journey Planner An online and a Mobile Application (2011)

17 *Laura V. Drews:* Multi-criteria GIS analysis for siting of small wind power plants - A case study from Berlin (2012)

18 *Qaisar Nadeem:* Best living neighborhood in the city - A GIS based multi criteria evaluation of ArRiyadh City (2012)

19 *Ahmed Mohamed El Saeid Mustafa:* Development of a photo voltaic building rooftop integration analysis tool for GIS for Dokki District, Cairo, Egypt (2012)

20 *Daniel Patrick Taylor*: Eastern Oyster Aquaculture: Estuarine Remediation via Site Suitability and Spatially Explicit Carrying Capacity Modeling in Virginia's Chesapeake Bay (2013)

21 *Angeleta Oveta Wilson:* A Participatory GIS approach to *unearthing* Manchester's Cultural Heritage '*gold mine'* (2013)

22 *Ola Svensson:* Visibility and Tholos Tombs in the Messenian Landscape: A Comparative Case Study of the Pylian Hinterlands and the Soulima Valley (2013)

23 *Monika Ogden:* Land use impact on water quality in two river systems in South Africa (2013)

24 *Stefan Rova:* A GIS based approach assessing phosphorus load impact on Lake Flaten in Salem, Sweden (2013)

25 *Yann Buhot:* Analysis of the history of landscape changes over a period of 200 years. How can we predict past landscape pattern scenario and the impact on habitat diversity? (2013)

26 *Christina Fotiou:* Evaluating habitat suitability and spectral heterogeneity models to predict weed species presence (2014)